

2015

## Feasibility and Supply Analysis of U.S. Geothermal District Heating and Cooling System

Xiaoning He

Follow this and additional works at: <https://researchrepository.wvu.edu/etd>

---

### Recommended Citation

He, Xiaoning, "Feasibility and Supply Analysis of U.S. Geothermal District Heating and Cooling System" (2015). *Graduate Theses, Dissertations, and Problem Reports*. 5785.  
<https://researchrepository.wvu.edu/etd/5785>

This Dissertation is protected by copyright and/or related rights. It has been brought to you by the The Research Repository @ WVU with permission from the rights-holder(s). You are free to use this Dissertation in any way that is permitted by the copyright and related rights legislation that applies to your use. For other uses you must obtain permission from the rights-holder(s) directly, unless additional rights are indicated by a Creative Commons license in the record and/ or on the work itself. This Dissertation has been accepted for inclusion in WVU Graduate Theses, Dissertations, and Problem Reports collection by an authorized administrator of The Research Repository @ WVU. For more information, please contact [researchrepository@mail.wvu.edu](mailto:researchrepository@mail.wvu.edu).

# **Feasibility and Supply Analysis of U.S. Geothermal District Heating and Cooling System**

**Xiaoning He**

**Dissertation submitted  
to the Benjamin M. Statler College of Engineering and Mineral Resources  
at West Virginia University**

**in partial fulfillment of the requirements for the degree of**

**Doctor of Philosophy in  
Chemical Engineering**

**Brian Anderson, Ph.D., Chair  
Timothy Carr, Ph.D.  
Randall Jackson, Ph.D.  
Richard Turton, Ph.D.  
John Zondlo, Ph.D.**

**Department of Chemical Engineering**

**Morgantown, West Virginia  
2015**

**Keywords: Geothermal energy, Direct use, Levelized cost of heat, Supply analysis  
Copyright 2015 Xiaoning He**

## **ABSTRACT**

### **Feasibility and Supply Analysis of U.S. Geothermal District Heating and Cooling System**

**Xiaoning He**

Geothermal energy is a globally distributed sustainable energy with the advantages of a stable base load energy production with a high capacity factor and zero SO<sub>x</sub>, CO, and particulates emissions. It can provide a potential solution to the depletion of fossil fuels and air pollution problems. The geothermal district heating and cooling system is one of the most common applications of geothermal energy, and consists of geothermal wells to provide hot water from a fractured geothermal reservoir, a surface energy distribution system for hot water transmission, and heating/cooling facilities to provide water and space heating as well as air conditioning for residential and commercial buildings.

To gain wider recognition for the geothermal district heating and cooling (GDHC) system, the potential to develop such a system was evaluated in the western United States, and in the state of West Virginia. The geothermal resources were categorized into identified hydrothermal resources, undiscovered hydrothermal resources, near hydrothermal enhanced geothermal system (EGS), and deep EGS. Reservoir characteristics of the first three categories were estimated individually, and their thermal potential calculated. A cost model for such a system was developed for technical performance and economic analysis at each geothermally active location. A supply curve for the system was then developed, establishing the quantity and the cost of potential geothermal energy which can be used for the GDHC system.

A West Virginia University (WVU) case study was performed to compare the competitiveness of a geothermal energy system to the current steam based system. An Aspen Plus model was created to simulate the year-round campus heating and cooling scenario. Five cases of varying water flow rates and temperatures were simulated to find the lowest levelized cost of heat (LCOH) for the WVU case study. The model was then used to derive a levelized cost of heat as a function of the population density at a constant geothermal gradient. By use of such functions in West Virginia at a census tract level, the most promising census tracts in WV for the development of geothermal district heating and cooling systems were mapped.

This study is unique in that its purpose was to utilize supply analyses for the GDHC systems and determine an appropriate economic assessment of the viability and sustainability of the systems. It was found that the market energy demand, production temperature, and project lifetime have negative effects on the levelized cost, while the drilling cost, discount rate, and capital cost have positive effects on the levelized cost by sensitivity analysis. Moreover, increasing the energy demand is the most effective way to decrease the levelized cost. The derived levelized cost function shows that for EGS based systems, the population density has a strong negative effect on the LCOH at any geothermal gradient, while the gradient only has a negative effect on the LCOH at a low population density.

## ACKNOWLEDGEMENTS

It has been a productive, enjoyable, and a full of memory five years staying in West Virginia University in Morgantown, WV. I would like to acknowledge the following people and organizations that helped me in various ways throughout the duration of this project.

First I would like to sincerely thank my advisor, Dr. Brian Anderson, who guides me into the geothermal research and supports me since then. I am encouraged by his enthusiasm and dedication to the energy field, and have learned many things from him. I am grateful for those trips to Cornell University, Stanford University, and Portland that would not have been possible without his supports. Those are not only great opportunities to learn and to interact with new people, but also enjoyable times to new places.

I would like to thank U.S. Department of Energy (DOE) for providing funding to this project. I would also like to thank Dr. Chad Augustine from National Renewable Energy Laboratory for his help in my research.

I would like to thank my committee members: Dr. Timothy Carr, Dr. Randall Jackson, Dr. Richard Turton, and Dr. John Zondlo. I am grateful for their advice and help.

I would like to thank my colleges and my friends: Dr. Srinath Velaga, Dr. Nagasree Garapati, Dr. Manohar Gaddipati, Dr. Patrick McGuire, Madhur Bedre, Jason Peluchette, Taiwo Ajayi, Manish Nandanwar, and Prathyusha Sridhara. It is a wonderful experience working with them. I would like to thank Ms. Lisa Saurborn and the WVU facility office for their help in completing my research. I would also like to thank Dr. Jeff Tester and his geothermal research group members: Maciej Lukawski, Koenraad Beckers, whose collaboration has helped my research.

Finally, I would like to thank my parents and my wife for their supports, love, and encourages throughout my life.

Xiaoning He

March 4<sup>th</sup>, 2015

# Table of Contents

<b>Chapter 1 The Geothermal Basics</b> .....	1
1.1 Earth as a Heat Engine .....	1
1.2 Using Geothermal Energy for Heat and Power .....	2
1.3 Background and Motivation .....	6
1.4 World-wide Geothermal Development.....	7
1.5 Objective and Approach .....	9
<b>Chapter 2 Supply Analysis of Geothermal District Heating and Cooling Systems ..</b>	<b>11</b>
2.1 Introduction.....	11
2.2 Levelized Cost of Heat.....	12
2.3 Previous Studies on Geothermal Supply Analysis.....	14
2.4 Reservoir Characterization and Potential Estimation .....	19
2.4.1 Geothermal Resources Categorization .....	19
2.4.2 Identified Hydrothermal Resources.....	20
2.4.3 Undiscovered Hydrothermal Resources .....	22
2.4.4 Near Hydrothermal EGS Resources .....	24
2.4.5 Deep EGS Resources.....	25
2.5 Energy Market Characterization .....	27
2.5.1 Barriers to the GDHC Development .....	28
2.5.2 Energy Demand Estimation.....	29
2.6 LCOH Model Development.....	31
2.6.1 Surface Facility Design and Economics.....	32
2.6.2 Well Design and Economics.....	41
2.6.3 Risk Analysis .....	44
2.6.4 Cost Model Implementation .....	45

2.7	Thermal Potential for GDHC System .....	46
2.7.1	Identified Hydrothermal Resources .....	46
2.7.2	Undiscovered Hydrothermal Resources .....	48
2.7.3	Near Hydrothermal EGS Resources .....	49
2.8	LCOH Estimation and Supply Curve Development .....	50
2.8.1	Identified Hydrothermal Resources .....	50
2.8.2	Undiscovered Hydrothermal Resources .....	55
2.8.3	Near Hydrothermal EGS Resources .....	57
2.8.4	The GDHC Supply Curve.....	59
2.9	Discussion .....	61
2.9.1	Population’s Effect on LCOH .....	61
2.9.2	Geothermal Gradient’s Effect on LCOH.....	62
2.9.3	Model Sensitivity.....	63
2.10	Conclusion .....	64
<b>Chapter 3 Techno-Economic Assessment of GDHC systems: A Case Study on West Virginia University.....</b>		<b>67</b>
3.1	Introduction.....	67
3.2	The Initial: West Virginia Geothermal Hot Spot.....	68
3.3	Modeling the GDHC System on WVU Campus .....	70
3.3.1	Existing Heating and Cooling Basics .....	71
3.3.2	Proposed Heating and Cooling System .....	71
3.3.3	LCOH Calculation for WVU Case Study.....	74
3.4	Empirical LCOH Function Derivation.....	76
3.5	Results and Discussion .....	77
3.5.1	West Virginia Geothermal Maps .....	77

3.5.2	Campus GDHC Characterization .....	79
3.5.3	Campus GDHC Cost Analysis .....	82
3.5.4	LCOH Functions and State Wide Estimation.....	85
3.6	Conclusion .....	90
<b>Chapter 4 Conclusions and Recommendations.....</b>		<b>92</b>
4.1	Significance and Conclusions .....	92
4.2	Recommendations.....	94
Reference .....		96
Appendix A: Geothermal Reservoir Characteristics and LCOH.....		105
Table A-1: Identified Hydrothermal Resources and Near Hydrothermal EGS .....		105
Table A-2: Undiscovered Hydrothermal Resources .....		132
Appendix B: WV Geothermal Temperature Maps .....		135

## List of Figures

Figure 1.1: Heat flow map of the conterminous United States by SMU Geothermal Laboratory (Blackwell, et al., 2011). .....	2
Figure 1.2: The Lindal diagram shows different geothermal utilizations by temperature ranges (Gudmundsson, et al., 1985).....	3
Figure 1.3: Schematic layout of a geothermal district heating and cooling system. DWP is deep well pump, SDT is storage and degassing tank, CP is circulation pump, PLB is peak load boiler, htw is hot water, and C is convention heating (Marcel, 2007). .....	4
Figure 1.4: Schematic of a two-well enhanced geothermal power generation system in hot rocks in a low permeability crystalline basement formation (Tester, et al., 2006).....	5
Figure 1.5: World average energy consumption per person ( $\times 10^9$ J/pp/yr) and population growth since 1970, data from (Glassley, 2010). .....	6
Figure 1.6: CO <sub>2</sub> emission from fossil fuels, data from (EIA, 2011) and global mean surface temperature, data from (NASA, 2012).....	7
Figure 1.7: Number of installed countries and installed capacity of geothermal direct use. ....	8
Figure 1.8: Installed capacity of the worldwide geothermal power generation since 1950. It is expected to reach 70,000 MW <sub>e</sub> in 2050.....	9
Figure 2.1: Zhangbei area, China available wind power supply, plotted based on data from Kline, et al., 2008.....	13
Figure 2.2: Predicted levelized cost of electricity and cost breakdown for new generation resources in 2019, based on data from Annual Energy Outlook, 2014, U.S. EIA.....	14
Figure 2.3: Flow diagram to develop the supply curve of GDHC application. ....	19
Figure 2.4: The favorability factor map of undiscovered hydrothermal resources in the western U.S. A warmer color indicates a higher probability to find the hydrothermal resources (Williams, et al., 2009). ....	23
Figure 2.5: Map of underground temperature at 4.5 km of the continental U.S (Tester, et al., 2006). ....	26
Figure 2.6: Comparison of annual U.S. crude oil imports and renewable energy consumption from 2000 to 2014, based on data from U.S. EIA.....	27
Figure 2.7: Flow diagram to estimate the energy demand of the target location.....	29



Figure 2.8: The housing pattern with increase population and distribution network design. .....	33
Figure 2.9: Schematic of the building heating unit of a GDHC system. ....	36
Figure 2.10: Schematic of the absorption chiller, cooling provided at EVAP, geothermal hot water flows through HX-GEO.....	40
Figure 2.11: The drilling cost function with drilling depth. ....	43
Figure 2.12: Histogram of the identified hydrothermal resources mass flow rates and the predicted probability density curve.....	47
Figure 2.13: Pie chart of the remaining identified hydrothermal potential in each state, with a total of 47 GW <sub>th</sub> . ....	48
Figure 2.14: Pie chart of the undiscovered hydrothermal potential in each state, with a total of 159 GW <sub>th</sub> . ....	49
Figure 2.15: Maps of the identified hydrothermal resources, coupled with a western U.S. geothermal temperature map at 6.5 km.....	51
Figure 2.16: Cost breakdown of the GDHC projects of identified hydrothermal resources. .....	52
Figure 2.17: Temperature profile of main streams of the GDHC system in the Weiser area in Idaho. ....	53
Figure 2. 18: Year-round flow rate profile of the geothermal production water of the GDHC system in the Weiser area in Idaho, corresponding to the daily system energy production. ....	54
Figure 2.19: Supply curve of the identified hydrothermal resources, truncated at 50 GW <sub>th</sub> , in comparison with the current cost of heating by natural gas, which is \$ 9.2/MMBtu. ..	55
Figure 2.20: Cost breakdown of the GDHC projects of undiscovered hydrothermal resources. ....	56
Figure 2.21: Supply curve of the undiscovered hydrothermal resources, in comparison with the current cost of heating by natural gas, which is \$ 9.2/MMBtu.....	57
Figure 2.22: Supply curve of the near hydrothermal EGS, truncated at \$ 100/MMBtu, in comparison with the current cost of heating by natural gas, which is \$ 9.2/MMBtu. ....	58
Figure 2.23: Supply curve of the U.S. GDHC application with different categories of geothermal resources. ....	59

Figure 2.24: Supply curve of the U.S. GDHC application. .... 60

Figure 2.25: Partial enlargement of the supply curve, in comparison with the current natural gas heating cost, which is \$ 9.2/MMBtu. .... 60

Figure 2.26: Population served by identified hydrothermal resource based GDHC systems versus their LCOH. Blue dots are identified resources, and the trend line shows the predicted LCOH as a function of the population. .... 62

Figure 2.27: Geothermal gradients of the identified hydrothermal resources versus their calculated LCOH for the GDHC systems. .... 63

Figure 2.28: Sensitivity analysis of the cost model, showing energy demand has the most significant negative effect, while drilling cost has the most significant positive effect. .. 64

Figure 3.1: Geologic formations near Morgantown, WV at depth of 3 to 4 km, the Tuscarora and Oswego Sandstone are of interest for GDHC development.....69

Figure 3.2: Layout of the Evansdale campus buildings (classroom, greenhouse, and library) and pipeline, based on which the Aspen Plus heating model was built..... 73

Figure 3.3: Geothermal temperature map of West Virginia at 4.5 km, black dots show the locations of oil and gas wells from which SMU updated their temperature profiles. .... 78

Figure 3.4: Monthly heating and cooling demand of the Evansdale Campus, WVU..... 79

Figure 3. 5: Return temperature versus mass flow rate at selected supply temperatures to provide campus peak heating demand, dashed line indicates the minimum requirement for the return temperature. .... 80

Figure 3.6: Minimum mass flow rate versus supply temperature to supply campus heating demand. Dashed lines indicate one production and two production wells' maximum flow rate. Red dots indicate the selected pairs of temperature and flow rate for cost estimation. .... 81

Figure 3.7: LCOH for the WVU GDHC project with selected temperature and flow rate. .... 85

Figure 3. 8: Geothermal gradient map of WV, with a warmer color indicating a higher geothermal gradient. .... 86

Figure 3.9: Population density map of WV, with a warmer color indicating a higher population density..... 86

Figure 3.10: Census tracts map of WV, coupled with their estimated LCOH, with a warmer color representing a lower LCOH. Lowest LCOH is found at Morgantown, WV. .... 89

Figure 3.11: Plot showing the variation of LCOH function with population density and geothermal gradient. .... 90

## List of Tables

Table 2.1: Summary of geothermal power potential and levelized cost of electricity from previous supply analysis studies. ....	15
Table 2.2: Residential buildings heating/cooling consumptions (MMBtu/household) by U.S. climate regions in 2009.....	30
Table 2.3: Commercial buildings heating/cooling consumption (trillion Btu) of the mountain and the pacific region, in western U.S., 2003. ....	30
Table 2.4: Cost constants for pipeline capital cost calculation. ....	34
Table 2.5: Streams table of the building heating unit. ....	36
Table 2. 6: Streams table of the absorption chiller system. ....	39
Table 2.7: Stimulation cost breakdown for a 2,500-meter well based on practices from the Marcellus shale industry. ....	44
Table 2.8: Probabilistic metrics for risk analysis in the cost model, data follows a triangle distribution, in the format of (minimum value, most likely value, maximum value).....	45
Table 2.9: Favorability factor of different geothermal regions.....	48
Table 2.10: Cost summary for the simulated GDHC system at Weiser, ID. ....	52
Table 2.11: Cost summary for the simulated GDHC system in California with an undiscovered hydrothermal resource. ....	56
Table 2.12: Estimated thermal potential and the corresponding lowest LCOH from the western U.S. geothermal resources. ....	65
Table 3.1: Comparison of the geologic conditions between Gross Schoenebeck and Morgantown, WV, data from Hurter, et al. (Hurter, et al., 2002) and Castle and Byrnes (Castle and Byrnes, 2005).....	70
Table 3.2: Investigated cases of geothermal flow and temperature for WVU case study.	82
Table 3.3: Surface operation and maintenance cost estimation for case 2, in \$/per year, except for total direct cost, which is in \$. ....	83
Table 3.4: Cost summary of the proposed GDHC system on WVU campus, based on five selected temperature and flow rate cases. ....	83
Table 3.5: LCOH (\$/MMBtu) for the WVU campus GDHC system, in different geothermal water characteristics (case 1, 2, 3, 4, and 5) and different economic scenarios (case I, II, and III) .....	84

Table 3.6: Least square fitting results of LCOH function constants a, b, and n for different geothermal gradients ( $G$ ). ..... 87

Table 3.7: Potential places for GDHC systems development in WV, whose LCOH is less than \$ 30/MMBtu..... 88

# Chapter 1

## The Geothermal Basics

---

*“It is a well-known fact that the interior portions of the earth are very hot, the temperature rising, as observations show, with the approach to the center at the rate of approximately 1 °C for every hundred feet of depth. The difficulties of sinking shafts and placing boilers at depths of twelve thousand feet, corresponding to an increase in temperature of about 120 °C are not insuperable, and we could certainly avail ourselves in this way of the internal heat of the globe. In fact, it would not be necessary to go to any depth at all in order to derive energy from the stored terrestrial heat. The superficial layers of the earth ... are at a temperature sufficiently high to evaporate some extremely volatile substances, which we might use in our boilers instead of water.”*

--- Nikola Tesla

### 1.1 Earth as a Heat Engine

As the quote stated, people have been thinking of utilizing geothermal energy for a long time. In fact, hot springs have been used by mankind from time immemorial. However, the commercialization of geothermal energy did not start until the first success of the geothermal power generation in Italy in 1904. Since then, with growing concerns of fossil fuels depletion and environment deterioration, geothermal energy has experienced dramatic increase in attention.

During the millions of years of the Earth’s formation, the earth developed a solid inner core with a radius of 1,221-kilometers, and a liquid outer core of 2,200-kilometers, approximately. The temperature at the edge of the liquid outer core is about 4,000K. About 40% of the geothermal energy is from such remnant heat from the Earth’s core (Glassley, 2010). The other 60% of the heat is from the radioactive decay of the long-

lived isotopes of uranium ( $U^{238}$ ,  $U^{235}$ ), thorium ( $Th^{232}$ ) and potassium ( $K^{40}$ ). Heat transfer in the earth, dominated by conduction and convection, results in a heterogeneous terrestrial heat flow, ranging from  $30 \text{ mW/m}^2$  to more than  $150 \text{ mW/m}^2$ . Figure 1.1 shows the heat flow map of the continental United States by South Methodist University (SMU) Geothermal Lab (Blackwell, et al., 2011). As seen from Figure 1.1, the western region has a higher geothermal heat flow than the east region on average.

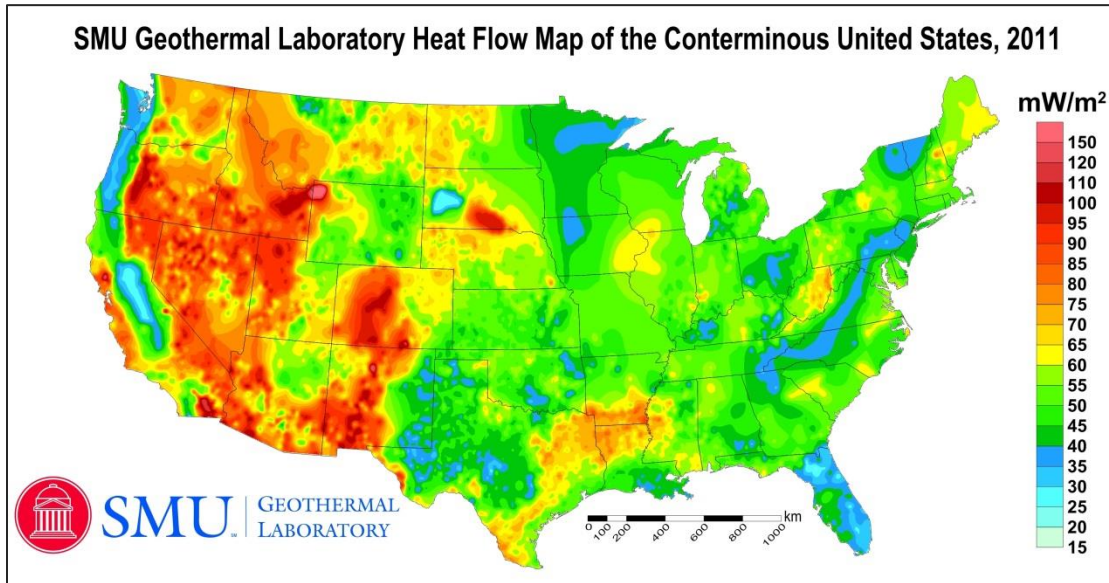


Figure 1.1: Heat flow map of the conterminous United States by SMU Geothermal Laboratory (Blackwell, et al., 2011).

## 1.2 Using Geothermal Energy for Heat and Power

Man has a long history of direct use of geothermal energy, back from when people began to use hot springs for baths, to modern geothermal utilizations, such as space heating or aquaculture farming. The classic Lindal diagram (Gudmundsson, et al., 1985) shown in Figure 1.2 provides a good overview of the geothermal utilizations based on different temperature ranges. Conventional power generation technics generally require geothermal temperatures greater than  $150 \text{ }^\circ\text{C}$ . For a lower temperature range ( $110$  to  $150 \text{ }^\circ\text{C}$ ), a binary cycle power generation is often used, which uses a secondary low boiling temperature fluid instead of water, to be vaporized and sent through a turbine. Geothermal district heating and cooling requires even lower temperatures. Given the

ubiquity of the temperature range (20 to 100 °C) for other low temperature cascading utilizations, direct use has the potential to be applied in most regions on the earth as long as there is a sufficient water supply and a large enough energy consumption market.

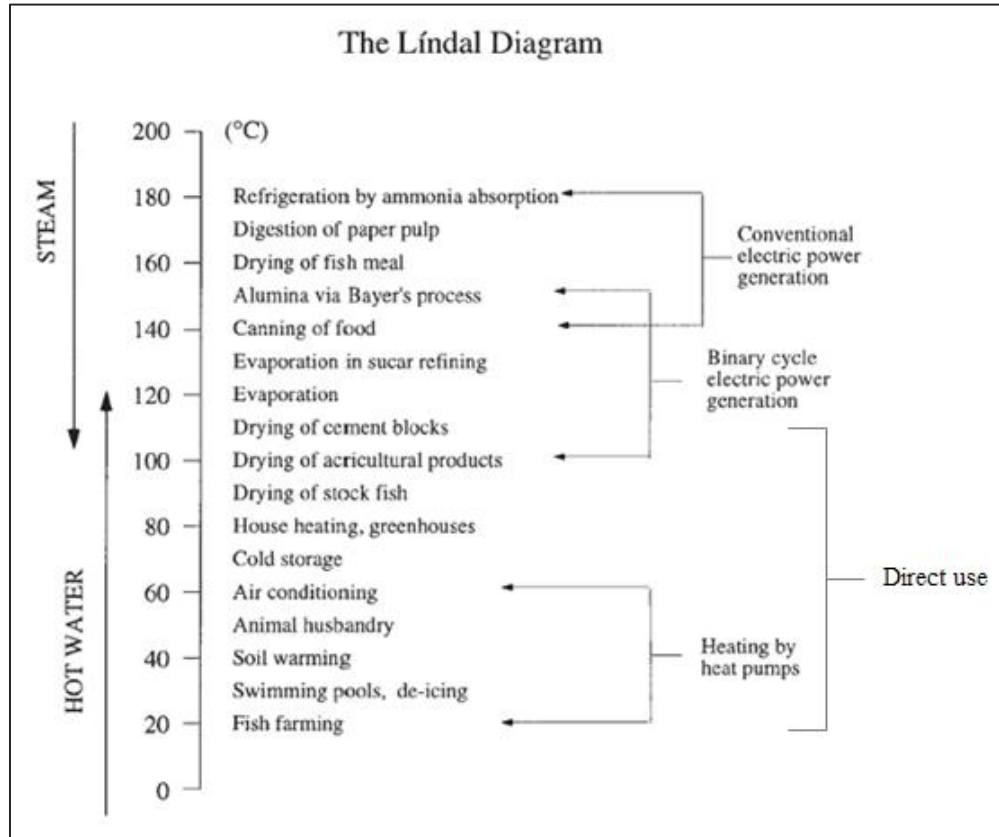


Figure 1.2: The Lindal diagram shows different geothermal utilizations by temperature ranges (Gudmundsson, et al., 1985).

Figure 1.3 shows a basic geothermal district heating and cooling (GDHC) utilization which consists of geothermal injection and production wells for hot water production, a surface energy distribution network for hot water distribution, and a surface energy conversion system for heating and cooling production. Because of the large amount of energy production and the huge capital and maintenance costs of a geothermal heating and cooling system, it would not be energetically nor economically efficient for individual users. A GDHC system should be carefully coupled with local geothermal resource availability and local energy demand to let them match one another, to ensure sufficient energy production and profits from selling energy. The monthly heating and



cooling demand should be carefully estimated, so that geothermal energy production can be controlled, and to prevent fast reservoir cooling. Return water from a GDHC system can further be used for cascading utilizations such as snow melting or fish farming whose temperature requirements are lower.

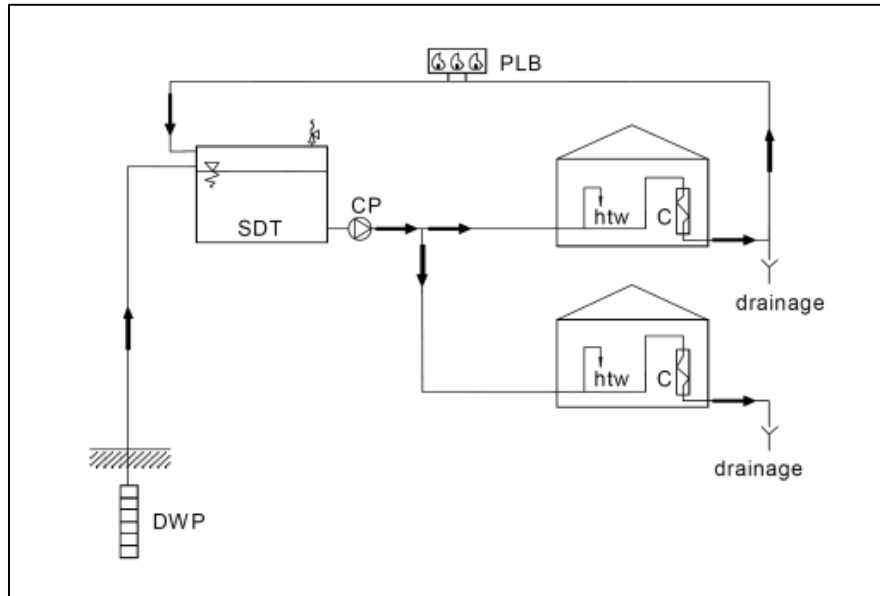


Figure 1.3: Schematic layout of a geothermal district heating and cooling system. DWP is deep well pump, SDT is storage and degassing tank, CP is circulation pump, PLB is peak load boiler, htw is hot water, and C is convention heating (Marcel, 2007).

The first geothermal power generation device was set up in Italy in 1904. After a century of development, the world installed geothermal power generation capacity has exceeded 10,000 MW<sub>e</sub> in at least twenty-four countries (Chamorro, et al., 2012). Figure 1.4 shows a two-well enhanced geothermal power generation system in hot rocks in a low permeability crystalline basement formation. Similar to geothermal district heating and cooling, wells are drilled to desired depths to access the rocks which are hot enough. With respect to different production temperatures, different power generation technics will be applied. The dry steam power plant uses high quality vapor-dominated hot steam to go directly through the turbine, which requires a high-temperature geothermal reservoir. For a median temperature reservoir with a liquid-dominated production fluid, the flash steam power plant is used. A binary power plant is used when the production

temperature is less than 150 °C. In case there is an aquifer layer underground and sufficient rock permeability, the heated geothermal water can be directly pumped to the surface, with return water from the geothermal utilization system re-injected back to the reservoir. Otherwise, artificial permeability improvement technologies should be used. Massive water fracturing is one of the most commonly used technics, which pumps millions of gallons of water into the reservoir to stimulate the rock through hydrofracturing or hydro-shearing, and forms pathways that allow water going through the reservoir to gain heat.

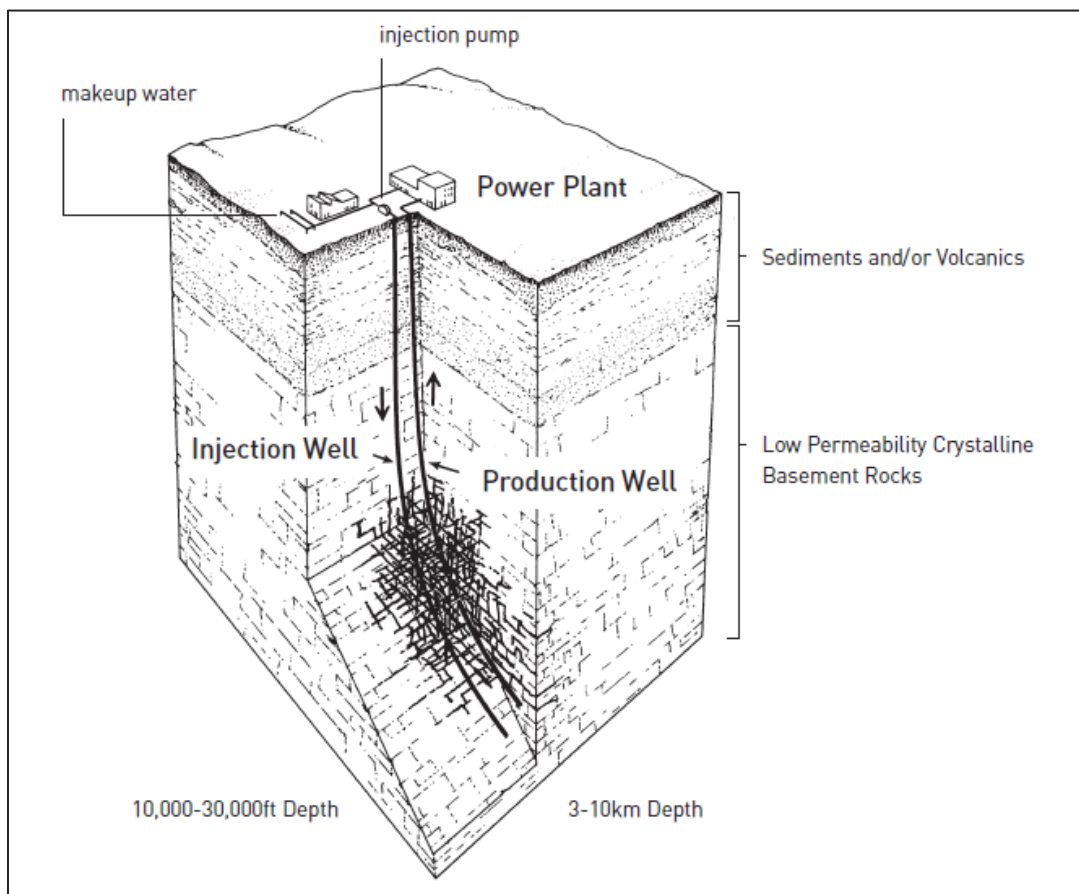


Figure 1.4: Schematic of a two-well enhanced geothermal power generation system in hot rocks in a low permeability crystalline basement formation (Tester, et al., 2006).

### 1.3 Background and Motivation

The 20th century witnessed some of the greatest technological advancements that affect every aspect of people's daily life. Since then, fossil fuels such as coal, oil and natural gas provide people a better living condition with electricity for heating and cooling, fast methods of transportations, and various industrial products. The improved living quality results in vast increases in energy per capita use; besides, the world population has expanded more than three times in the last fifty years, as shown in Figure 1.5. As a result, the consumption of fossil fuels has increased significantly, and the depletion problem rises. Asif predicted that the number of years to the exhaustion of coal for India, China, Russia and U.S. are 315, 83, 1034 and 305 years, respectively (Asif and Muneer, 2007).

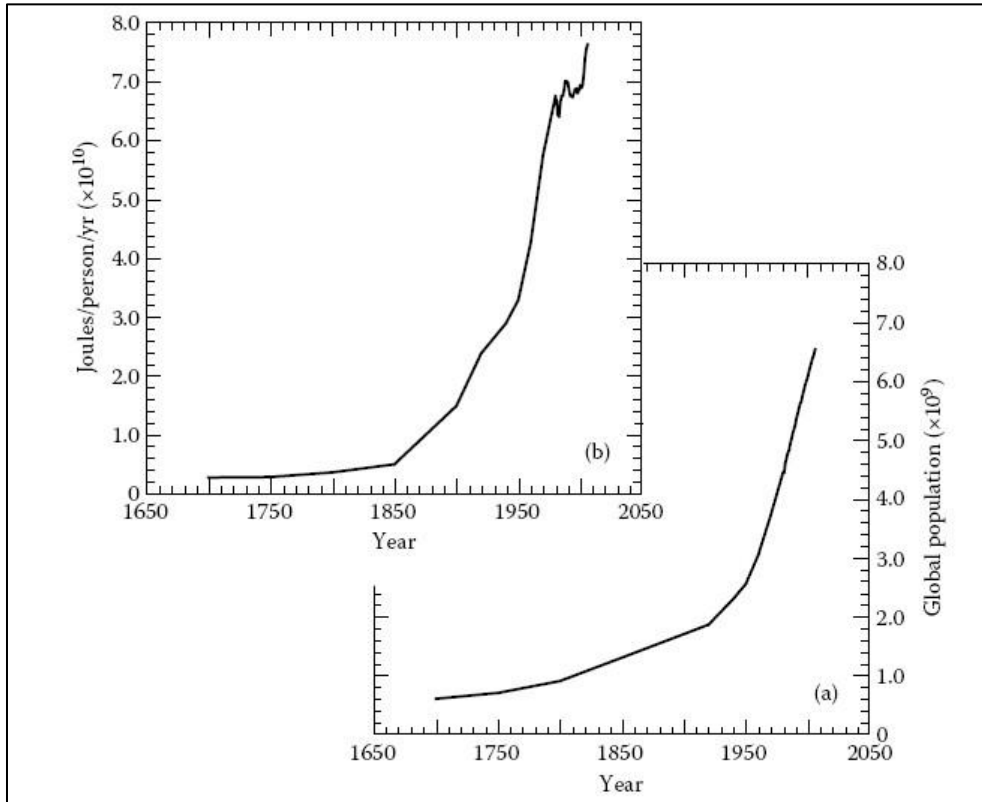


Figure 1.5: World average energy consumption per person ( $\times 10^9$  J/pp/yr) and population growth since 1970, data from (Glassley, 2010).

Using geothermal energy can efficiently reduce the fossil fuels consumption on the low temperature end uses like space heating. As of 2010, the U.S. installed capacity of

geothermal direct use reached 12,611 MW<sub>th</sub>, which produced 56,552 TJ of thermal energy in 2010 (Lund, 2010). Annual energy savings amounted to 27 million barrels of equivalent oil, and preventing 3.5 million tonnes of carbon and 12.8 million tonnes of CO<sub>2</sub> being released to the atmosphere, based on the data from Lawrence Livermore Laboratory (Kasameyer, 1997).

Another issue of intensively burning fossil fuels is its harm to the environment. The burning residue causes air pollution and vast greenhouse gas emission resulting in the greenhouse effect, as evidenced by elevated global temperature, polar ice melting and sea level increase (Lashof and Ahuja, 1990). Figure 1.6 shows the CO<sub>2</sub> emission from fossil fuels (coal, oil and natural gas), corresponding to the increasing global mean temperature since 1980 to 2010.

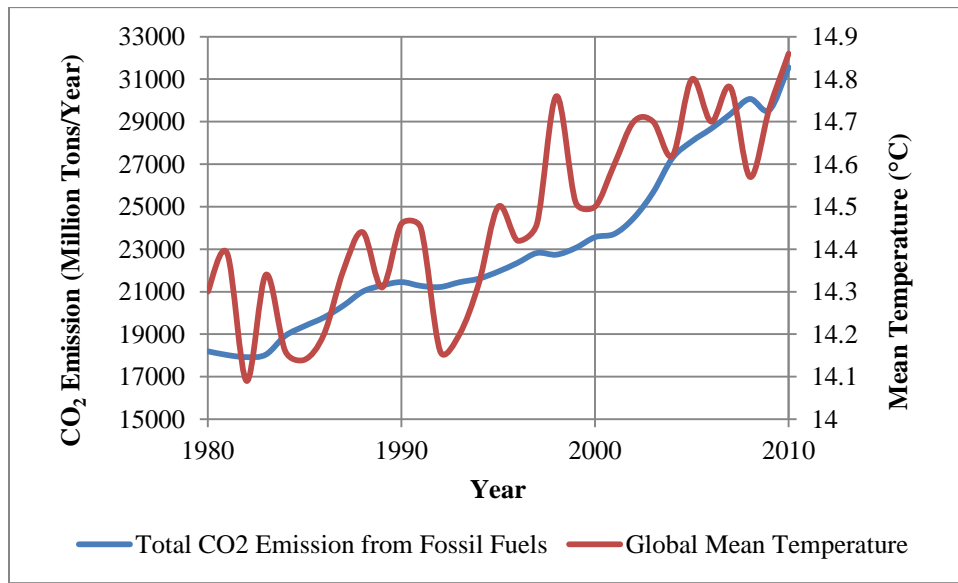


Figure 1.6: CO<sub>2</sub> emission from fossil fuels, data from (EIA, 2011) and global mean surface temperature, data from (NASA, 2012)

## 1.4 World-wide Geothermal Development

Geothermal direct use has been growing rapidly during the last 15 years. Figure 1.7 shows the number of installed country and the total installed capacity of geothermal direct use around the world. There are 78 countries reported having geothermal direct use

installed by the end of 2009, while the number for 1995 is only 28. The worldwide installed capacity in 2009 and 1995 is 50,583 MW<sub>th</sub> and 1,000 MW<sub>th</sub>, respectively. The five countries with the largest installed capacity are the United States, China, Sweden, Norway, and Germany. Among the overall installed capacity in 2010, the geothermal heat pump accounts for 69.7%, followed by the geothermal space and water heating, which is 23.9%, and the geothermal greenhouse heating, which is 3.1% (Lund, et al., 2010).

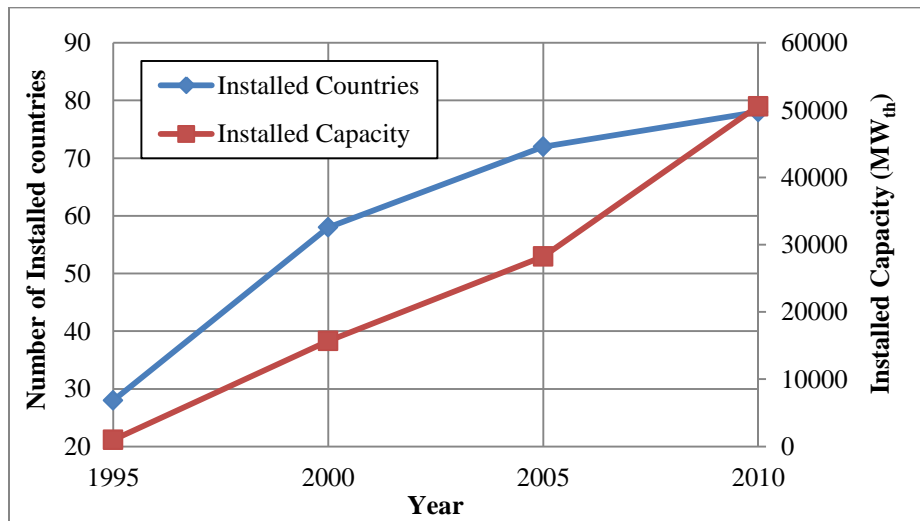


Figure 1.7: Number of installed countries and installed capacity of geothermal direct use.

As of 2012, there are 24 countries reported having geothermal power generation, with a total installed capacity about 10,898 MW<sub>e</sub>, corresponding to 67,246 GWh of electricity each year. The installed capacity doubled in the last three decades, and is expected to reach 70,000 MW<sub>e</sub> worldwide by 2050 (Chamorro, et al., 2012), as shown in Figure 1.8. The five countries with the largest installed capacity are the United States, Philippines, Indonesia, Mexico and Italy. Currently geothermal power generation projects are mainly served by hydrothermal resources, and the flash steam power plant dominates the power generation technics.

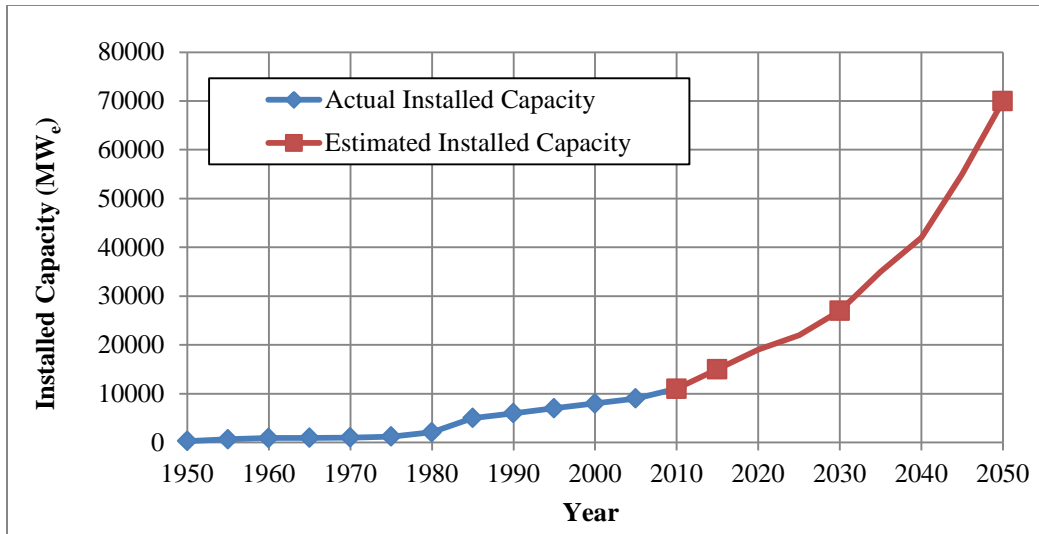


Figure 1.8: Installed capacity of the worldwide geothermal power generation since 1950. It is expected to reach 70,000 MW<sub>e</sub> in 2050.

## 1.5 Objective and Approach

This project focuses on the evaluation of the opportunities to develop the GDHC systems in the United States from the view of technical and economic feasibility. With the help of the GDHC systems, huge amounts of fossil fuels consumption and greenhouse gas emissions can be reduced, which will help the United States energy industry restructure to a more renewable and sustainable oriented supply system, and to protect the national energy security.

To accomplish this, In Chapter 2 the hydrothermal geothermal resources and near hydrothermal EGS in the western U.S. were identified, and their thermal potential estimated. Then a techno-economic model to calculate the levelized cost of heat (LCOH) of the GDHC system was developed. By estimating the LCOH for each of the identified resource, a supply curve of the GDHC application was finally developed, which is able to answer the questions such as how much geothermal energy can be potentially used for the GDHC systems in the United States, and where to develop such systems in order to get the minimum LCOH. In Chapter 3 a West Virginia University (WVU) case study on GDHC application based on the deep EGS resource was conducted to evaluate potential economic advantages in comparison with the current steam system. A series of LCOH

equations which are as functions of population density at different geothermal gradients were then derived. Finally, the LCOH was calculated for every census tract in West Virginia to develop the GDHC system. Those census tracts with the lowest LCOH were found and mapped by ArcGIS. Chapter 4 briefly provides conclusions and recommends future works for the development and research of the GDHC application.

# Chapter 2

## Supply Analysis of Geothermal District Heating and Cooling Systems

---

### 2.1 Introduction

Supply analysis reveals the relation between a given good's price and its quantity in modern market. The supply curve is the most straightforward way to illustrate the supply analysis results. A typical supply curve usually has a positive slope, which means that at a low price, only the most efficient producers can make a profit, with limited product amount; at a high price, even the high cost producer can also make a profit, and hence large amount of products available.

Supply analysis has been accepted as a powerful tool in both traditional and renewable energy research for estimation of energy reserves, as well as for the cost of energy, e.g. Analysis on the oil market by Blair (Blair, 1978) and Kilian (Kilian, 2006), coal market by Gordon (Gordon, 1975), and solar energy market by Cook, et al. (Cook, et al., 2010). Supply analysis has also been used for geothermal energy research since the 1990s. There are two main applications of geothermal energy, which is power generation and direct use, however, all the supply analysis have only been concentrating on the geothermal power generation, e.g. (Petty, et al., 1992 and 2007) and (Augustine, et al., 2010). In the light of the foregoing, the first aspect of this study is the supply analysis of a nationwide geothermal direct use. It answers the following two questions: How much geothermal energy is available for the geothermal district heating and cooling application and how much it costs to deliver the energy in respect of the first question. The other aspect of this study is to map the paired energy potential and energy cost, and it answers another question: where to develop the geothermal district heating and cooling application first with concerns of the energy adequateness and economical costs. Answers to these



questions help to develop a comprehensive national renewable energy strategy and framework with respect to geothermal energy and also address the economic environmental balance issue.

## **2.2 Levelized Cost of Heat**

Traditional supply curve consists of two parts: the x-axis represents the accumulated quantity of the good in the market and the y-axis represents the price at which can make a profit. An example is shown in Figure 2.1, which shows the wind power's supply curve in Zhangbei area, China. In this study the quantity of the good is simply the geothermal energy potential, which is directly related to the geothermal resources' quality and quantity. However, how to define the "price" that can make a profit is more complicated. The basic economics tells that the selling price should at least cover all the investments in the producing process. The geothermal energy is an extremely capital-intensive industry with three capital investment phases: 1) Exploration and drilling of test and production wells; 2) Construction of surface energy conversion facilities; and 3) Discounted future re-drilling and well simulation (Tester, et al., 2006). How to find the optimum price which is related to both the one-time upfront investments and the various day-to-day operation costs over the project's lifetime is very important. The geothermal energy industry is also very location-sensitive. The quality of the resources has a significant impact on the wells drilling and completion costs, which attribute up to 60% of the overall capital investments (Sanyal, 2004). Even for the resources with similar geologic settings, differences in energy demand and energy market structure also impact. Therefore, the levelized cost of heat (LCOH) is used in this study, which is a convenient summary measure of the competitiveness of one energy generating technology. It represents the present value of the overall cost to build and operate an energy generating plant over the project's lifetime.

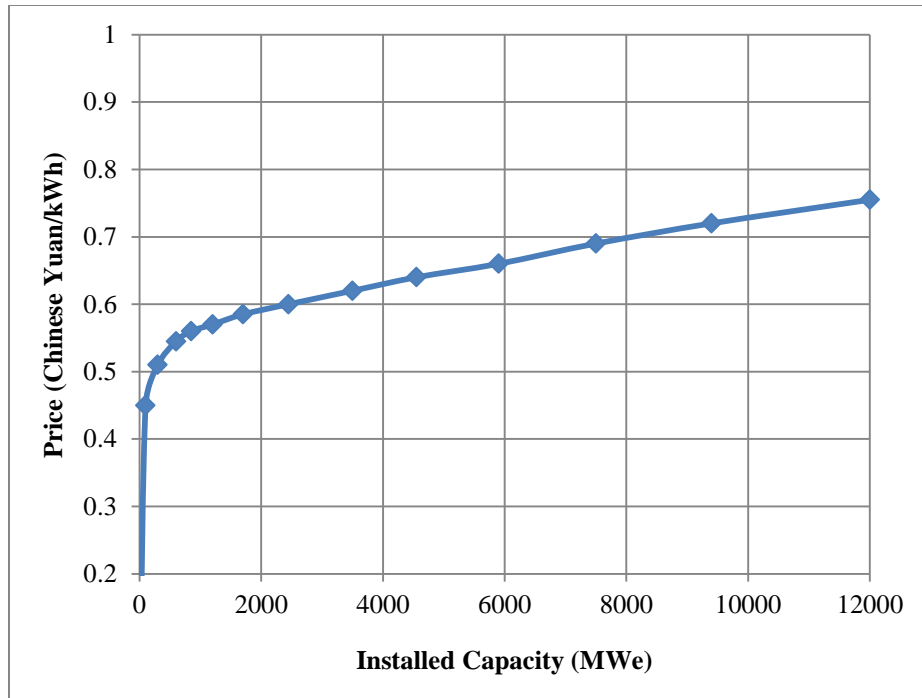


Figure 2.1: Zhangbei area, China available wind power supply, plotted based on data from Kline, et al., 2008.

The LCOH is related to the system’s capital cost, fuel cost, fixed and variable operation and maintenance (O&M) cost, financing cost, and so on. For one kind of energy resource, the specific technology used converting it to power or heat and the regional characteristics such as the resource availability and energy consumption market are also key elements for the LCOH calculation. Figure 2.2 shows the predicted levelized cost of electricity (LCOE) and their cost breakdown for different technologies in the U.S. in 2019. It shows that for electricity generation, geothermal energy is very competitive to other forms of energy resources because of its advantages of the high capacity rate, long project lifetimes with a stable base load output and near zero fuel cost.

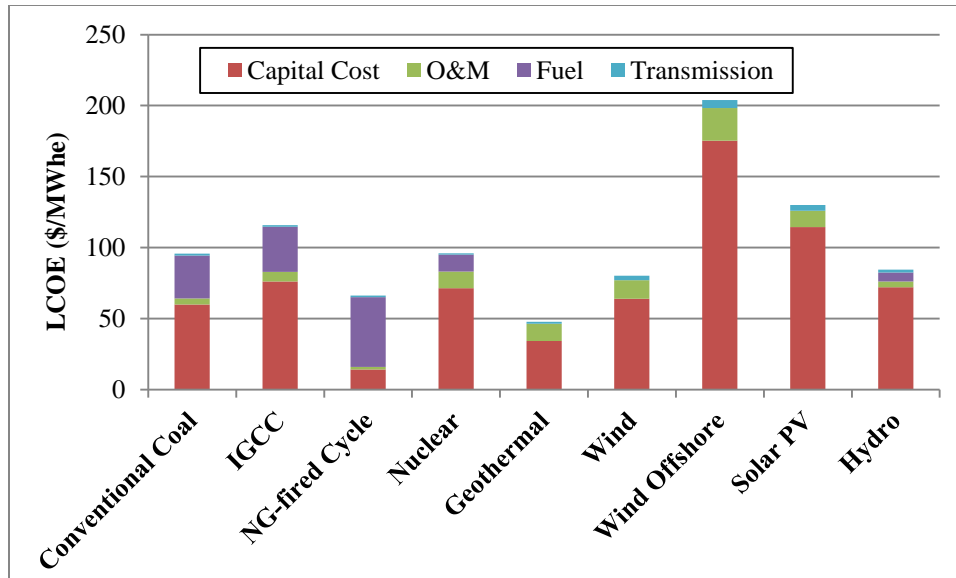


Figure 2.2: Predicted levelized cost of electricity and cost breakdown for new generation resources in 2019, based on data from Annual Energy Outlook, 2014, U.S. EIA.

In this study, an Excel-based calculation model was developed to calculate LCOH of the GDHC system. The model can provide a comprehensive simulation of the proposed system, and help the designers, engineers, operators and utilities with extensive technical and economic information about the GDHC system. The model uses a matrix of about 20 user-defined variables to cover every aspect of the system. In general categories, the variables account for geothermal resource characteristics, wells exploration and production, market configuration, heating/cooling facilities, and economic settings. The output results provide a year-round monitoring of the geothermal production temperature, flow rate, and the overall energy production, as well as economic analysis throughout the project's lifetime.

### 2.3 Previous Studies on Geothermal Supply Analysis

Previous work on supply analysis of geothermal energy have only been focused on geothermal power generation, e.g. Petty, et al., 1992 and 2007, and Augustine, et al., 2010. As time goes on, more geothermal exploration activities, as well as more advanced energy utilization technology have been developed. Thus, the latter report has covered more categories of geothermal resources than the former ones with lower estimated cost.

A summary including the estimated power potential and their corresponding levelized cost of electricity from these reports is listed in Table 2.1.

Table 2.1: Summary of geothermal power potential and levelized cost of electricity from previous supply analysis studies.

Source	Category	Potential, GW <sub>e</sub>	Region	Cost Model	Potential, GW <sub>e</sub> less than \$ 50/MWh
Petty, et al., 1992	Identified hydrothermal	27.4	Western U.S.	IM-GEO	12.5
	Undiscovered hydrothermal	22.6			9.5
Petty and Porro, 2007	Hydrothermal	27.6	Western U.S. & Southwestern U.S. for coproduced	GETEM	<10.0
	EGS	54.7			0
	Co-produced with oil, gas	44.0			21.0
Augustine, et al., 2010	Identified hydrothermal	6.4	Western U.S. & entire lower 48 states for EGS	GETEM & @Risk	3.0
	Undiscovered hydrothermal	30.0			0
	Near-hydro EGS	7.0			2.5
	Deep EGS	15,908.0			0

The first report was published in 1992, in which Petty et al. reviewed 54 hydrothermal resources in the western U.S. The report focused only on eleven western states, which were Arizona, California, Colorado, Hawaii, Idaho, Nevada, New Mexico, Montana, Oregon, Utah, and Washington. The report identified 45 hydrothermal resources in these states where surface manifestation such as hot springs or geysers or if a well had been drilled into the resources were observed and other 9 unities representing the undiscovered

resources in the nine states, except Arizona and Hawaii. The report also cut off the database with a minimum reservoir temperature at 110 °C, because at that time the coolest geothermal water used for power generation was 108 °C, by a power plant in Amedee, California. The characteristics of the geothermal resources were mainly from two sources: the U.S. Geologic Survey (USGS) Circular 790 (Muffler and Guffanti, 1979), and the Bonneville Power Authority study (Bloomquist, 1985). Three parameters were selected to define a geothermal resource, which were the reservoir temperature, reservoir depth, and flow rate. Due to the extreme lack of exploration activities and data, power potential and the corresponding levelized cost were roughly estimated. Extensive personal knowledge and judgments from the investigation team and consulted experts had been used. Cost estimations were made with the use of IM-GEO, a cost model specifically developed for the geothermal power generation by a team led by Dan Entingh (Entingh, et al., 1988) in late 1980s. As a result, the report estimated 27.4 GW<sub>e</sub> from the identified hydrothermal resources, and 22.6 GW<sub>e</sub> from the undiscovered hydrothermal resources. The majority of the identified resources could provide electricity at a cost less than \$ 120/MWh. About half of the undiscovered ones could provide electricity at a cost less than \$ 75/MWh. The cost estimation only examined the economic feasibility of the resource itself. Political, environmental, regulatory and market constrains were not considered in this report.

In 2007, Petty and Porro updated the supply analysis of geothermal power generation with expanded geothermal resources and a new cost model the – Geothermal Electric Technology Evaluation Model (GETEM), developed by Princeton Energy Resources International (Petty and Porro, 2007). GETEM is an Excel-based techno-economic analysis tool for computing costs for a set of user-defined input variables that address four dozen project criteria based on a baseline profile of the input values that reflect current technical capabilities and economic conditions (Entingh, 2006). The updated supply analysis covered not only the hydrothermal resources, but also the enhanced geothermal systems (EGS) and the geothermal fluid coproduced in oil and gas industry. The updated report also expanded its focus to 12 more southeastern states (mainly for coproduced geothermal system), which were Alabama, Arkansas, Georgia, Kansas, Louisiana, Mississippi, North Carolina, Oklahoma, South Carolina, Tennessee, Texas, and Virginia. The study extensively reviewed and investigated the geothermal resources

based on more than 10 reports from the USGS (Priest, et al., 2000), state geologic survey office (Garside, 1994), SMU Geothermal Lab (Blackwell and Richards, 2004), and private firms such as GeothermEx (Klein, et al., 2004), and identified more than 220 hydrothermal and convective EGS sites. By collecting the physical characteristics of the resources, and with the advantage of the GETEM, the updated supply analysis estimated the levelized cost of electricity based on resource types (Hydrothermal or EGS) and utilization technologies (binary or flash). Methods for potential estimation were similar to the previous one, by assuming a series of constant conversion rate to get the power potential from the original heat stored in the reservoir, which is called the Volume Method. As a result, they estimated 27.6 GW<sub>e</sub> from the hydrothermal resources, 44 GW<sub>e</sub> from the coproduced resources, and 54.7 GW<sub>e</sub> from the EGS resources. The levelized cost of electricity was estimated at least \$ 40/MWh, and that of over 90% of the resources were less than \$ 80/MWh. Another improvement comparing to the previous supply analysis was that they introduced the impacts of geothermal industry's R&D and learning ability. The updated report not only gave economic analysis based on year 2007, but also predicted the cost of energy in year 2015 and year 2030 with advanced technology.

In 2010, Augustine, et al. reviewed any possible available reports and papers to estimate the geothermal power potential, in particular, the most recent national geothermal assessment conducted by USGS (Williams, et al., 2008) and the *Future of Geothermal Energy* report from Massachusetts Institute of Technology to characterize the EGS resources (Tester, et al., 2006). The study identified 241 hydrothermal resources, and gave reasonable guesses for the undiscovered resources, and it for the first time covered all the continental U.S. (48 states) for the EGS resources. Methods for power potential and cost of energy estimation remained similar with the former studies. The most significant improvement was that more effort had been focused to predict the cost decrease due to different levels of funding. The study adopted a possible data range for each system's technology performance metric from the updated geothermal technical risk assessment (Young, et al., 2010), and gave probabilistic results of the power potential as well as the LCOE. As a result, Augustine et al. estimated 36.4 GW<sub>e</sub> from the hydrothermal resources, and 15,915 GW<sub>e</sub> from the EGS resources, of which 7 GW<sub>e</sub> is near hydrothermal EGS. Estimation of EGS resources covered much larger area than any

other study, with 48 states from underground 3 km to 10 km, while Petty and Porro, 2007 only covered eleven western states from 3 km to 6 km. The levelized cost of electricity was estimated at least \$ 30/MWh, and that of the most of the undiscovered hydrothermal resources were less than \$ 100/MWh. Developments for the most of the EGS resources were predicted to be not economically feasible.

Besides the above mentioned cost models IM-GEO, and GETEM (continuing being updated by National Renewable Energy Laboratory, latest version is August 2012 Beta), there have been several other models developed by national laboratories or universities for the same purpose, such as the System Advisor Model (Gilman and Bobos, 2012), and the Cost of Renewable Energy Spreadsheet Tool (Gifford and Grace, 2011) from U.S. National Renewable Energy Laboratory, the HEATMAP<sup>®</sup> from the Washington State University Energy Program and the software for direct use applications from Geo-Heat Center, Oregon Institute of Technology. However, none of these cost models consider reservoir characteristics impacts on the energy cost except GETEM, which was specifically designed for geothermal power generation. Therefore, a new cost model comprehensively considering the reservoir characteristics and the surface utilities for geothermal direct use is in need, and is developed in the present study.

No study is being conducted on the supply analysis of other geothermal applications currently. There are case studies based on specific GDHC or GDH systems, e.g. He and Anderson's case study on West Virginia University (He and Anderson, 2012), Erdogmus, et al. and Yildirim, et al.'s studies on Izmir Institute of Technology (Erdogmus, et al., 2006), (Yildirim, et al., 2006), and Lei and Valdimarsson's case study on the district heating system in Tianjing area, China (Lei and Valdimarsson, 2009), but lack of a national supply characterization of such application. This study focuses on the approach to characterize the supply curve of geothermal district heating and cooling systems in the United States. In this project, geothermal resources were categorized; resources characteristics were identified; resources' thermal potential and corresponding cost of energy were estimated; finally, the supply curve was generated. Though focusing on different types of utilization, the supply analysis of geothermal power generation gives reasonable assumptions on the market settings and provides inspiring methods for

reservoir characterization. Some of them were adopted in this study for the supply analysis of geothermal district heating and cooling. The innovation of this study is to expand the supply analysis into the GDHC application, and for the first time to include energy market in the geothermal research.

## 2.4 Reservoir Characterization and Potential Estimation

Figure 2.3 shows the flow diagram to develop the supply curve in this study. The primary steps include the resources characterization and cost estimation. The following discusses how geothermal energy is categorized, how the reservoir is characterized and how the potential is estimated for each category of the resources.

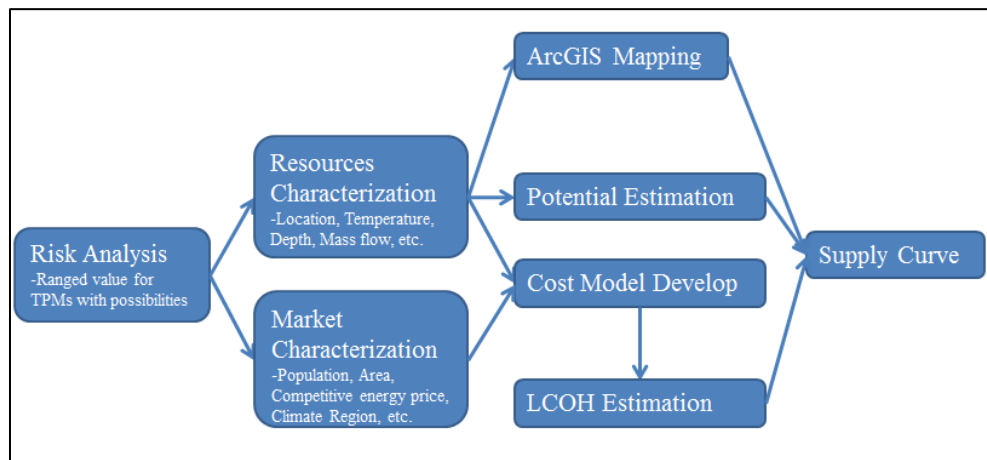


Figure 2.3: Flow diagram to develop the supply curve of GDHC application.

### 2.4.1 Geothermal Resources Categorization

For a long time, the geothermal resources were classified by their reservoir temperatures into low, intermediate, and high enthalpy resources (Lee, 1996). However, it cannot illustrate the significant reservoir differences regarding to the permeability and porosity in the geothermal research. In this study, the geothermal resources were categorized by the reservoir technology into two kinds, which are the conventional hydrothermal resources and the enhanced geothermal systems (EGS). Hydrothermal resources have the common ingredients of water (hydro) and heat (thermal). The ground water trapped in



porous rocks or the running water along the fractured rock surfaces and faults is heated by the hot magma near the earth surface. Some of the hydrothermal resources can be observed directly, like the hot springs and the geysers. Others can be accessible by drilling wells into the reservoir. Hydrothermal resources were further classified into the identified ones and the undiscovered ones. EGS resources are also known as the hot dry rock (HDR) resources, which indicate that although hot, these resources lack sufficient permeability for energy extraction. Reservoir stimulation technologies are usually used to enhance the reservoir permeability for practical applications. EGS resources were further classified into the near hydrothermal EGS resources and the deep EGS resources in this study. Due to lack of available data for deep EGS resources, the following only discusses the first three categories of the geothermal resources.

#### 2.4.2 Identified Hydrothermal Resources

Since GDHC shares the same reservoirs with geothermal power generation, the latest national assessment of geothermal power potential USGS Fact Sheet 2008–3082 (Williams, et al., 2008) was consulted. It identified 241 moderate (90 to 150 °C) and high temperature (greater than 150 °C) hydrothermal resources located in thirteen western states: Arizona, California, Colorado, Idaho, Montana, New Mexico, Nevada, Oregon, Utah, Washington, Wyoming, Alaska, and Hawaii. This study also identified twelve more low temperature (less than 90 °C) hydrothermal resources because of the versatile design temperatures of various heating/cooling systems by consulting other reports such as USGS Circular 726 (White and Williams, 1975), USGS Circular 790 (Muffler and Guffanti, 1979), and USGS Circular 892 (Reed, 1982). The reservoir temperature and depth data used in the study were from in situ measurements in exploration and production wells when available, or from calculation of the chemical geothermometers. Chemical geothermometers are based on the concept that chemical or isotopic constituents in the water are established at higher temperatures, but will persist when the water cools as it flows to the surface (Karingithi, 2009). Equation 2.1 shows the equation of K-Mg chemical geothermometer used by the USGS assessment (Giggenbach, et al., 1988), where  $T_R$  is the reservoir temperature, and  $c_K$  and  $c_{Mg}$  are the molar concentration

of the potassium and magnesium in the production water. The reservoirs' temperatures and depths data were retrieved from the USGS Energy Data Finder.

$$T_R = \frac{4410}{14.0 + \log\left(\frac{c_K^2}{c_{Mg}}\right)} - 273.15 \quad (2.1)$$

Estimation of intensive properties such as temperature is usually easier than that of extensive properties such as flow rate. Without actual wells drilled, it is not possible to give an estimate. The method to determine each reservoir's mass flow rate in this study was derived from the Volume Method, as shown in Equation 2.2. The Volume Method was used in the past USGS assessments for geothermal power potential (Nathenson, 1975), (Muffler and Cataldi, 1978), (Muffler, 1979), (Lovekin, 2004), and (Williams, 2004). Equation 2.2 illustrates the process by which thermal energy stored underground is converted to electricity production:

$$\dot{W}_e = \frac{\eta_e}{t} \times [R_g (\rho C V)_{rock} (T_R - T_0) - m_{WH} T_0 (s_{WH} - s_0)] \quad (2.2)$$

In this equation,  $t$  is the lifetime of the project (typically assumed 30 years); for each reservoir,  $\rho C$  is the volumetric specific heat of the reservoir rock;  $V$  is the volume of the reservoir;  $T_R$  is the reservoir temperature;  $T_0$  and  $s_0$  is the temperature and the entropy per unit mass of water at reference state;  $m_{WH}$  is the overall mass of production water,  $s_{WH}$  is the entropy per unit mass of water at the well head;  $R_g$  represents the fraction of heat recovered from the rock; and  $\eta_e$  represents the overall utilization efficiency from exergy to electricity. It is assumed that for an identified hydrothermal reservoir,  $m_{WH}$  obtained at the well head during the lifetime depends only on the volume of the reservoir  $V$ . With larger reservoir volume, the fractures in the reservoir are larger, allowing more flow rate of water going through the reservoir. Thus, for any reservoir with temperature  $T_R$  given, the power potential  $\dot{W}_e$  depends only on the mass of water  $m_{WH}$ . The Volume Method illustrates the theoretical basis of how the potential is calculated in the cost model GETEM. Equation 2.3 was used in this study to find the mass flow rate by GETEM, with

power potential and reservoir temperature data retrieved from the USGS Energy Data Finder for each resource:

$$\dot{m}_R = \frac{m_{WH}}{t} = \frac{GETEM(\dot{W}_e, T_R)}{t} \quad (2.3)$$

The thermal potential  $\dot{Q}$  was calculated by Equation 2.4 for each resource by assuming the return temperature  $T_r$  at 40 °C.

$$\dot{Q} = \dot{m}_R \times C_{water} \times (T_R - T_r) \quad (2.4)$$

### 2.4.3 Undiscovered Hydrothermal Resources

Due to uncertainties of locations of the undiscovered hydrothermal resources, there is no way to estimate them one by one. This study used an analogous method as in the geothermal power generation supply analysis, as shown in Equation 2.5. The preferred geologic conditions or manifestations of undiscovered hydrothermal resources are the same with those of the identified hydrothermal resources. For example, from the studies of the known geothermal systems, young felsic magmatism has a strong spatial correlation with geothermal energy (Smith and Shaw, 1979); higher underground heat flow is usually relevant to a larger possibility of geothermal reservoir occurrence; all the quaternary faults have a strong statistical significance for the correlation within 4 km distance of geothermal occurrences (Williams and DeAngelo, 2008). Therefore, it is safe to use the spatial correlations of such preferred geologic factors that facilitate the formation of geothermal resources to estimate undiscovered resources. The favorability factor  $\alpha$ , is the statistical integrated strength result of the preferred factors, representing the possibility of the occurrence of hydrothermal resources. The thermal potential of the undiscovered hydrothermal  $\dot{Q}'$  in one region is  $\alpha$  times of that of the identified hydrothermal resources  $\dot{Q}$  in the same region. Such indicator favorability theory has also been used to estimate undiscovered resources in other industries such as mineral (Pan, 1993) and petroleum industry (Gao, et al., 2000).

$$\dot{Q}' = \alpha \times \dot{Q} \quad (2.5)$$

In the latest USGS geothermal assessment, Williams, et al. investigated 5 evidence layers of heat flow, quaternary magmatism, quaternary faulting, seismicity, and tectonic stress (Williams, et al., 2009) to estimate the favorability factors of undiscovered hydrothermal resources in each state, as shown in Figure 2.4. The favorability factor for each state in this study was calculated to be the area average favorability factor, as shown in Equation 2.6, where  $i$  indicates each of the region with its unique favorability factor in the target state, and  $A$  is the region area.

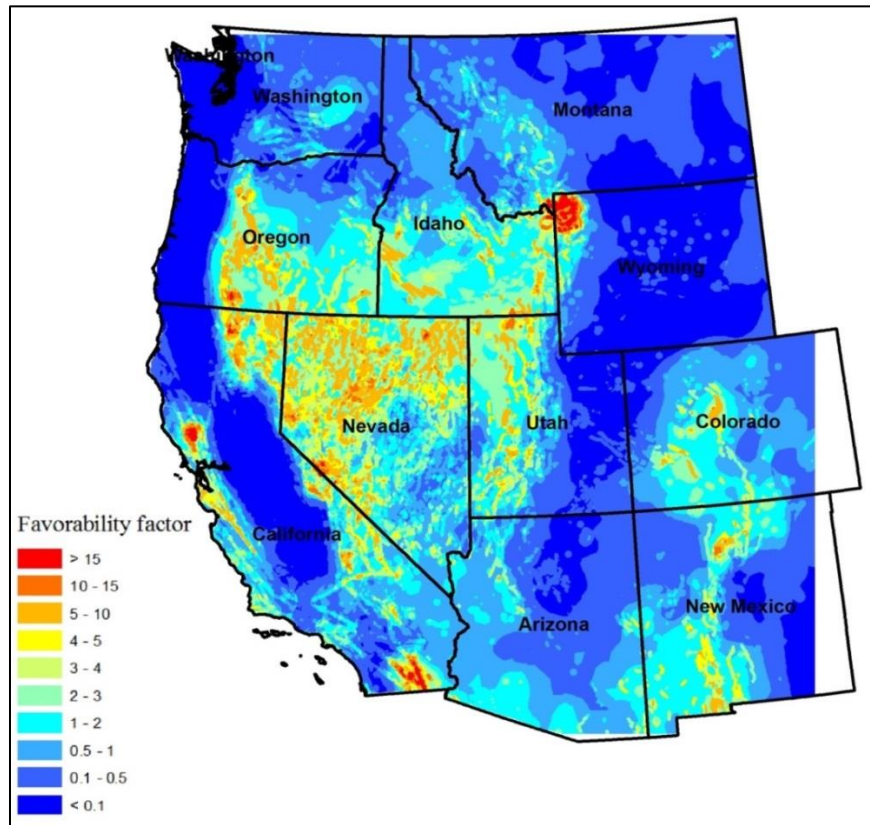


Figure 2.4: The favorability factor map of undiscovered hydrothermal resources in the western U.S. A warmer color indicates a higher probability to find the hydrothermal resources (Williams, et al., 2009).

$$\alpha = \frac{\sum(\alpha_i \times A_i)}{\sum A} \quad (2.6)$$

This study assumed the same reservoirs' characteristics of all the undiscovered resources in the same state. And the reservoirs' characteristics (depth, temperature, and flow rate) were assumed more similar to those of the larger identified resources with larger thermal potential than the smaller ones. The reservoirs' characteristics (depth, temperature, and flow rate) were estimated by calculating the mean-potential-weighted average of each of these parameters from the identified hydrothermal sites in each state, as shown in Equation 2.7 to 2.10.

$$\beta_i = \dot{Q}_i / \sum \dot{Q}_i \quad (2.7)$$

$$d_R' = \sum (d_{Ri} \times \beta_i) \quad (2.8)$$

$$T_R' = \sum (T_{Ri} \times \beta_i) \quad (2.9)$$

$$\dot{m}_R' = \sum (\dot{m}_{Ri} \times \beta_i) \quad (2.10)$$

Where  $d_R', T_R', \dot{m}_R'$  is the depth, temperature, and flow rate of the undiscovered resources,  $\beta_i$  is the potential weighted factor,  $d_{Ri}, T_{Ri}, \dot{m}_{Ri}, \dot{Q}_i$  is the depth, temperature, flow rate, and thermal potential of the identified resources in the same state.

#### 2.4.4 Near Hydrothermal EGS Resources

Reservoir temperature and mass flow rate are the most important factors when determining the economics of a geothermal resource. The near hydrothermal EGS is defined as the geothermal resource around the hydrothermal site but lack sufficient permeability to let water through. Comparing to the deep EGS, the near hydrothermal EGS has a higher reservoir temperature at a shallower depth. So it is one kind of the least expensive EGS resource, and should be exploited first. Recently the U.S. Department of Energy and Ormat Technologies, Inc. announced the first EGS power plant connected to the commercial electricity grid, which is operating based on a near hydrothermal EGS resource, and is producing 1.7 MW<sub>e</sub> of electricity.

There has not been a formal assessment of near hydrothermal EGS resources until now. Estimation of their thermal potential is preliminary and based on assumptions. Based on the definition of the resource, the reservoir temperature of the near hydrothermal EGS is

the same as that of the hydrothermal resource being surrounded. Since thermal potential is only determined by the reservoir temperature and the mass flow rate, as shown in Equation 2.4, with temperatures being the same, the mass flow rate is the only one to distinguish the near hydrothermal EGS from the hydrothermal resources. Thus, it was assumed in this study that thermal potential of each near hydrothermal EGS  $\dot{Q}_{near}$  is the thermal potential difference between the mean and the high-end estimation of its corresponding hydrothermal resources, as shown in Equation 2.11:

$$\dot{Q}_{near} = \dot{Q}(95\text{ percentile}) - \bar{Q} \quad (2.11)$$

As for estimation of the reservoir mass flow rate, Darcy's Law describes the flow rate through a porous medium is related to the permeability, the viscosity, the pressure gradient, and the drainage cross section. Although water viscosity can be determined easily in this case, the remaining parameters are dependents on the specific reservoir and of the hydraulic fracturing process technic. Therefore, estimation of the flow rate of an EGS is very site specific. Exploration drilling and in-situ well logging must be conducted. Without the exploration data, McVeigh assumed the mass flow rate as 54 kg/s based on the current hydraulic fracture technology (McVeigh, et al., 2007). Augustine assumed the flow rate as 30 kg/s and 60 kg/s for the current and improved technology scenario (Augustine, et al., 2010). In this study, for near hydrothermal EGS the mass flow rate was assumed to be 40 kg/s, 60 kg/s, and 80 kg/s. Calculations related to near hydrothermal EGS have considered these three different levels of production rates to provide a comprehensive view of such resources. For calculations based on other flow rates, one can interpret the results by assuming a linear relation in the 40 to 60 kg/s or 60 to 80 kg/s region.

#### 2.4.5 Deep EGS Resources

Conventional hydrothermal resources usually exist at depth 3 km or less. The near hydrothermal EGS can be considered as the extensions of the hydrothermal resources, and also exist at a shallower depth. Deep EGS resources are the geothermal resources deeper than 3 km, with dry and impermeable rocks. Artificial permeability increasing

technologies like hydraulic fracturing are needed to reach the economic production rate. Because of the nature of the EGS resources, their thermal potential is enormous (Mock, et al., 1997). The latest systematic assessment of the U.S. EGS resources is the MIT report (Tester, et al., 2006). It used a series of temperature-at-depth maps developed by the SMU Geothermal Lab, from 3.5 km to 10 km, to estimate the EGS potential with the above mentioned Volume Method. Figure 2.5 shows one of the temperature maps of the continental U.S. at depth 4.5 km. The MIT report estimated  $13,267,370 \times 10^{18}$  Joules of potential from deep EGS, which is approximately 132,673 times of the U.S. annual energy consumption, with extremely high levelized cost. Therefore, another trial to estimate potential of the EGS is not recommended. Instead, this study conducted a techno-economic case study of the EGS based GDHC system at WVU campus. Details are discussed in Chapter 3.

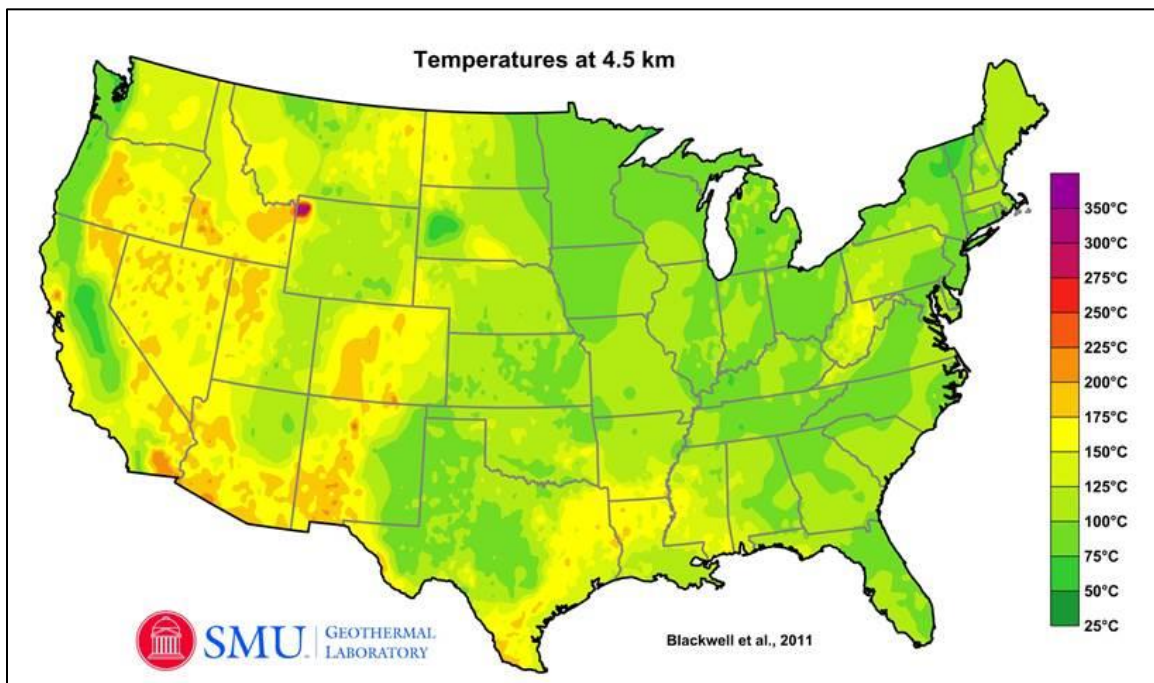


Figure 2.5: Map of underground temperature at 4.5 km of the continental U.S (Tester, et al., 2006).

## 2.5 Energy Market Characterization

The demand and supply is the most fundamental basics of modern market. A careful market research is very essential for the success of any product, including renewable energy. Figure 2.6 shows the sharp decrease of annual U.S. crude oil imports corresponding to the rapid increase in renewable energy consumption. Based on the preliminary research, market demand impact on the economics of a GDHC project is much stronger than that on the economics of a geothermal power generation project. It is because the GDHC system is very location sensitive: geothermal heating and cooling must be consumed at the same location where it is produced, or the severe energy loss during the long hot water distribution will very much corrode the advantage of the low energy cost. However, the geothermal power plant can operate at a remote area, while the electricity is still able to be transferred thousands of miles away efficiently. This is why the previous geothermal power supply analysis is “*not constrained by the potential market*” (Petty, et al., 1992). But in this study, the size of the energy market is a crucial factor. Since the supply analysis is based on a site-by-site thermal potential and cost estimation, the energy market demand was also estimated site-by-site.

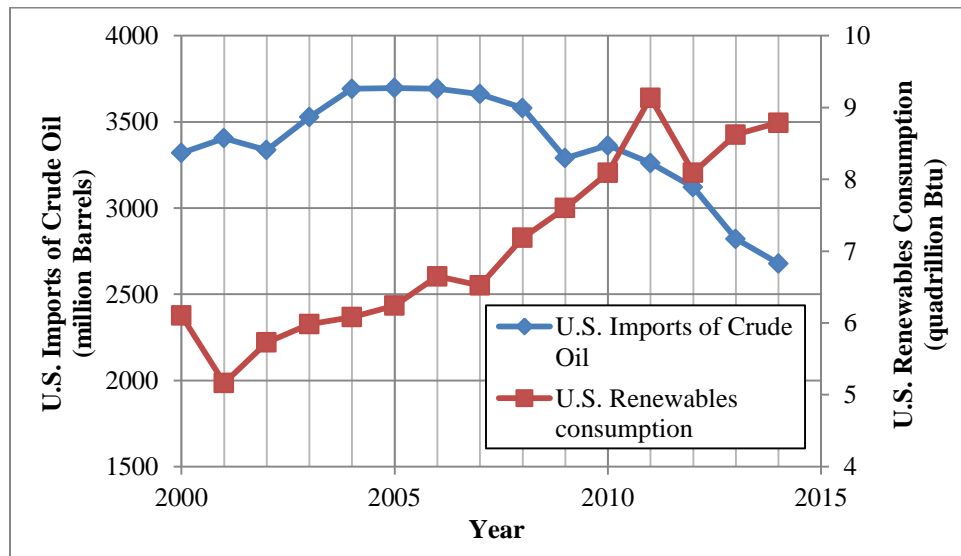


Figure 2.6: Comparison of annual U.S. crude oil imports and renewable energy consumption from 2000 to 2014, based on data from U.S. EIA.



### 2.5.1 Barriers to the GDHC Development

Bloomquist and Lund identified some barriers to the development of geothermal district heating system from a survey based on 271 communities, among which only one community responded with interests (Bloomquist and Lund, 2000). For example, local authorities' unawareness of the geothermal energy benefits and local leaders' lack of the necessary knowledge to develop the system have shown to be detrimental to the expansion of geothermal energy. Thorsteinsson further studied 21 operating geothermal district heating systems and concluded the barriers into three categories: technical feasibility – most of the high quality hydrothermal resources have been developed into large scale power generation systems, while the technology to extract the huge EGS resources is immature; economic feasibility – the low cost of alternative energy forms such as natural gas and oil; social/political feasibility – the public and the leaders have inadequate knowledge of geothermal energy, and the geothermal research is severely underfunded (Thorsteinsson, 2008).

People tend to accept new things gradually. For example, the world's largest geothermal system – Reykjavik geothermal district heating system in Iceland, took nearly a century to develop from serving one house at the beginning to providing 61% of the total population of Iceland with hot water (Gunnlaugsson, 2008). One important assumption in this study was that, unlike the above situation, people would completely adopt geothermal energy as their primary heating and cooling source as soon as the GDHC system is built. No simulations were included to describe people's attitude of unfamiliar with geothermal energy to liking geothermal energy. Studying such expanding process of a renewable energy system is beyond the scope of this project. A good suggestion for future work is to add another system metric to represent the portion of people willing to use geothermal energy in the target area. A good example is explained in Labay and Kinnear's research to explore customers' decision process in the adoption of solar energy (Labay and Kinnear, 1981). But in this study, it was simply assumed that the capacity of a GDHC system should meet the overall heating and cooling demands of the whole population.

## 2.5.2 Energy Demand Estimation

This study aims to cover both the residential and the commercial buildings' heating and cooling demands. Since the energy consumption very much depends on the climate and the day-to-day ambient temperature, this study focuses to find the maximum heating and cooling demand, so that it can be used as the design capacity of the surface energy conversion facilities. Figure 2.7 shows the flow diagram of the energy demand estimation process.

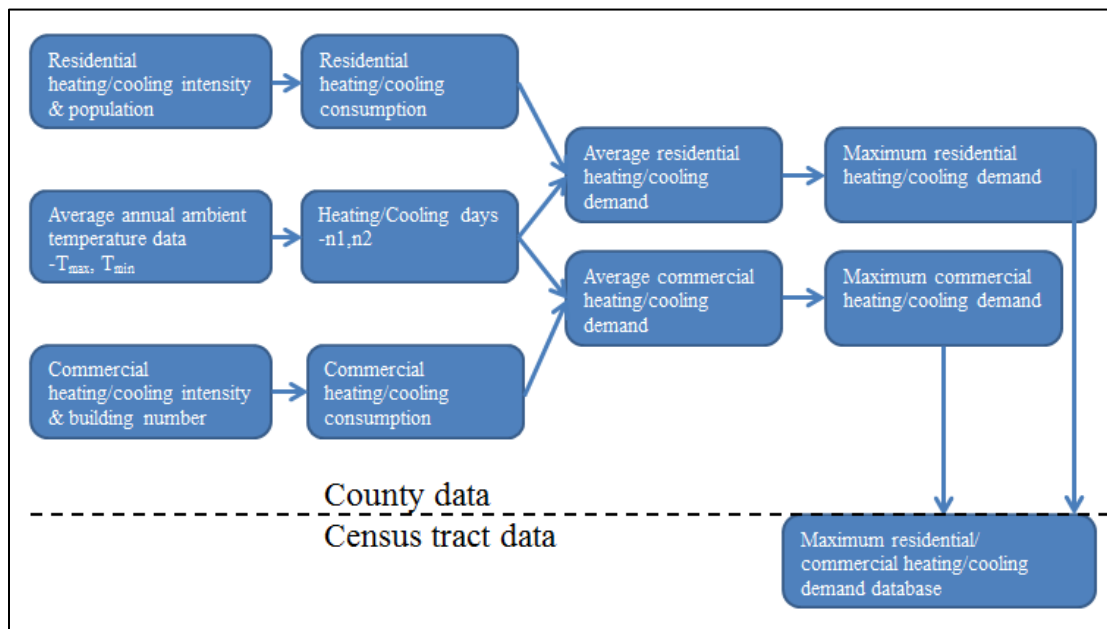


Figure 2.7: Flow diagram to estimate the energy demand of the target location.

This study estimated the overall energy demand with the overall population and the energy consumption intensity per capita for residential section, and with the overall building number and the energy consumption intensity per building for commercial section. The county and census tract based population data was found from the Topologically Integrated Geographic Encoding and Referencing database (TIGER) from U.S. Census Bureau. The commercial building number was found from the latest Commercial Buildings Energy Consumption Survey (CBECS) by U.S. EIA in 2003. The U.S. EIA estimates the consumptions of residential household's end-uses by the climate regions. Their heating and cooling intensities for different regions are shown in Table 2.2.

The CBECS estimates the consumptions of commercial building's end-uses by the census regions. Their heating and cooling intensities are shown in Table 2.3.

Table 2.2: Residential buildings heating/cooling consumptions (MMBtu/household) by U.S. climate regions in 2009.

Climate Region	Space Heating, $\delta_{SH}$	Water Heating, $\delta_{WH}$	Cooling, $\delta_C$
Very Cold/Cold	60.5	18.3	2.0
Mixed-Humid	37.8	16.2	6.5
Mixed-Dry/Hot-Dry	18.2	15.3	8.7
Hot-Humid	11.9	11.7	14.5
Marine	26.4	14.5	1.2

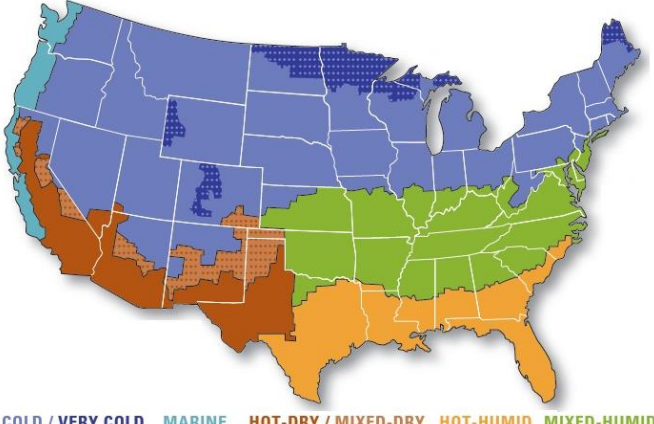
U.S. Climate Region Map	 <p style="font-size: small; color: blue; text-align: center;">COLD / VERY COLD    MARINE    HOT-DRY / MIXED-DRY    HOT-HUMID    MIXED-HUMID</p>
-------------------------	---

Table 2.3: Commercial buildings heating/cooling consumption (trillion Btu) of the mountain and the pacific region, in western U.S., 2003.

Census Region	Space Heating, $\Delta_{SH}$	Water Heating, $\Delta_{WH}$	Cooling, $\Delta_C$
Mountain	167	41	31
Pacific	131	68	55

This study assumed a trigonometric function to curve-fit the year-round ambient temperature. The function of the day-to-day ambient temperature  $T_{ab}$  is shown in Equation 2.12:

$$T_{ab} = (T_{abMax} - T_{abMin}) \times \sin\left(\frac{\pi}{365n}\right) + T_{abMin} \quad (2.12)$$

The maximum and minimum ambient temperatures for each location were found from the National Climatic Data Center database. It was also assumed that days with temperature lower than 18.3 °C accounted into space heating days, while days with temperature greater than 18.3 °C accounted into cooling days. The total heating days  $n_H$  and cooling days  $n_C$  can be calculated by Equation 2.13:

$$\begin{cases} n_H = 365 \times \frac{18.3 - T_{abMin}}{T_{abMax} - T_{abMin}} \\ n_C = 365 - n_H \end{cases} \quad (2.13)$$

Thus, taking the residential part as an example, the peak heating and cooling demands were calculated by Equation 2.14 and 2.15, where  $hh$  is the household number and  $ppl$  is the population. The commercial part was estimated with the similar process.

$$\text{Heating: } \begin{cases} T_{abMax} > 18.3, \dot{H}_{peak} = \left( \frac{\delta_{SH} \times hh}{n_H} + \frac{\delta_{WH} \times hh}{365} \right) \times \frac{ppl_{Census}}{ppl_{County}} \times \frac{\pi/365 \times n_H}{\sin(\pi/365 \times n_H)} \\ T_{abMax} < 18.3, \dot{H}_{peak} = \left( \frac{\delta_{SH} \times hh}{n_H} + \frac{\delta_{WH} \times hh}{365} \right) \times \frac{ppl_{Census}}{ppl_{County}} \times \pi \end{cases} \quad (2.14)$$

$$\text{Cooling: } \begin{cases} T_{abMax} > 18.3, \dot{C}_{peak} = \left( \frac{\delta_C \times hh}{n_C} \right) \times \frac{ppl_{Census}}{ppl_{County}} \times \frac{\pi/365 \times (n_C - n_H)}{\cos(\pi/365 \times n_H) - \cos(\pi/365 \times n_C)} \\ T_{abMax} < 18.3, \dot{C}_{peak} = 0 \end{cases} \quad (2.15)$$

## 2.6 LCOH Model Development

As mentioned in section 2.3, none of the existing cost models can be perfectly implemented into this study considering the GDHC system's feature of energy production and consumption balance. This part of the study discusses how to develop the cost model for GDHC system and calculates the LCOH. Six categories of parameters have been used to characterize the system. They are:

- 1) Resource parameters – Geothermal temperature, geothermal gradient, etc.

- 2) Market parameters – Population density, energy intensive, climate data, etc.
- 3) Capital parameters – Well drilling and exploration, stimulation cost, heating and cooling unit cost, etc.
- 4) O&M parameters – Reservoir O&M, surface facility O&M, make-up wells.
- 5) Financial parameters – Discount rate, lifetime, capacity factor, etc.
- 6) Risk parameters – Possible ranges for the above selected parameters.

With these parameters, the cost model first accesses the reservoir database to get the essential reservoir characteristics, and then calculates target heating/cooling demand; based on local energy demand, the cost model defines the wells' production rate and designs the corresponding surface heating and cooling unit, as well as the distribution system. Finally, it calculates the levelized cost of energy and annual energy production as well as a series of economic parameters such as capital cost, O&M cost, project cash flow details, etc. The following part discusses two modules which constitute the cost model, namely – surface facility design and economics, and well design and economics. They were developed in Excel spreadsheets, with necessary reservoir database and economic factor database. The cost model was designed to function as a standalone or be called in as an Excel-customized macro by other programs.

### 2.6.1 Surface Facility Design and Economics

Surface equipment for a GDHC system mainly consists of a distribution network, a series of heat exchangers for heating, and an absorption chiller system for cooling. This part of the study illustrates the surface equipment layout, the necessary design and their cost evaluation.

The GDHC system aims to provide heating and cooling to a large number of people. The assumption that every person at the target area would accept the geothermal energy at the beginning eliminates concerns about gradual expansion of the distribution network. Since geothermal reservoirs exist in different locations with different population densities, a general living pattern was assumed and imposed on the design of the distribution network. As shown in Figures 2.8a, 2.8c, and 2.8d, it was assumed that houses are spaced geographical-uniformly throughout the whole area. A uniform distance between two

buildings was assumed as  $D_{NN}$ , which decreases with increase in population and number of houses. When the population reaches a point such that  $D_{NN}$  reaches a required minimum, people tend to live in apartment buildings rather than building more houses. The described housing pattern is repeated by more number of apartment buildings with larger building stories until the population reaches saturation. It is to be noted that at low population density, people tend to live closely as shown in Figure 2.8b, rather than the assumed scenario illustrated in Figure 2.8a. However, the use of a GDHC system in a low population density area may not be economically feasible since its cost per capita is expected to be much higher. Developing GDHC for such a scenario is not the interest of this study.

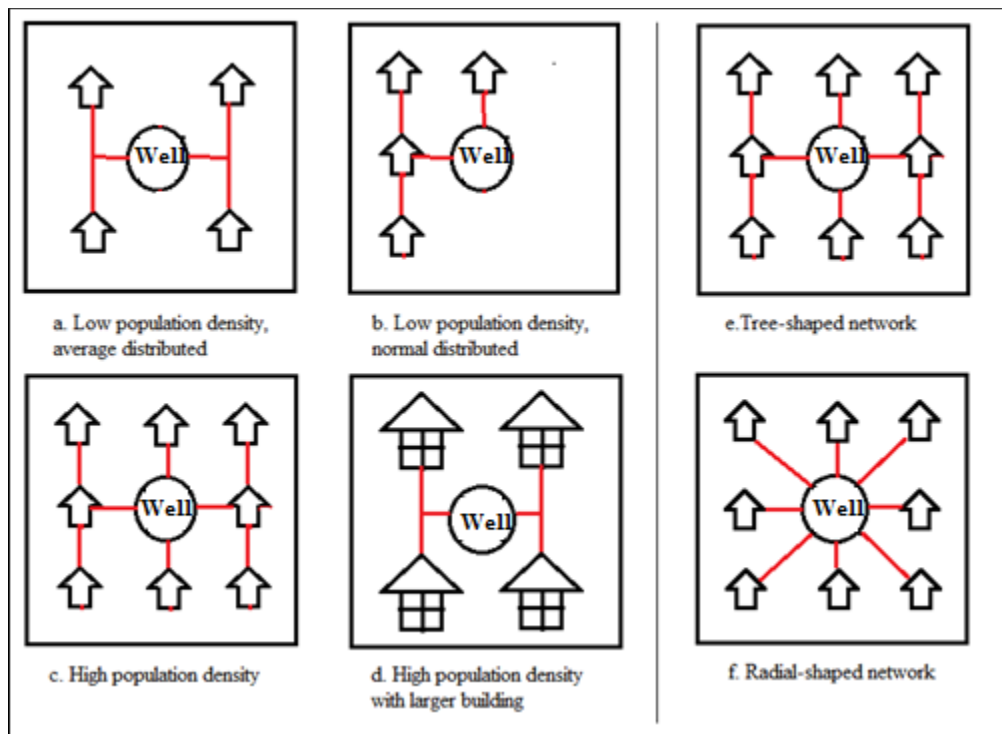


Figure 2.8: The housing pattern with increase population and distribution network design.

The geothermal production wells were assumed to be located at the center of the target area. Based on the Xia’s research on Hong Kong’s cooling distribution network (Xia, et al., 2011), a tree-shaped design shown in Figure 2.8e, is more economical than a radial-shaped design shown in Figure 2.8f, when the service nodes are greater than ten. Furthermore, the length of the pipeline  $L$  is a function of the service nodes number  $N$  and

the average distance between two nodes  $D_{NN}$ , as shown in Equation 2.16. Based on Ogden's research on the hydrogen transition strategies, the average distance between two nodes  $D_{NN}$ , is a function of the target area  $A$  and nodes number  $N$ , as shown in Equation 2.17.

$$L = D_{NN} \times N^{1.04} \quad (2.16)$$

$$D_{NN} = \sqrt{0.15 \times A / N} \quad (2.17)$$

As a result, the length of the distribution line was calculated in Equation 2.18,

$$L = \begin{cases} ppl < 1500, L = 0.4 \times A^{0.5} \times (ppl/3)^{0.54} \\ 1500 < ppl < 5000, L = 0.4 \times A^{0.5} \times (ppl/6)^{0.54} \\ ppl > 5000, L = 0.4 \times A^{0.5} \times (ppl/8)^{0.54} \end{cases} \quad (2.18)$$

The capital cost of the pipeline  $CAP_{pipe}$  was calculated in Equation 2.19 to 2.21, based on Persson and Werner's research on hot water distribution cost based on European cities (Persson and Werner, 2011).

$$CAP_{pipe} = L \times c_0 \quad (2.19)$$

$$c_0 = c_1 + D \times c_2 \quad (2.20)$$

$$D = 0.0486 \times \ln(G_s / L) + 0.0007 \quad (2.21)$$

Where  $c_0$ ,  $c_1$ , and  $c_2$  are cost constants for the pipeline, as shown in Table 2.4,  $D$  is the pipeline diameter, and  $G_s$  is the annual energy provided through the pipeline.

Table 2.4: Cost constants for pipeline capital cost calculation.

	$c_1$ , \$/m	$c_2$ , \$/m <sup>2</sup>
Outer area, population <1500	198.716	1818.448
Median, 1500<population<5000	281.624	2270.1
Inner city, population >5000	376.316	2660.952

Equation 2.22 to 2.26 were used to estimate the pumping cost  $PC$ , where  $\Delta P_f$  is the pressure drop due to the friction,  $f$  is the friction coefficient,  $\rho$  is water density,  $v$  is the water flow velocity,  $Re$  is the Reynolds number,  $e$  is electricity rate,  $\dot{V}$  is the volume flow rate,  $\dot{m}_p$  is the mass flow rate,  $\eta_{pump}$  is the pump efficiency, and  $t$  is the pumping time. The friction coefficient  $f$  was calculated by Equation 2.23 for turbulent flow ( $10^4 > Re > 4 \times 10^8$ ), where  $\varepsilon$  is the average roughness for steel pipes, and was assumed to be 0.045 mm (Chen, 1979).

$$-\Delta P_f = \frac{2 \times f \times \rho \times v^2 \times L}{D} \quad (2.22)$$

$$\frac{1}{\sqrt{4f}} = -2 \times \log \left\{ \frac{\varepsilon}{3.7065D} - \frac{5.0452}{Re} \log \left[ \frac{1}{2.8257} \left( \frac{\varepsilon}{D} \right)^{1.1098} + \frac{5.8506}{Re^{0.8981}} \right] \right\} \quad (2.23)$$

$$v = \frac{\dot{V}}{\pi D^2 / 4} \quad (2.24)$$

$$\dot{V} = \dot{m}_p / \rho \quad (2.25)$$

$$PC_{surface} = \frac{e}{\eta_{pump}} \times (\Delta P_f) \times \dot{V} \times t \quad (2.26)$$

A basic building heating unit is shown in Figure 2.9, with a shell and tube heat exchanger outside the building (OUT-HXER), and a hot water radiator inside the building (RADIATOR). The geothermal hot water is sent to each building and go through the shell side of the heat exchanger. Another loop of water is circulating through the tube side of the heat exchanger and the radiator. The use of the secondary loop of water inside the building helps to prevent hot corrosive geothermal water from scaling the indoor pipes which are usually installed inside the walls and are hard to replace.



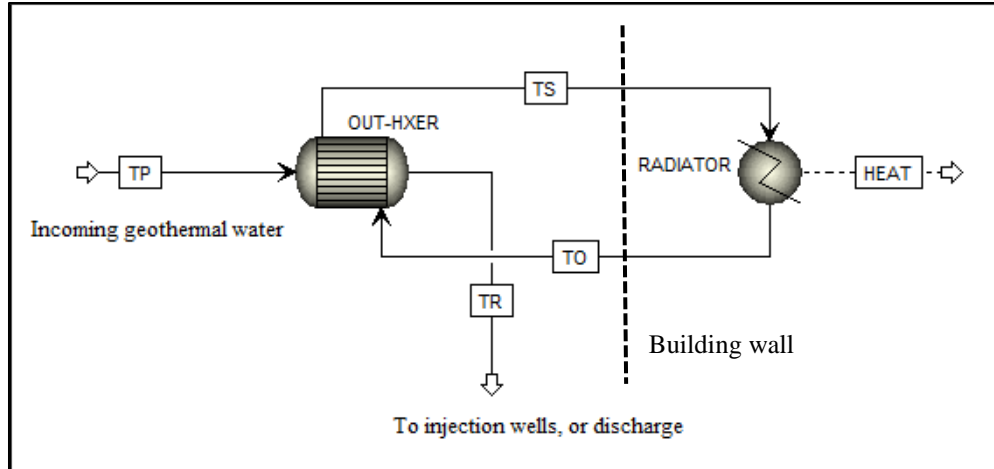


Figure 2.9: Schematic of the building heating unit of a GDHC system.

The theory of heat exchanger design has been well developed, e.g. (Fraas, 1989), and (Shah and Sekulic, 2003). The size of the OUT-HXER was determined by a set of user defined parameters at reference state, which are shown in Table 2.5.

Table 2.5: Streams table of the building heating unit.

Stream	From	To	Value at reference state
$T_p$	Production well	OUT-HXER	85 °C to 210 °C, from reservoir database
$T_r$	OUT-HXER	Reinjection well	43 °C
$T_s$	OUT-HXER	RADIATOR	80 °C
$T_o$	RADIATOR	OUT-HXER	40 °C
$HEAT$	RADIATOR	Inside building	Peak heating demand

The size of the OUT-HXER was calculated by Equation 2.27 and 2.28, where  $A_{HX}$  is the heat transfer area,  $\dot{H}_0$  is the estimated peak heating demand,  $U$  is the heat transfer coefficient,  $F$  is the correction factor, and subscript 0 indicates the reference state. The

OUT-HXER was assumed to be a single shell pass, two tube passes heat exchanger, and the correction factor  $F$  was found from Bowman, et al.'s chart for a 1-2 heat exchanger (Bowman, et al., 1940).

$$A_{HX} = \dot{H}_0 / (U \times F \times LMTD_{out0}) \quad (2.27)$$

$$LMTD_{out0} = \frac{(T_{p0} - T_{s0}) - (T_{r0} - T_{o0})}{\ln((T_{p0} - T_{s0}) / (T_{r0} - T_{o0}))} \quad (2.28)$$

For the hot water radiator inside the building, the film coefficients of the streams inside and outside of the tubes were assumed to be constant. Therefore, the overall heat transfer coefficient was also assumed to be constant. Then the Valdimarsson's equation was used to calculate the normal operating states based on the reference state of the hot water radiator, as shown in Equation 2.29 (Valdimarsson, 1993).

$$\left(\frac{\dot{H}}{\dot{H}_0}\right)^{1.3} = \frac{LMTD_{in}}{LMTD_{in0}} = \frac{[(T_s - T_{room}) - (T_o - T_{room})] / \ln[(T_s - T_{room}) / (T_o - T_{room})]}{[(T_{s0} - T_{room}) - (T_{o0} - T_{room})] / \ln[(T_{s0} - T_{room}) / (T_{o0} - T_{room})]} \quad (2.29)$$

The temperature drop of the water inside the radiator was assumed to be 40 °C, and the heating demand was assumed to follow the sine function throughout the whole year with the peak demand occurs at minimum ambient temperature, as shown in Equation 2.30 and Equation 2.31:

$$T_s - T_o = 40 \quad (2.30)$$

$$\dot{H} = \dot{H}_0 \times \cos\left(\frac{\pi}{365} \times n\right) \quad (2.31)$$

The  $T_s$  and  $T_o$  was then solved on a daily basis. The mass flow rate of the geothermal production water was calculated by Equation 2.32, where  $T_r = T_o + 3$ .

$$\dot{m}_p = \dot{H} / [C_{water} \times (T_p - T_r)] \quad (2.32)$$

The capital cost of the heat exchanger  $CAP_{HX}$  was calculated by Equation 2.33 (Stevenson, 2014), where  $c_3$  is the cost constant for heat exchangers.

$$CAP_{HX} = c_3 \times \exp[8.821 - 0.30863 \times (\ln A_{HX}) + 0.0681 \times (\ln A_{HX})^2] \quad (2.33)$$

A centralized single-effect water/lithium bromide absorption chiller was assumed in this study, as illustrated in Figure 2.10. Design of the absorption chiller system consulted Somers' work (Somers, et al., 2011). Table 2.6 shows the stream table of the absorption chiller system. The distribution network is switched to deliver chilled water to each building in summer. The absorption chiller system mainly has three phases, which are the evaporation, absorption, and regeneration. The low pressure water (stream 9) goes through the evaporator, evaporates into the steam, and extracts energy from the surrounding environments, which provides cooling. The use of the valves and the pump is to decrease the evaporator feeding's pressure in order to stimulate the evaporation process. The pure steam (stream 10) is then absorbed by the concentrated LiBr solution at the absorber. The use of LiBr solution can significantly increase its capability of absorbing steam. Then the LiBr solution (stream 1) is heated up by a series of heat exchangers so that water can be flashed back into steam (stream 6) for the next loop of the evaporation process. The geothermal hot water is used in one of the heat exchangers (HX-GEO). So the incoming temperature of stream GEOIN was equal to the geothermal production temperature, while the return temperature of stream GEOOT was calculated by assuming a pinch temperature of the heat exchanger HX-GEO to be 5 °C. Table 2.6 shows the streams properties for providing a 6.3 MW<sub>th</sub> cooling demand. For other cooling demands, this model is simulated to determine the flow rates of the streams, while the temperatures and pressures are the same. Therefore, mass flow of the geothermal production water at heat exchanger HX-GEO was calculated by Equation 2.34, where  $\dot{Q}_{HX}$  is the net duty of HX-GEO calculated by the Aspen Plus model.

$$\dot{m}_p = \dot{Q}_{HX} / [C_{water} \times (T_p - T_r)] \quad (2.34)$$

Table 2. 6: Streams table of the absorption chiller system.

Stream	1	2	3	4	5	6
Temperature, °C	32.70	32.69	64.80	65.76	90.00	89.90
Pressure, kPa	0.67	7.46	7.46	7.46	7.46	7.46
Flow rate, kg/s	32.40	32.40	32.40	32.40	32.40	2.68
LiBr fracture, %	21.84	21.84	21.84	21.84	21.84	0
Vapor fracture,%	0.00	0.00	0.00	0.00	12.00	100.00

Table 2.6 continued

Stream	7	8	9	10	11	12	13
Temperature, °C	78.40	40.20	1.31	1.30	89.90	53.30	43.15
Pressure, kPa	7.46	7.46	0.67	0.67	7.46	7.46	0.67
Flow rate, kg/s	2.68	2.68	2.68	2.68	29.72	29.72	29.72
LiBr fracture, %	0	0	0	0	25.75	25.75	25.75
Vapor fracture,%	100.00	0.00	9.30	100.00	0.00	0.00	1.10

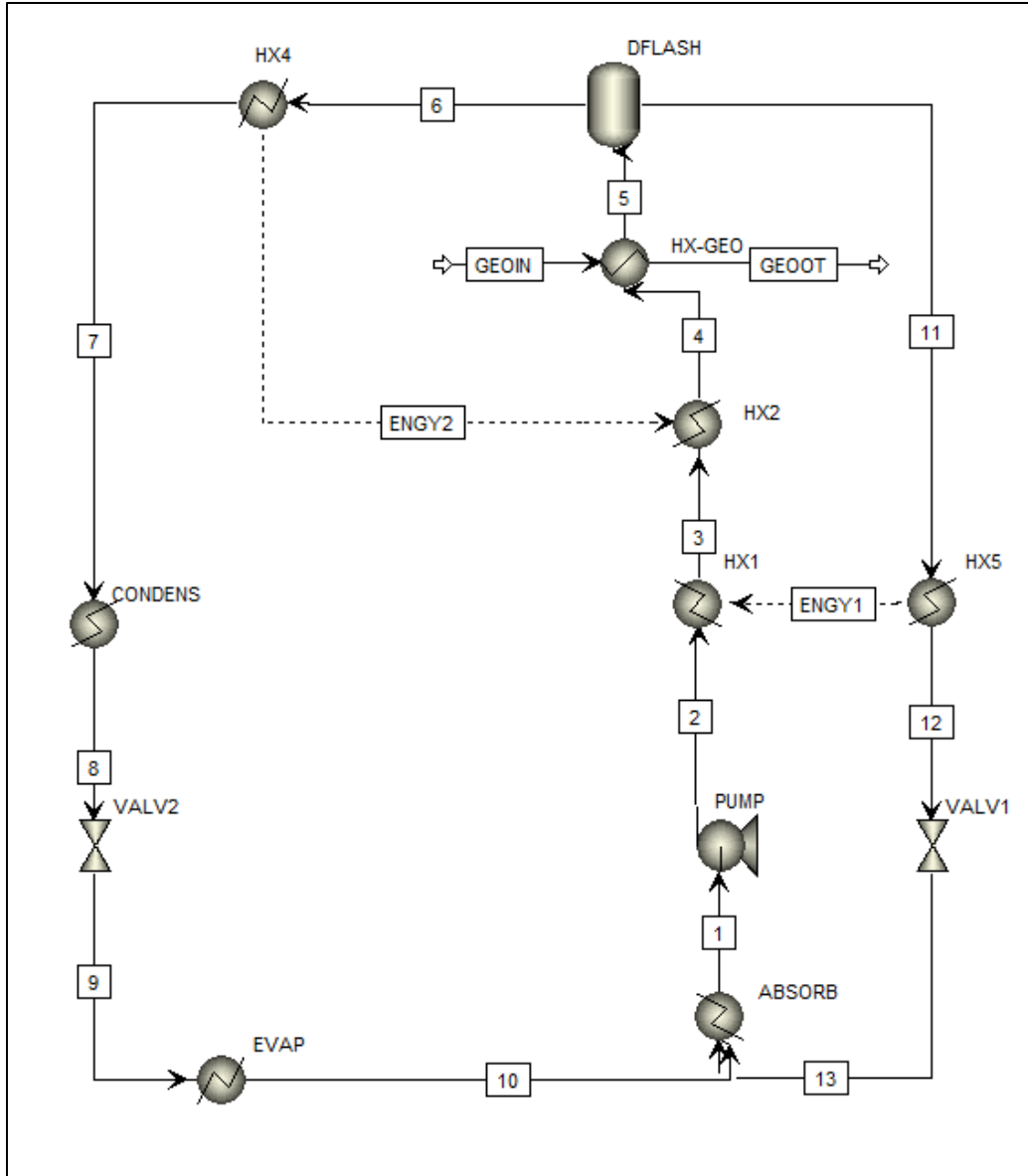


Figure 2.10: Schematic of the absorption chiller, cooling provided at EVAP, geothermal hot water flows through HX-GEO.

The capital cost of the absorption chiller  $CAP_{AC}$  was calculated by Equation 2.35 to 2.37, where  $CAP_{abs}$  is the absorption tank cost,  $CAP_{pump}$  is the centrifugal pump cost,  $\dot{C}_0$  is the estimated peak cooling demand,  $c_4$  and  $c_5$  are cost constants for the absorption tank and the pump (Mahone, 1998).

$$CAP_{AC} = CAP_{HX} + CAP_{abs} + CAP_{pump} \quad (2.35)$$

$$CAP_{abs} = c_4 \times \dot{C}_0 \quad (2.36)$$

$$CAP_{pump} = c_5 \times \dot{C}_0 \quad (2.37)$$

The annual operation and maintenance cost (O&M) of the surface facilities was calculated by investigating the direct cost, such as the labor cost  $c_{labor}$  and the fixed cost (tax and depreciation), as shown in Equation 2.38 (Turton, et al., 2008).  $c_{labor}$  is found from the Bureau of Labor Statistics (BLS, 2013).

$$OM_{surface} = 2.065 \times c_{labor} + 0.246 \times (CAP_{pipe} + CAP_{HX} + CAP_{AC}) \quad (2.38)$$

## 2.6.2 Well Design and Economics

Geothermal drilling technology has been adapted from oil and gas practices, and has matured in the past 30 years since the development of the Geysers geothermal power plants in California. The maximum well production rate in this study was assumed to be 40 kg/s, and preliminary research has shown that for most of the target areas, three production wells are enough to provide sufficient energy for heating and cooling purposes. The injection-production wells arrangement was assumed to follow the oil field practice, with well spacing around 500 meters to ensure maximum energy extraction and minimum thermal drawdown for such a geothermal system with 30 years lifetime. With the exception of wells in EGS reservoirs, wells were assumed to be drilled to the depth from the USGS database identified in section 2.4 to reach the desired temperature and sufficient fracture for water flow. Subsequently, the number of production wells is calculated based on the required mass flow estimated in the surface design part in section 2.5. For deep EGS wells, the high cost of deep drilling will offset the advantage of the high temperature. The optimum among these scenarios must be discussed case by case, and is not included in this study.

Geo-fluid pumping is also needed, for injection wells to overcome the friction losses and for production wells to lift the production water to the surface. The setting depth of the pump  $d_{pump}$  and its capacity  $\dot{W}_{pump}$  were calculated by Equation 2.39 and 2.40, where  $P_R$  is the reservoir pressure,  $f_R$  is the overall friction. The cost of the pump was calculated by

Equation 2.41. Calculations of annual pumping cost in the well field followed the same as described in section 2.5.

$$d_{pump} = d_R - \frac{P_R}{\rho \times (1 + f_R)} \quad (2.39)$$

$$\dot{W}_{pump} = 40 \times d_{pump} / \eta_{pump} \quad (2.40)$$

$$CAP_{pump} = c_5 \times \dot{W}_{pump} \quad (2.41)$$

There are not enough geothermal drilling data available to give an accurate estimation of the overall exploration to completion stages of geothermal wells. However, the oil and gas well drilling industry is well established with thousands of wells drilled every year. For this part of the study, collaborating with Cornell University geothermal group, the MIT Depth Dependent (MITDD) drilling index was updated with the latest available drilling data, and was used for the drilling cost estimation. The overall drilling expense and overall drilling depth database were updated to 2009 based on the Joint Association Survey on Drilling Costs 2009 (JAS) from the American Petroleum Institute. For an assumed drilling depth interval, the cost per meter data was calculated, then a unified polynomial function was used to fit all the data from all the drilling intervals, as shown in Equation 2.42. Figure 2.11 pictures the function between the drilling depth and the drilling cost.

$$CAP_{drill} = 1.1592 - 1.908 \times 10^{-14} \times d_R^4 + 4.0292 \times 10^{-10} \times d_R^3 - 2.5874 \times 10^{-6} \times d_R^2 + 8.5065 \times 10^{-3} \times d_R \quad (2.42)$$

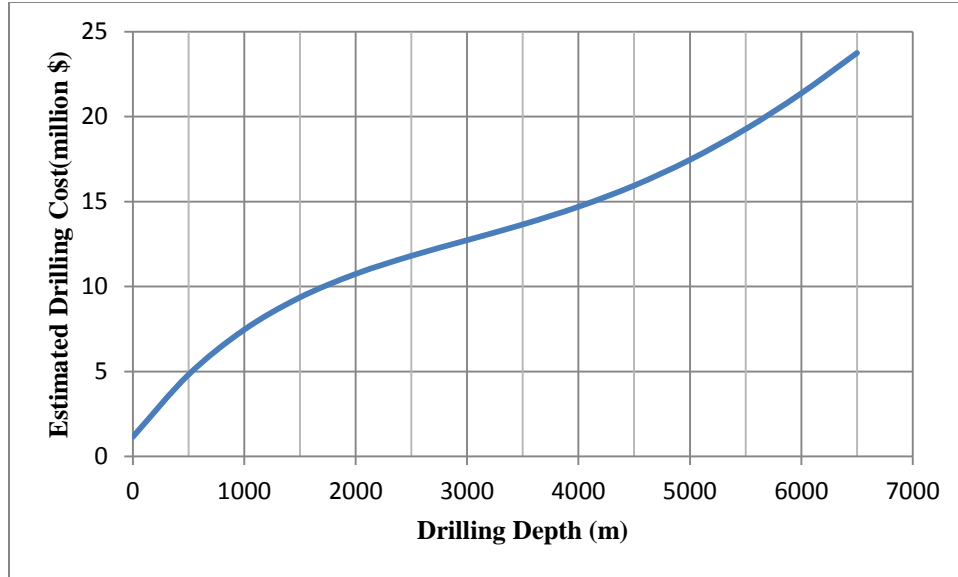


Figure 2.11: The drilling cost function with drilling depth.

The exploration wells are used by geologists to explore and confirm the existence of geothermal energy. The success of the exploration wells is essential to an economical drilling activity. Cost of exploration wells is usually less than that of production wells, but depends on the successful rate. The cost of exploration  $CAP_{expl}$  was calculated by Equation 2.43, where  $c_6$  is cost constant, and  $\chi$  is the exploration successful rate.

$$CAP_{expl} = 0.58 \times \exp(c_6 \times d_R) \times \frac{1}{\chi} \quad (2.43)$$

For near hydrothermal EGS reservoirs, well stimulation is needed to increase the porosity and permeability of the reservoir. The cost of stimulation  $CAP_{fracture}$  is mainly the cost of huge amount of water used to fracture the reservoirs, and hence the pumping cost and water storage cost. Practices from the Marcellus shale industry suggest a cost range at \$ 1500 to \$ 1800 per meter of hydraulic fracturing. For a depth of 2500 meter reservoir, 0.8 million kilograms of water is needed to pump into the reservoir in 24 hours, creating a 69 MPa pressure to stimulate the rocks. The detailed cost is shown in Table 2.7, calculation based on cost per unit mass of water from Hefley and Seydor's research on Marcellus shale gas explorations (Hefley and Seydor, 2011). Estimations for the stimulation cost of the near hydrothermal EGS resources in this study followed the same process.



Table 2.7: Stimulation cost breakdown for a 2,500-meter well based on practices from the Marcellus shale industry.

Item	Cost, \$
Water	648
Pump fuel	8,000
Storage	180,000
Pipeline	475,200
Sand	1,600
Total	665,448

The annual operation and maintenance cost (O&M) of the well side was calculated as 25% of the labor cost  $c_{labor}$  and 1% of the capital investment, as shown in Equation 2.44.

$$OM_{well} = 0.25 \times c_{labor} + 0.01 \times (CAP_{pump} + CAP_{drill} + CAP_{expl} + CAP_{fracture}) \quad (2.44)$$

### 2.6.3 Risk Analysis

In 2009, the US Department of Energy Geothermal Technology Program conducted a detailed risk analysis of the EGS technology (Young and Augustine, 2010). This part of the study consulted some of the probabilistic metrics which are also essential for the economics of the hydrothermal resources and near hydrothermal EGS from the risk analysis report. Moreover, the reservoir temperature profiles from the USGS database are also in a range of values with possibilities. With these probabilistic metrics, estimations of resources' thermal potential and their LCOH are expected in in a range of values with possibilities. Table 2.8 lists the probabilistic metrics which were used in this study. The Palisade decision tool @Risk was used to conduct Monte Carlo simulations for the risk analysis in this study.

Table 2.8: Probabilistic metrics for risk analysis in the cost model, data follows a triangle distribution, in the format of (minimum value, most likely value, maximum value).

Type Metrics	Identified hydrothermal resources	Undiscovered hydrothermal resources	Near-hydro EGS resources	Reference
Reservoir temperature	Data directly or estimated from USGS database			USGS
Exploration success rate	(0.2, 0.35, 0.5)	(0.1, 0.17, 0.25)	(0.2, 0.35, 0.5)	Young and Augustine, 2010
Non-well exploration cost, $\times 10^6$ \$	(0.513, 1.174, 2.002)		(0.417, 1.314, 2.534)	
Drilling cost multiplier	(0.59, 0.86, 1.18)			
Stimulation cost multiplier	NA	NA	(0.9, 2.6, 5.0)	

#### 2.6.4 Cost Model Implementation

Levelized cost of energy has been used in many renewable energy researches. It is a measurement of the overall competitiveness of a particular type of energy technology. It represents the cost per unit energy of building and operating an energy-providing technology over an assumed financial life (EIA, 2013). To this point, the capital costs and the O&M costs of the surface facilities and the geothermal wells have been discussed. The levelized cost of thermal energy for GDHC systems was calculated by Equation 2.45.

$$LCOH = \frac{\sum(CAP + OM + PC)}{\sum G_s} \quad (2.45)$$

Here a constant discount rate  $r$  was used to discount future expense back to the present, and the project lifetime was assumed to be 30 years. The capital investment was calculated by Equation 2.46.

$$\sum CAP = (CAP_{surface} + CAP_{well}) \quad (2.46)$$

Annual O&M and pumping cost were calculated by Equation 2.47.

$$\sum (OM + PC) = (OM_{surface} + OM_{well} + PC_{surface} + PC_{well}) \times \frac{(1+r)^{30} - 1}{r \times (1+r)^{30}} \quad (2.47)$$

The overall energy provided in 30 years was calculated by Equation 2.48.

$$\sum G_s = G_s \times \frac{(1+r)^{30} - 1}{r \times (1+r)^{30}} \quad (2.48)$$

For all the resources,  $CAP_{surface}$  is the sum of  $CAP_{pipe}$ ,  $CAP_{HX}$ , and  $CAP_{AC}$ ;  $CAP_{well}$  is the sum of  $CAP_{pump}$ ,  $CAP_{drill}$ , and  $CAP_{expl}$ , noting that  $CAP_{well}$  also includes  $CAP_{fracture}$  for near hydrothermal EGS resources. The cost model calculated the LCOH for the 253 identified hydrothermal resources, 20 regions for the undiscovered hydrothermal resources, and the other 253 near hydrothermal EGS resources sequentially, and generated the supply curve.

## 2.7 Thermal Potential for GDHC System

### 2.7.1 Identified Hydrothermal Resources

Total available mass flow rate of each identified hydrothermal resource was first estimated. A summary of the reservoir characteristics is in Appendix A-1. Figure 2.12 shows the histogram of the mass flow. It is seen that mass flow is mostly less than 120 kg/s, and therefore, a maximum of three production wells would be sufficient.

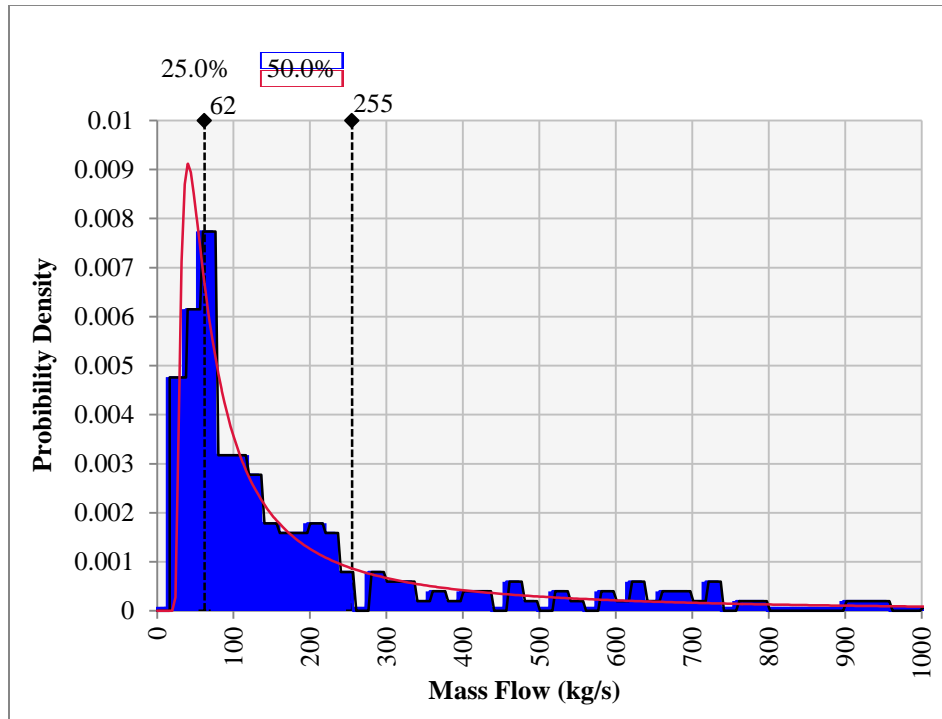


Figure 2.12: Histogram of the identified hydrothermal resources mass flow rates and the predicted probability density curve.

The overall thermal potential was then estimated with a mean of 72,577 MW<sub>th</sub>, a 95% probability of 33,250 MW<sub>th</sub> and a 5% probability of 113,535 MW<sub>th</sub> by Monte Carlo simulations. Currently, there are quite a few numbers of resources already under development or in operation, mainly for geothermal power generation and space heating. The installed power generation capacity from identified hydrothermal resources is 2,479 MW<sub>e</sub> (Augustine, et al., 2011), and that of space heating is around 215 MW<sub>th</sub> (Lund, et al., 2011). If assuming an overall 10% efficiency of thermal energy to power generation, the remaining thermal potential from identified hydrothermal resources would have a mean of 47,566 MW<sub>th</sub>. Figure 2.13 shows the pie chart of the hydrothermal potential distribution in each state, which shows that identified resources are concentrated in the state of California, Nevada, Alaska, and Oregon.

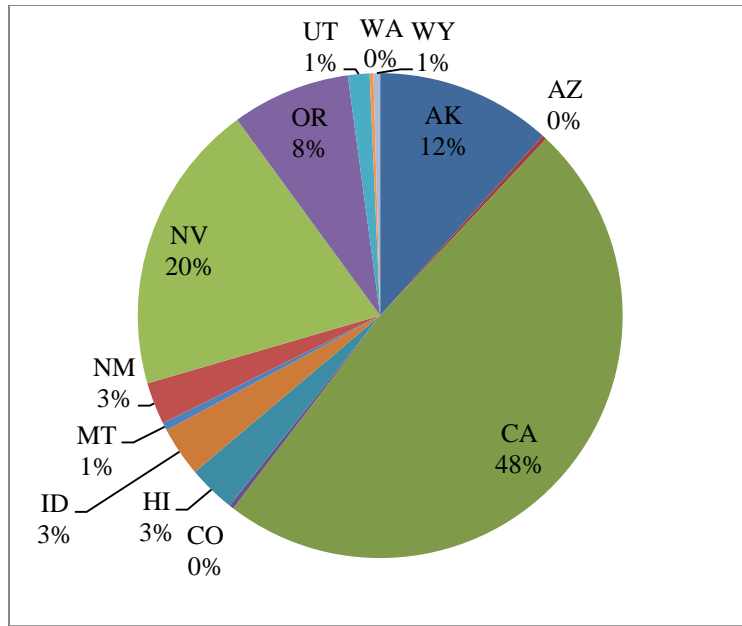


Figure 2.13: Pie chart of the remaining identified hydrothermal potential in each state, with a total of 47 GW<sub>th</sub>.

### 2.7.2 Undiscovered Hydrothermal Resources

For undiscovered hydrothermal resources, the favorability factor presents the ratio of the undiscovered hydrothermal resources to the identified hydrothermal resource. The calculated favorability factor for each state is shown in Table 2.9.

Table 2.9: Favorability factor of different geothermal regions.

Alaska	2.64	New Mexico	1.13
Arizona	0.71	Nevada	3.40
California	1.50	Oregon	1.70
Colorado	1.02	Utah	1.44
Hawaii	13.45	Washington	0.39
Idaho	1.85	Wyoming	0.59
Montana	0.43		

A summary of the reservoir characteristics of the undiscovered hydrothermal resources is in Appendix A-2. Thermal potential of the undiscovered hydrothermal resources is calculated with a mean of 159,566 MW<sub>th</sub>, a 95% probability of 70,953 MW<sub>th</sub>, and a 5% probability of 253,071 MW<sub>th</sub>. Figure 2.14 shows the pie chart of the undiscovered hydrothermal potential distribution in each state, which shows that undiscovered resources are concentrated in the state of California, Nevada, Hawaii, and Alaska. This is quite evident from the favorability map in Figure 2.4. And regions with more identified resources are more likely to have more undiscovered resources. Such states (CA, NV, HI, AK, OR) should be more focused when exploring geothermal energy.

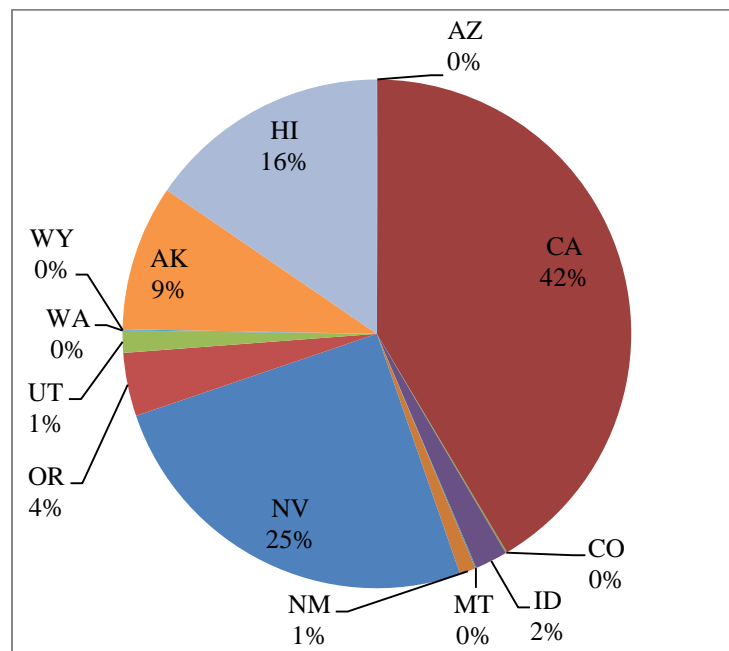


Figure 2.14: Pie chart of the undiscovered hydrothermal potential in each state, with a total of 159 GW<sub>th</sub>.

### 2.7.3 Near Hydrothermal EGS Resources

The near hydrothermal EGS has the same reservoir depth and temperature with its proximal hydrothermal reservoir. The thermal potential of each near hydrothermal EGS is the thermal potential difference between the mean and the high-end estimation of its corresponding hydrothermal resources. A list of the calculated near hydrothermal resource is shown in Appendix A-1. The overall thermal potential was estimated at

40,958 MW<sub>th</sub>. The top five resources with the most thermal potential were all found in California, which are Salton See area (8,393 MW<sub>th</sub>), Geysers area (3,432 MW<sub>th</sub>), Brawley (2,080 MW<sub>th</sub>), Coso area (1,415 MW<sub>th</sub>), and Medicine Lake area (1,375 MW<sub>th</sub>).

## **2.8 LCOH Estimation and Supply Curve Development**

### **2.8.1 Identified Hydrothermal Resources**

As stated in section 2.5, the GDHC system must be built at a populated location, so that the geothermal hot water can be consumed without much of the energy loss. There are some of the geothermal resources identified in this study with very few people living near them. With the levelized cost model, the calculated levelized costs at such locations were extremely high, more than \$ 150/MMBtu. In the following analysis, those locations with unreasonably high levelized cost are neglected. Figure 2.15 shows the calculated LCOH of the identified hydrothermal resources coupled with a geothermal temperature map at 6.5 km. The color of the dot indicates the calculated LCOH, while the size of the dot indicates the population size. A cost summary of each resource is shown in Appendix A-1. All the resources with competitive levelized cost can be characterized as with median or high reservoir temperature, with median or low drilling depth, and with large population size.

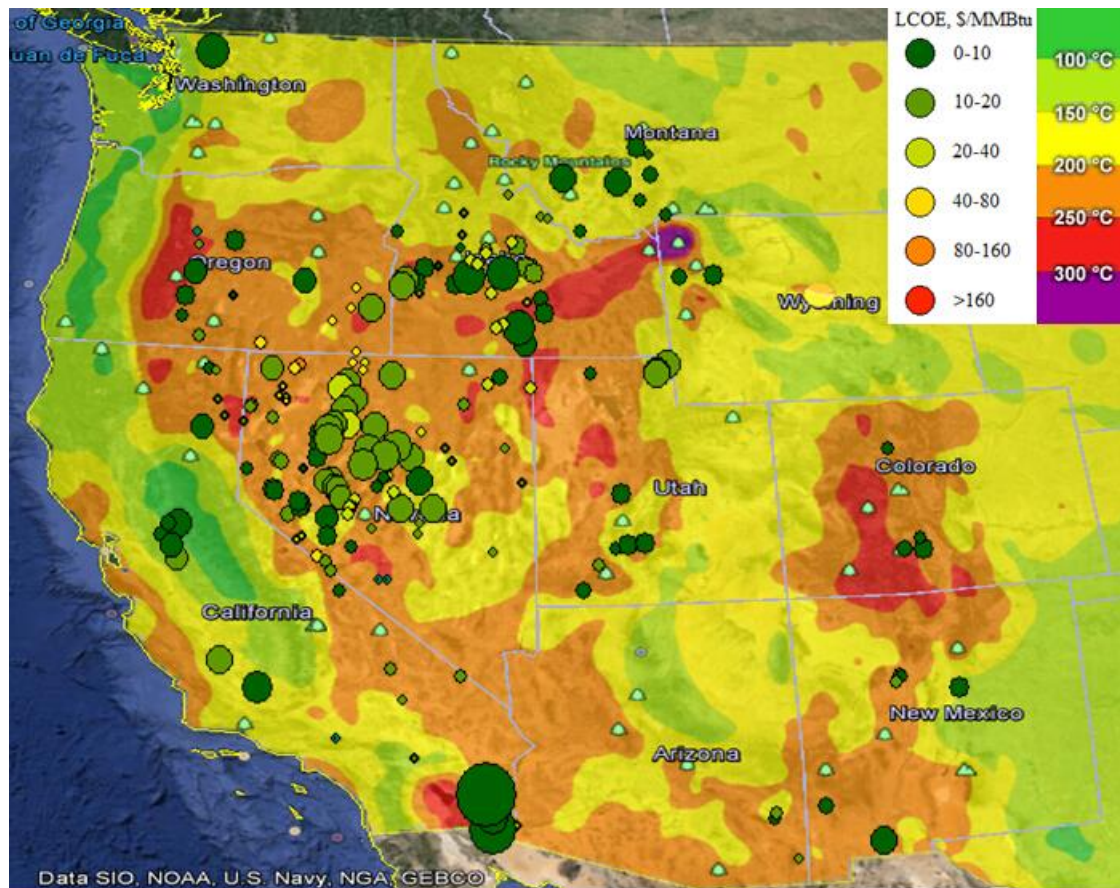


Figure 2.15: Maps of the identified hydrothermal resources, coupled with a western U.S. geothermal temperature map at 6.5 km.

It is not practical to show the LCOH calculation of all the resources. Instead, Figure 2.16 shows the overall cost breakdown by sorting the resources into nine different categories by population and depth. The overall cost during 30 years is around \$ 40 to 60 million. It is clear that overall cost increases with the depth increases because of the significant well capital increase. The overall cost also increases with the population increases because of the significant surface capital increase. The surface capital dominates the investment when the drilling depth is smaller than 1000 meters, while the wells capital dominates the investment when the drilling depth is larger than 1000 meters.



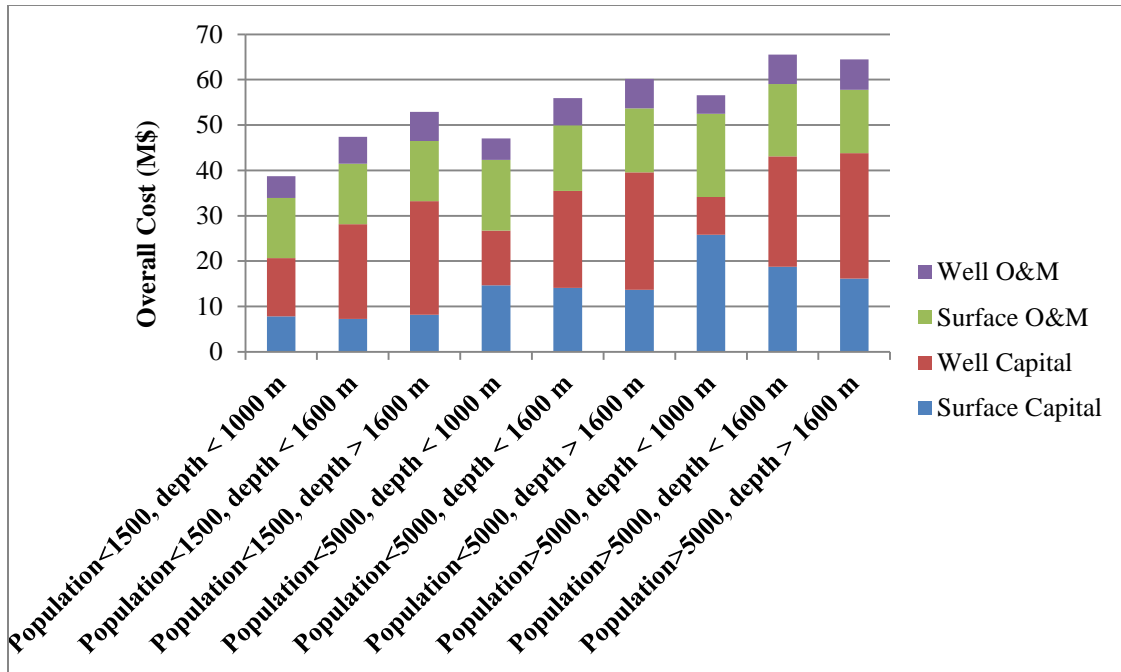


Figure 2.16: Cost breakdown of the GDHC projects of identified hydrothermal resources.

Among all the identified hydrothermal resources, the Weiser area in Idaho has the lowest levelized cost, at a mean of \$ 6.74/MMBtu. Table 2.10 shows the cost summary of the GDHC project at the Weiser area. The overall cost during 30 years is \$ 84 million, and the overall energy provided is  $12.5 \times 10^6$  MMBtu.

Table 2.10: Cost summary for the simulated GDHC system at Weiser, ID.

Capital Investment	Wells Drilling	$16.9 \times 10^6$ \$
	Wells Exploration & Miscellaneous	$3.0 \times 10^6$ \$
	Production Wells Pumps	$1.1 \times 10^6$ \$
	Injection Wells Pumps	$1.3 \times 10^6$ \$
	Surface Heating/Cooling	$1.9 \times 10^6$ \$
	Distribution System	$23.0 \times 10^6$ \$
O&M	Wells Field	$0.4 \times 10^6$ \$/y
	Surface Heating/Cooling	$1.6 \times 10^6$ \$/y
	System pumping	$0.4 \times 10^6$ \$/y

Figure 2.17 shows the year-round temperature profiles of the main streams of the surface heating/cooling facility, if the GDHC system is built at the Wesier area. The incoming temperature of the geothermal water  $T_p$  is constant throughout the year at 90 °C. During the space heating days, the supply temperature of the hot water radiator  $T_s$  increases with the ambient temperature  $T_{ab}$  decreases due to heating demand increases. During the space cooling days, the geothermal hot water is directly used in the absorption chiller system. And the supply temperature  $T_s$  is the same to the production temperature  $T_p$ .

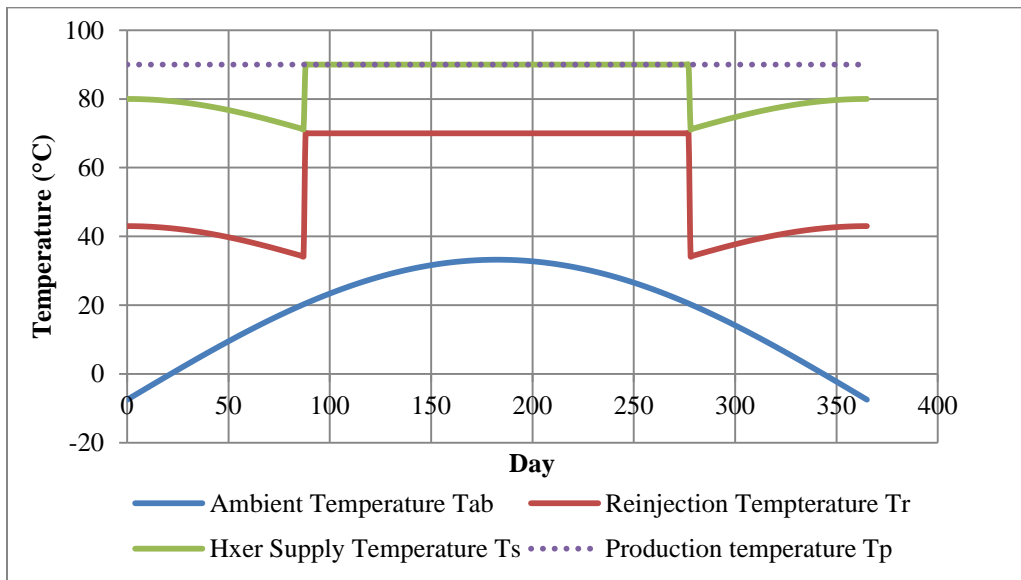


Figure 2.17: Temperature profile of main streams of the GDHC system in the Weiser area in Idaho.

Figure 2.18 shows the year-round mass flow rate profile of the geothermal production water regarding to the daily heating or cooling demand, if the GDHC system is built at the Wesier area. The maximum flow of production water is at the peak heating demand with 210 kg/s, which requires six production wells. Since the cooling demand is much smaller than the heating, the required flow rate in summer is therefore much less than that in winter.

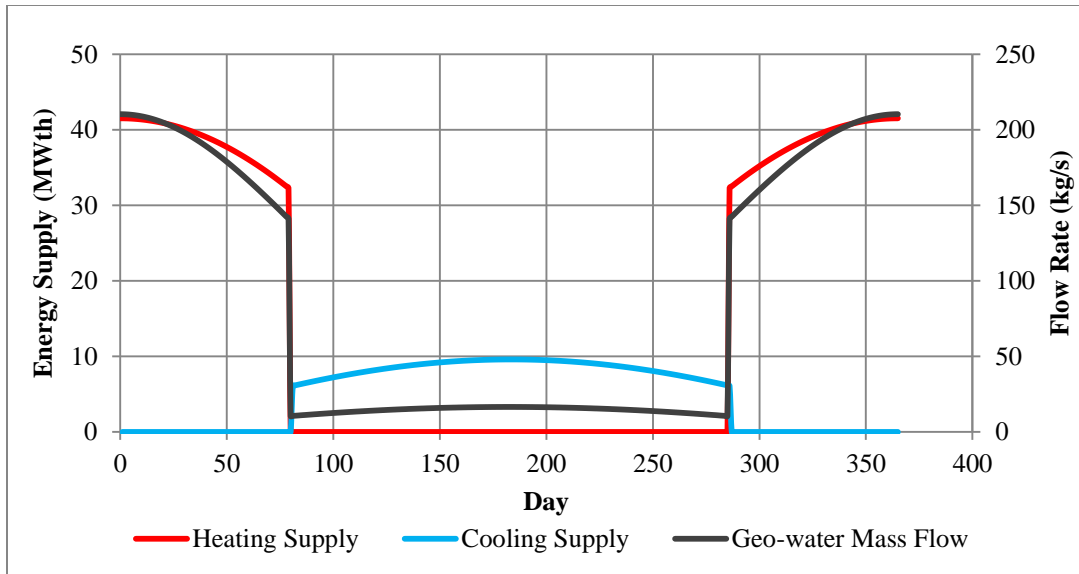


Figure 2. 18: Year-round flow rate profile of the geothermal production water of the GDHC system in the Weiser area in Idaho, corresponding to the daily system energy production.

The supply curve was then plotted based on each resource’s paired thermal potential and the LCOH. Here, as shown in Figure 2.19, the supply curve is truncated at 50 GW<sub>th</sub> to emphasize the resources with the lowest levelized cost, which are likely to be developed first. There are around 5 to 8 GW<sub>th</sub> of thermal energy which can be utilized under \$ 40/MMBtu. According to Edenhofer, et al., the cost of heating from any form of renewable energy becomes competitive to others when the price is not more than \$ 40/MMBtu (Edenhofer, et al., 2011). In comparison with the current cost of residential heating by natural gas, which is \$ 9.2/MMBtu (EIA, 2013), there is only a very small amount of identified hydrothermal energy which can be utilized cheaper than this cost, while the most of the identified resources are still above that cost.

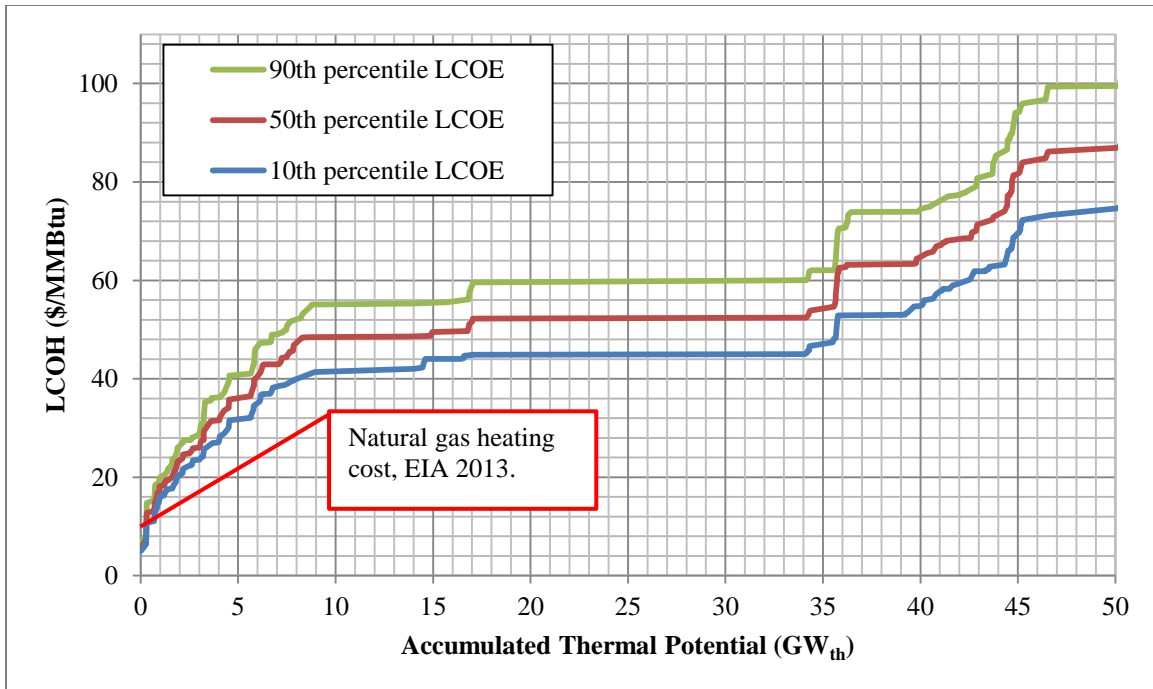


Figure 2.19: Supply curve of the identified hydrothermal resources, truncated at 50 GW<sub>th</sub>, in comparison with the current cost of heating by natural gas, which is \$ 9.2/MMBtu.

## 2.8.2 Undiscovered Hydrothermal Resources

For undiscovered hydrothermal resources, the reservoir characteristics are more like the larger identified geothermal reservoirs in each region. However, the local energy demand cannot be determined since the location is unknown. When estimating the LCOH for this category of the resource, local energy demand was assumed to be that of the most populated place in that region. Figure 2.20 shows the overall cost breakdown of undiscovered hydrothermal resources. It is clear that overall cost still follows the trend as found from the identified ones, increasing with the increase in drilling depth and population. But for each column, the well capital increases because of the increasing exploration cost, and hence increase the overall cost. Among all the undiscovered resources, the ones in California with temperature greater than 150 °C has the lowest LCOH at \$ 8.39/MMBtu. Table 2.11 shows the cost summary if the GDHC project built in that region. The overall cost during 30 years is \$ 78 million, and the overall energy provided is  $9.3 \times 10^6$  MMBtu.

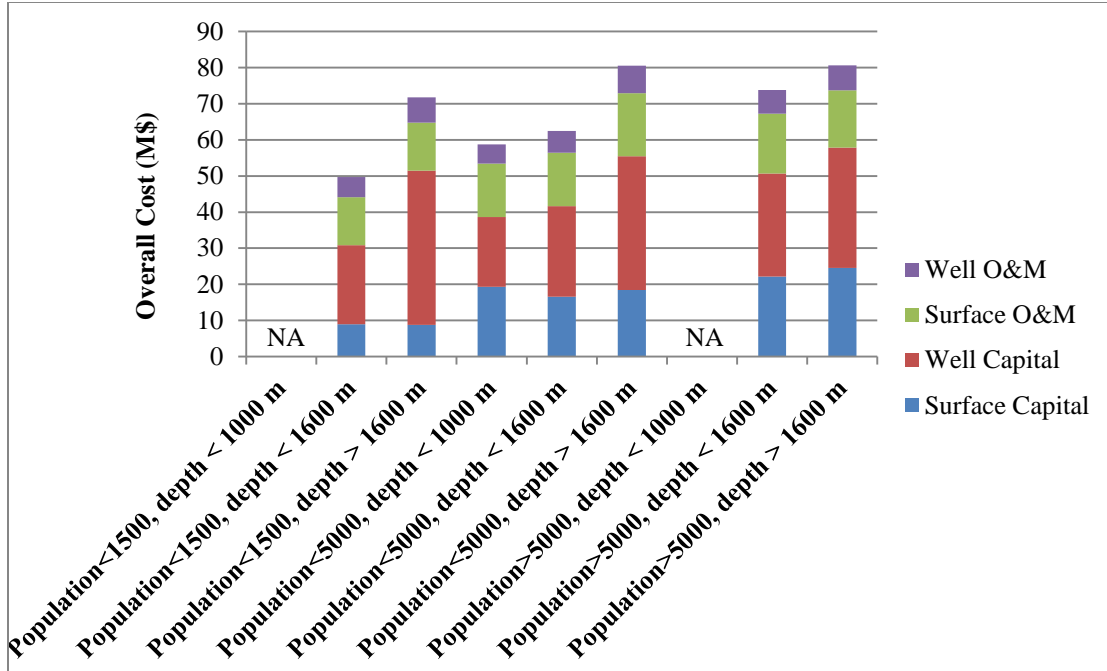


Figure 2.20: Cost breakdown of the GDHC projects of undiscovered hydrothermal resources.

Table 2.11: Cost summary for the simulated GDHC system in California with an undiscovered hydrothermal resource.

Capital Investment	Wells Drilling	$23.3 \times 10^6$ \$
	Wells Exploration & Miscellaneous	$10.5 \times 10^6$ \$
	Production Wells Pumps	$0.56 \times 10^6$ \$
	Injection Wells Pumps	0 \$
	Surface Heating/Cooling	$0.7 \times 10^6$ \$
	Distribution System	$19.8 \times 10^6$ \$
O&M	Wells Field	$0.4 \times 10^6$ \$/year
	Surface Heating/Cooling	$1.0 \times 10^6$ \$/year
	System pumping	$0.1 \times 10^6$ \$/year

The supply curve of the undiscovered hydrothermal resources is shown in Figure 2.21. There is about  $65 \text{ GW}_{\text{th}}$  of the hydrothermal resources undiscovered in California which

have a LCOH less than the current natural gas heating. Furthermore, there are up to 120  $\text{GW}_{\text{th}}$  of undiscovered resources which have a LCOH less than \$ 40/MMBtu, which will be the most valuable resources, and to be developed first in future geothermal studies.

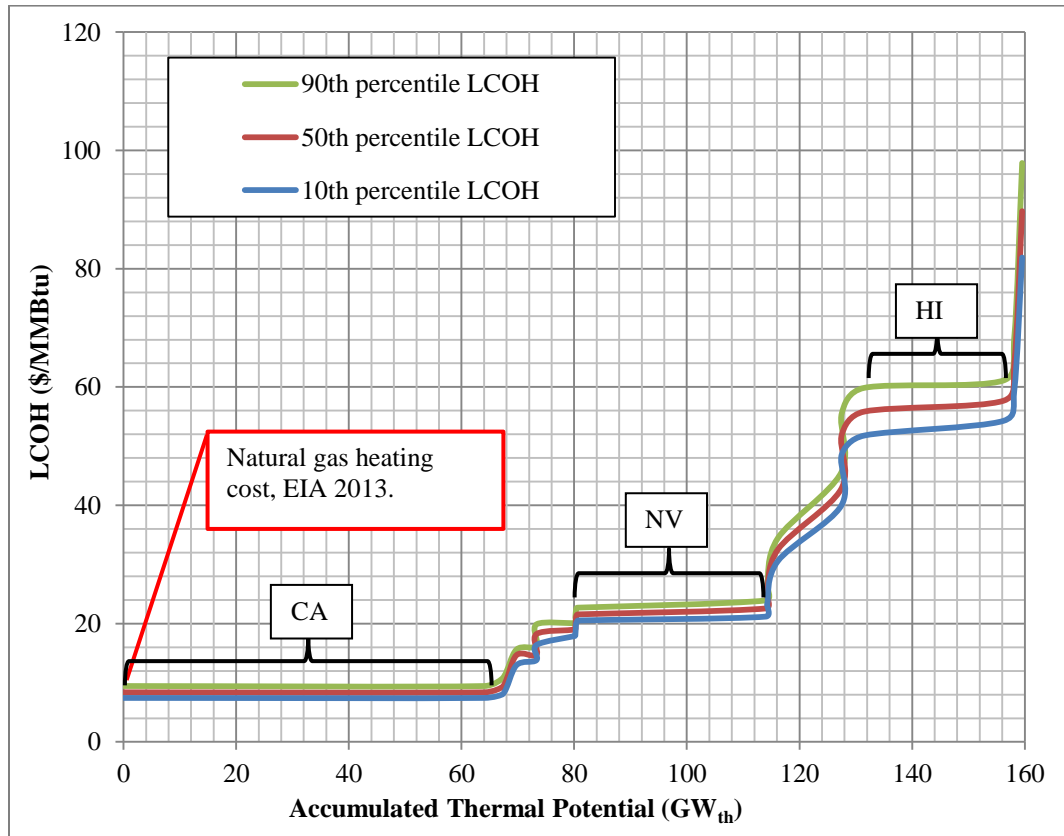


Figure 2.21: Supply curve of the undiscovered hydrothermal resources, in comparison with the current cost of heating by natural gas, which is \$ 9.2/MMBtu.

### 2.8.3 Near Hydrothermal EGS Resources

The LCOH of the near hydrothermal EGS is very similar to that of the identified hydrothermal ones, except that for the near hydrothermal EGS, artificial permeability-increasing technology (e.g. hydraulic fracturing) is required, which increases the well drilling capital. Among all the near hydrothermal EGS resources, the Weiser area in Idaho still has the lowest LCOH at \$ 7.87/MMBtu. The cost summary is similar to what is presented in Table 2.10, except that there is an added stimulation cost of about \$ 13 million to the well capital. The overall cost during 30 years is \$ 91.6 million, and the

overall energy provided is  $12.5 \times 10^6$  MMBtu. Figure 2.22 shows the supply curves of the near hydrothermal EGS resources with different flow rates.

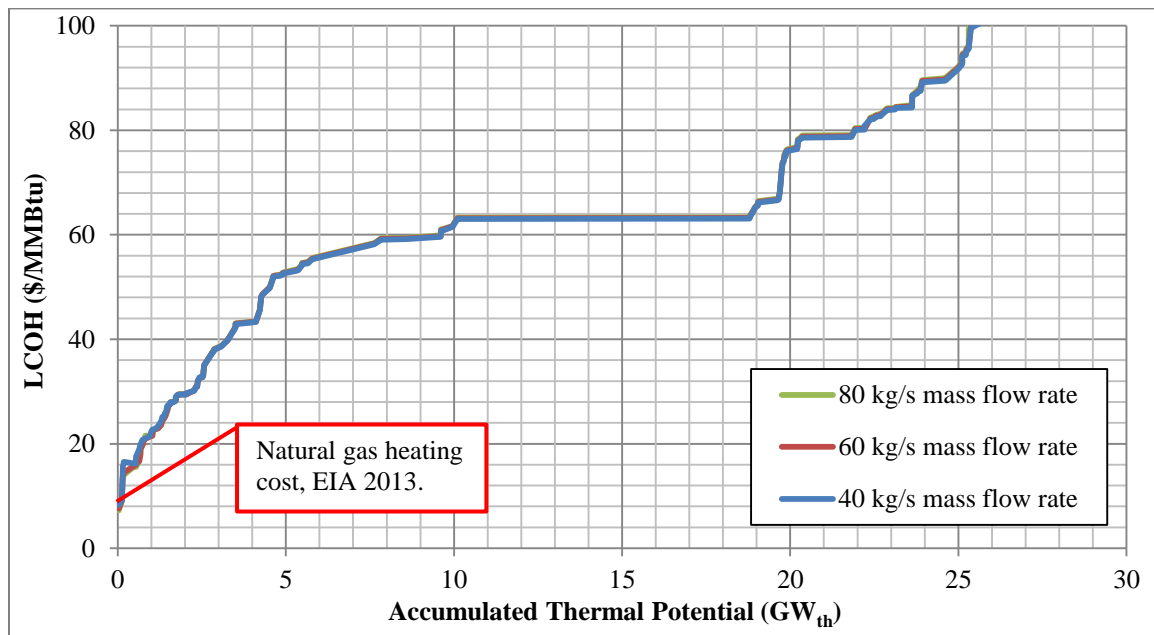


Figure 2.22: Supply curve of the near hydrothermal EGS, truncated at \$ 100/MMBtu, in comparison with the current cost of heating by natural gas, which is \$ 9.2/MMBtu.

Due to the uncertainty of the mass flow rate of each EGS reservoir, 40 kg/s, 60 kg/s, 80 kg/s were used as flow rate inputs for each case. Theoretically, with increasing flow rate, the levelized cost decreases because of the decreased number of production wells. The several resources at the left end of the supply curve in Figure 2.22 do follow such pattern: the levelized cost of the 80 kg/s scenario is the lowest, while that of the 40 kg/s scenario is the highest. For the other resources in this study, most locations only have a small energy demand, usually below 10 MW<sub>th</sub>. Therefore, one production well with a 40 kg/s water flow rate is sufficient to provide the energy demand. Increase in mass flow rate will not efficiently decrease the levelized cost. As a result, supply curves for the three different mass flow rate scenarios overlap for the most parts as shown in Figure 2.22.

## 2.8.4 The GDHC Supply Curve

Figure 2.23 shows the supply curve of three categories of geothermal resources, Figure 2.24 combines them together, and Figure 2.25 partially enlarges the part with reasonable cost. The near hydrothermal EGS resource is always coupled with its corresponding hydrothermal one with a slightly higher cost. Since most of the low cost hydrothermal resources have already been developed into power generation, their corresponding EGS resources may be good choices for expanding the existing system. There are also a large amount of hydrothermal resources undiscovered with a very low LCOH, which deserve more attentions in the future geothermal exploration.

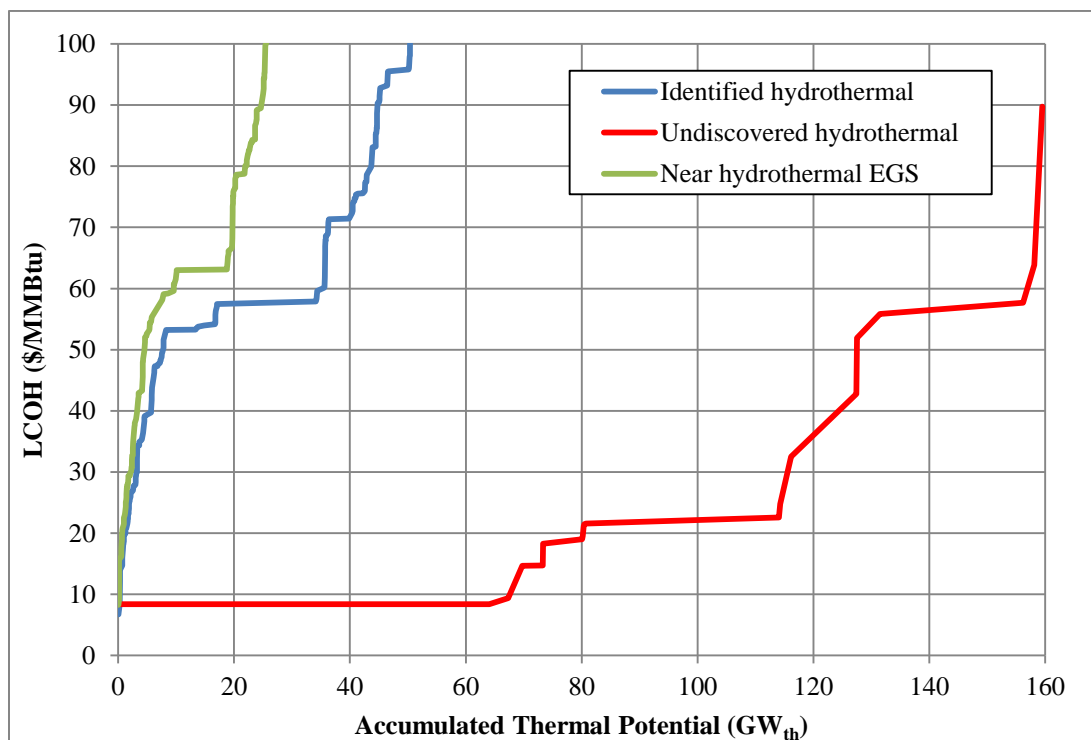


Figure 2.23: Supply curve of the U.S. GDHC application with different categories of geothermal resources.



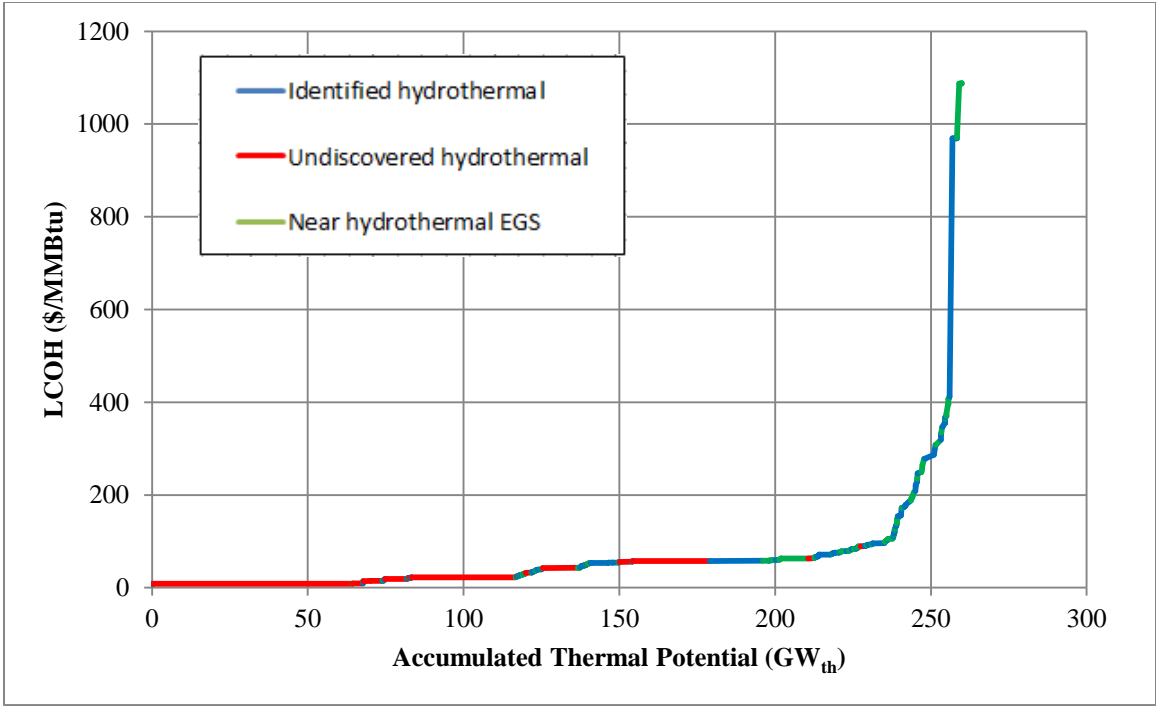


Figure 2.24: Supply curve of the U.S. GDHC application.

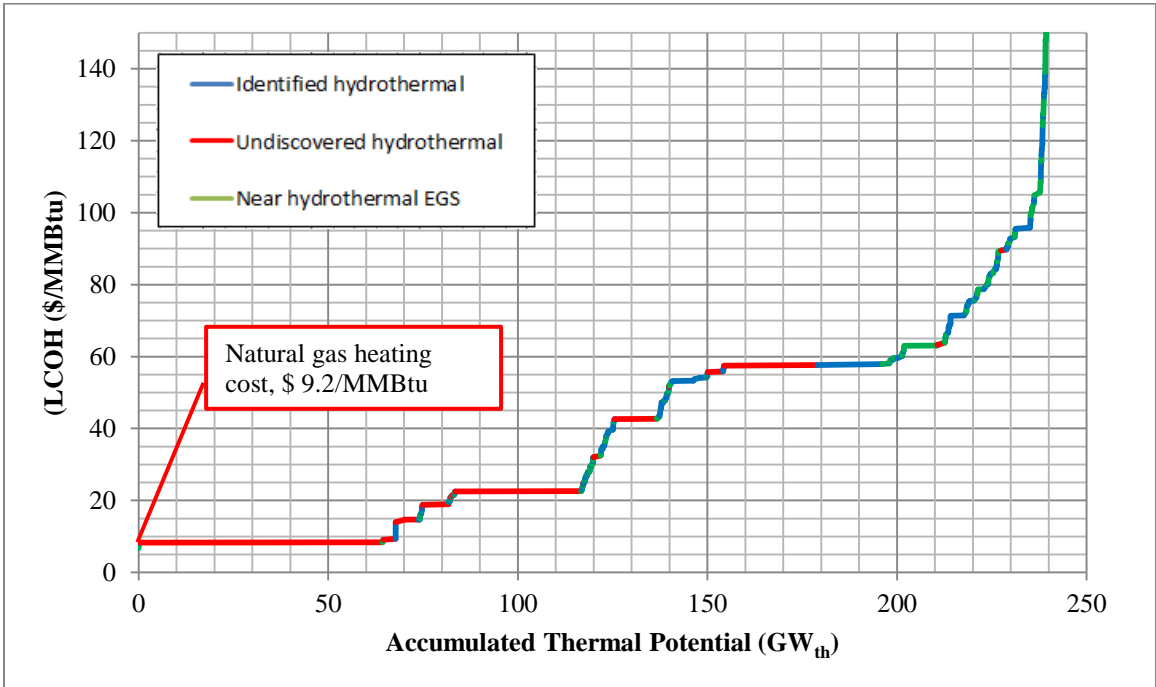


Figure 2.25: Partial enlargement of the supply curve, in comparison with the current natural gas heating cost, which is \$ 9.2/MMBtu.

## 2.9 Discussion

Discussions of the LCOH in this part of the study are based on results from identified hydrothermal resources and near hydrothermal EGS resources. Some of the system inputs such as population and reservoir gradient are uncontrolled factors. The following part discusses such uncontrolled factors' effects on the LCOH.

### 2.9.1 Population's Effect on LCOH

The population has a significant effect on the LCOH of a GDHC system. Figure 2.26 shows the population served by the identified hydrothermal resources based GDHC systems versus their LCOH. It shows that a resource with a larger population tend to have a lower LCOH, while a resource with a smaller population tend to have a higher LCOH. The predicted trend line in Figure 2.26 was fitted with a polynomial function by the least square error regression analysis, as shown in Equation 2.49. A larger population means a larger annual energy production, which is the denominator of the LCOH calculation, and hence decreases the LCOH. However, a larger population also means larger surface heating/cooling facilities, a larger distribution network, and more production wells. Thus, the constant in Equation 2.49 can be interpreted as the minimum LCOH with saturated population of a particular location.

$$LCOH = 10202 \times ppl^{-0.7495} + 1.6469 \quad (2.49)$$

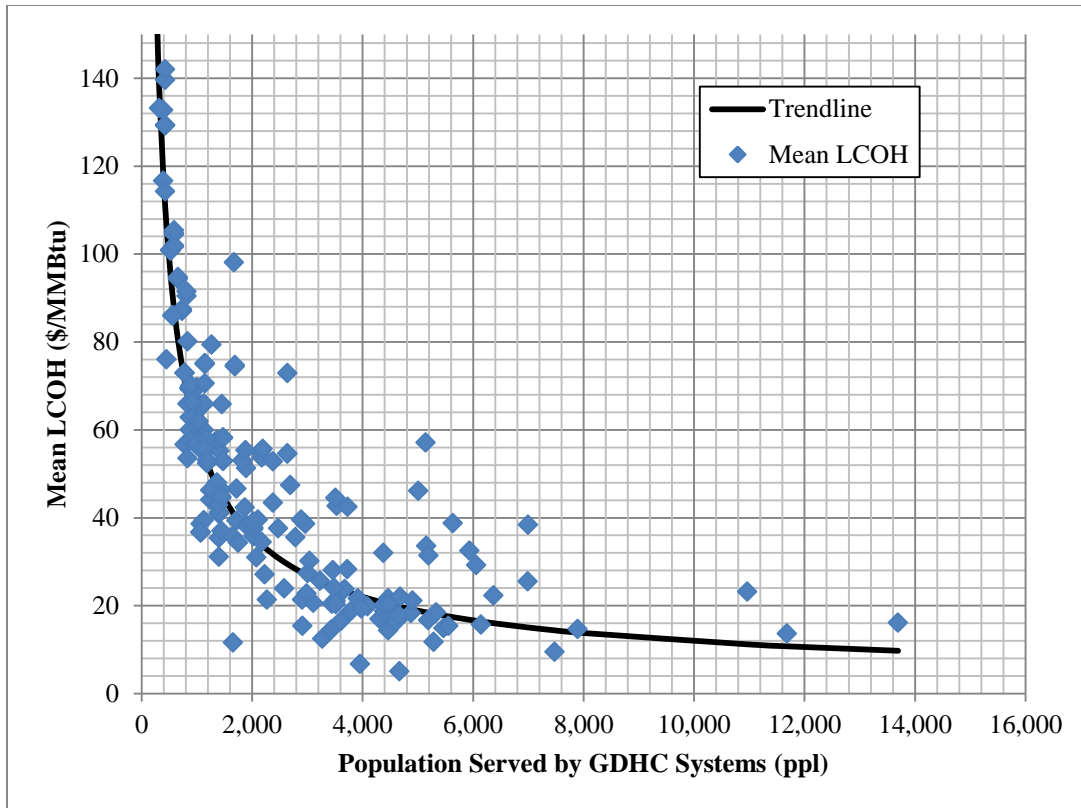


Figure 2.26: Population served by identified hydrothermal resource based GDHC systems versus their LCOH. Blue dots are identified resources, and the trend line shows the predicted LCOH as a function of the population.

### 2.9.2 Geothermal Gradient's Effect on LCOH

The effect of the geothermal gradient is not significant to the LCOH, but locations with higher gradients still tend to have a lower LCOH, as shown in Figure 2. 27. Most of the geothermal gradients of the identified resources are less than 0.2 °C/m, while the corresponding LCOH range from \$ 10 to 140 per MMBtu. For hydrothermal resources and near hydrothermal EGS resources, the reservoir depths are fixed. Efforts to lower the drilling depth cannot ensure sufficient mass flow rate. This is the reason why gradient has little effect on the LCOH. However, it can be predicted that for a deep EGS based project, a higher gradient means less drilling capital and a higher production temperature and surely, a decrease in the LCOH.

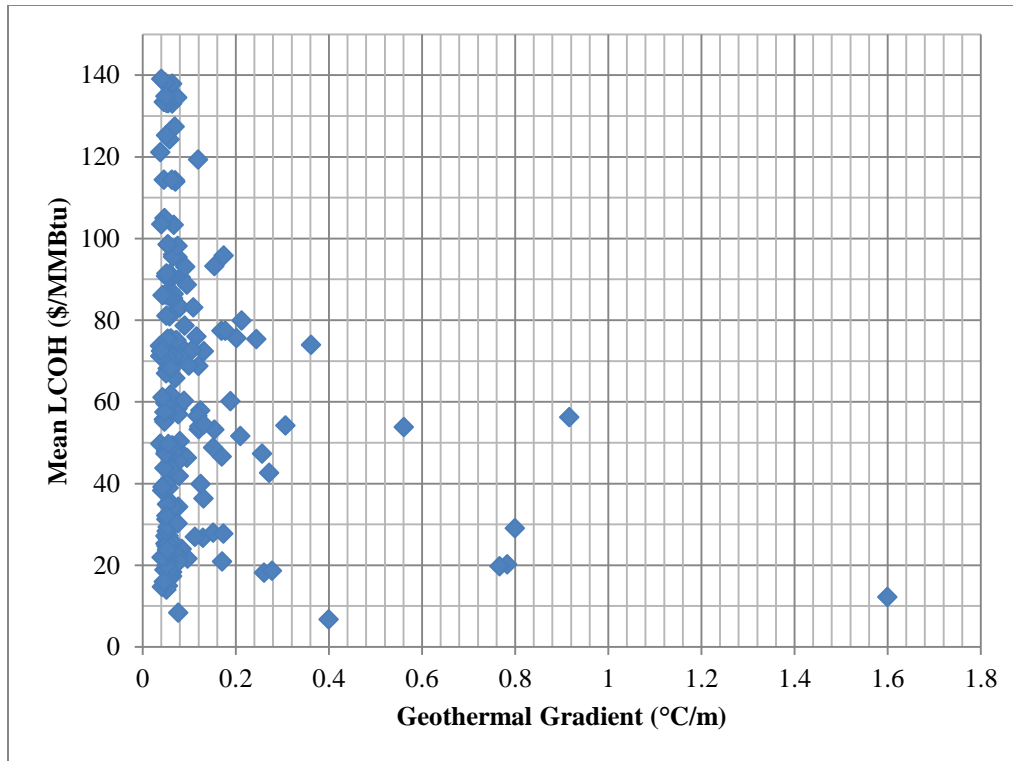


Figure 2.27: Geothermal gradients of the identified hydrothermal resources versus their calculated LCOH for the GDHC systems.

### 2.9.3 Model Sensitivity

To determine the sensitivity of the cost model, six technical or economic parameters from the model were selected, which are the energy demand, reservoir temperature, drilling cost, project lifetime, discount rate, and surface capital. Simulations were run for each parameter with -50%, -25%, +25% and +50% changes while the others stayed constant. Corresponding LCOH changes based on varies of the parameter were recorded. Results of the sensitivity analysis are shown in Figure 2.28. The energy demand has the most significant negative effect, while drilling cost has the most significant positive effect on LCOH. Moreover, increasing the energy demand is the most effective way to decrease LCOH. The project lifetime and reservoir temperature also have a negative effect on LCOH, while surface capital and discount rate have a positive effect on LCOH.

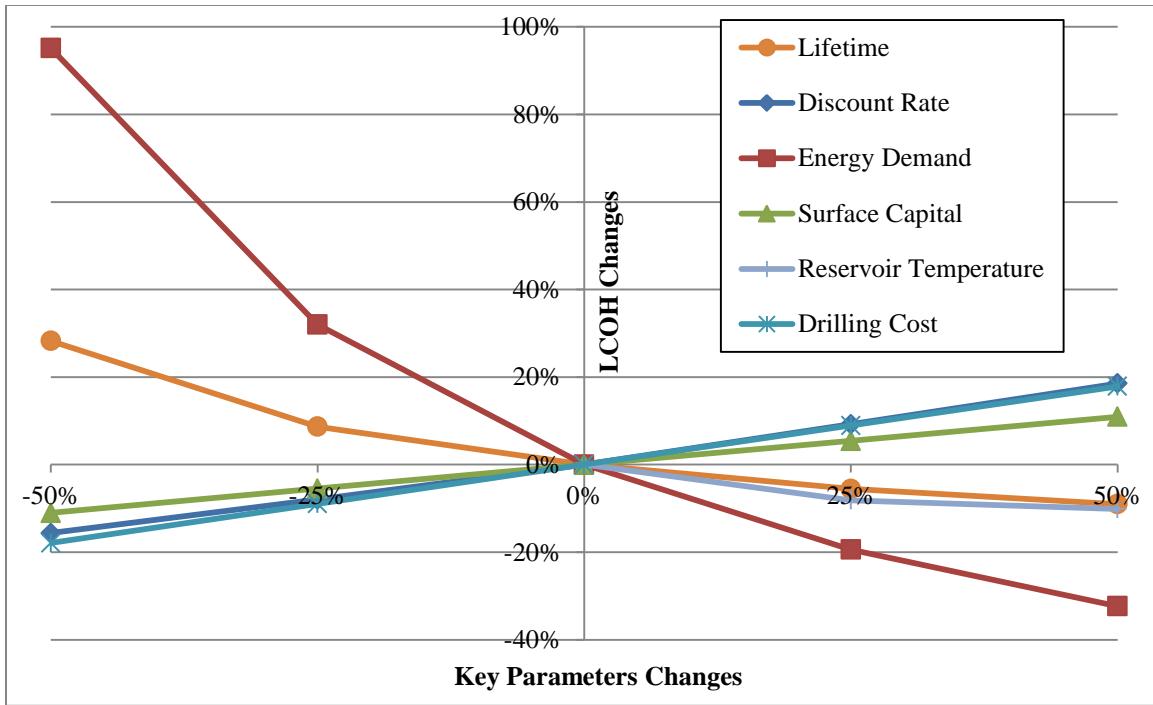


Figure 2.28: Sensitivity analysis of the cost model, showing energy demand has the most significant negative effect, while drilling cost has the most significant positive effect.

## 2.10 Conclusion

This part of the study focuses on the supply curve of geothermal district heating and cooling application. Geothermal resources were categorized into identified hydrothermal resources, undiscovered hydrothermal resources, near hydrothermal EGS resources and the deep EGS resources. Owing to the high cost of the deep EGS resources, only the first three categories have been discussed in this part of the study. 253 hydrothermal resources were identified from literature review, and 253 near hydrothermal EGS resources were assumed. Due to the uncertainties of the undiscovered resources, this category of hydrothermal resources was estimated by calculating their occurrence possibility in each state. As a summary, estimated thermal potential from each category of the resources is presented in Table 2.12. Following the fact that nearly half of the identified hydrothermal resources have already been developed into other applications such as power generation, the remaining potential from this category is about 47,566 MW<sub>th</sub>, which is concentrated in the states of California, Nevada, Alaska, and Oregon. Estimated thermal potential from

the undiscovered hydrothermal resources is about 159,566 MW<sub>th</sub>, which is concentrated in the states of California, Nevada, Hawaii, Alaska, and Oregon. Estimated thermal potential from the near hydrothermal EGS resources is about 40,958 MW<sub>th</sub>.

Table 2.12: Estimated thermal potential and the corresponding lowest LCOH from the western U.S. geothermal resources.

	5 Percentile, MW <sub>th</sub>	50 Percentile, MW <sub>th</sub>	95 Percentile, MW <sub>th</sub>	Lowest LCOH, \$/MMBtu
Identified hydrothermal resources	33,250	72,577	113,535	6.74
Undiscovered hydrothermal resources	70,953	159,566	253,071	8.39
Near hydrothermal EGS	40,958			7.87

This study also developed a cost model for the GDHC system, which enables a matrix of 20 user-defined inputs to characterize the geothermal resources as well as the target energy demand. The cost model was used for every resource to simulate the lifetime heating/cooling process, capital investment, and operation and maintenance activities. As a result, the lowest LCOH of identified hydrothermal resources to develop a GDHC system is at Weiser in Idaho, with a LCOH at \$ 6.74/MMBtu. That of the undiscovered hydrothermal resources is estimated at \$ 8.39/MMBtu in the state of California, and that of the near hydrothermal EGS resources is \$ 7.87/MMBtu, also at Weiser in Idaho. For similar geologic settings, LCOH for the identified hydrothermal resource is the lowest, while that for the undiscovered hydrothermal resource is the highest because of the high exploration cost. All the resources with competitive levelized cost can be characterized as with a median or high reservoir temperature, a median or low drilling depth, and with a large population size. Analysis of the results revealed that population has significantly

greater effect on LCOH than geothermal gradient. The energy demand has the most significant negative effect, while drilling cost has the most significant positive effect on LCOH. Increasing the energy demand is the most effective way to decrease LCOH.

Finally, the supply curve of GDHC application was developed. It shows the order in which resource should be developed based on the LCOH results. There are about 50% of the thermal potential with a levelized cost lower than \$ 40/MMBtu. With the exception of the lowest cost of the identified hydrothermal resource (Weiser area, ID) and its corresponding EGS resource, over 60 GW<sub>th</sub> of the potential is still undiscovered, with a cost lower than the natural gas heating. Moreover, there is another 35 GW<sub>th</sub> of the undiscovered hydrothermal resources with LCOH between less than \$ 25/MMBtu. The near hydrothermal EGS is the least expensive type of EGS resource. The levelized cost of the near hydrothermal EGS is a little higher than its corresponding identified hydrothermal resource. Thus in the supply curve, the near hydrothermal EGS and the identified hydrothermal resource are usually coupled. In fact, there is not much thermal potential available from identified hydrothermal resources, since most of the low cost resources have already been developed with other applications such as power generation. So the near hydrothermal EGS corresponding to the most competitive identified hydrothermal resources may be a good choice for expanding the existing system.

# Chapter 3

## Techno-Economic Assessment of GDHC Systems: A Case Study on West Virginia University

---

### 3.1 Introduction

Geothermal energy has the advantages of sustainable energy output with a high capacity factor, but hydrothermal geothermal resources only exist in very few locations worldwide. Exploitable geothermal resources require three elements at the same time, which are the hot enough reservoir, the water itself, and permeable subsurface structure so that the hot water could be delivered to the surface. However, most of the geothermal resources consist of impermeable subsurface structure. Therefore, technology of the enhanced geothermal system (EGS) would be used to enhance the rock permeability by injecting large amounts of water into the reservoir.

Currently there is no large scale commercial EGS project, but only experimental activities operating all over the world. For example, the Fenton Hill geothermal power plant in New Mexico, U.S. with a net capacity of 5 MW<sub>e</sub>, and the pilot plant in Soultz, France with a net capacity of 1.5 MW<sub>e</sub> (Tenzer, 2001). Augustine estimated that levelized cost of EGS power generation is at least \$ 0.27/kWh (Augustine, et al., 2010).

Preliminary study shows that low temperature end uses such as space and water heating, and air conditioning contribute up to 25% of the U.S. annual energy consumption. Developing geothermal district heating and cooling (GDHC) systems based on EGS could efficiently decrease the fossil fuels usage for such low temperature applications, especially in the populated eastern U.S. where hydrothermal resources are not common. This part of the study proposes an EGS based GDHC system on the campus of West



Virginia University (WVU) to evaluate its competitiveness as compared to the existing steam based heating and cooling system. Based on this case study, empirical functions for solving LCOH for EGS based GDHC systems are developed and the potential locations in West Virginia for developing such systems mapped. The objective is to provide a techno-economic benchmark for future EGS based GDHC systems development.

### **3.2 The Initial: West Virginia Geothermal Hot Spot**

In 2010, Frone, Richards, and Blackwell at Southern Methodist University (SMU) Geothermal Lab identified elevated geothermal temperatures in West Virginia. With the updated data from oil and gas field, the new temperature profile is significantly higher than the previously estimated in the MIT report – *The Future of Geothermal Energy* (Tester, et al., 2006). The high temperature geothermal region extends from the north central WV i.e. from Monongalia County where WVU is located, to Greenbrier County in the southeastern WV. This part of the study evaluates the potential to develop the EGS based GDHC systems in the state of West Virginia, beginning with a case study on West Virginia University campus.

Geothermal energy is essentially a ubiquitous resource for which its economics vary regionally. The resource availability on the supply side and the energy consumption on the demand side must be carefully evaluated when examining a potential geothermal project. The large size energy consuming population, dense arrangement of the campus buildings, and the elevated geothermal temperature profile, makes West Virginia University a potential location for the GDHC development.

The geologic cross section *D-D'* (Ryder, et al., 2009) from the U.S. Geologic Survey is the nearest geologic cross section to illustrate the geologic framework at WVU, as shown in Figure 3.1, which suggests no massive aquifer layer beneath WVU. WVU is located about 20 km north of the well (API 47-049-00244) owned by the Phillips Petroleum Company, as shown in Figure 3.1. The 100-meter-thick Tuscarora Sandstone at depth 3.3 km (10000 feet) is of interest, as the successful EGS project at Gross Schoenebeck in Germany also has very similar geologic conditions with that of West Virginia, as shown

in Table 3.1. The wells at Gross Schoenebeck were successfully stimulated by massive water fracture treatment which is a common reservoir fracturing method in oil industry, and an economical productivity was reached for a 70 kW geothermal power plant. The 30-meter-thick Oswego Sandstone at depth 3.6 km (12000 feet) is also of interest. The Oswego formation extends along the Appalachian basin to the central New York state where horizontal wells have been drilled, making it the fourth largest natural gas production formation in the state of New York (NYSDEC, 2011), suggesting that sufficient permeability may also be reached with proper stimulation at WVU.

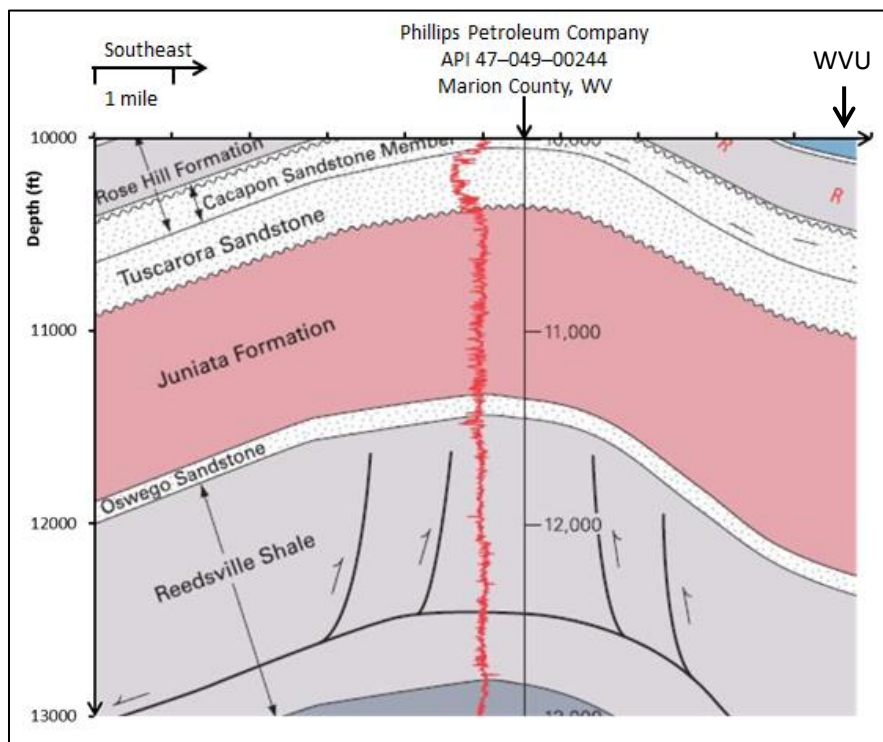


Figure 3.1: Geologic formations near Morgantown, WV at depth of 3 to 4 km, the Tuscarora and Oswego Sandstone are of interest for GDHC development.

Table 3.1: Comparison of the geologic conditions between Gross Schoenebeck and Morgantown, WV, data from Hurter, et al. (Hurter, et al., 2002) and Castle and Byrnes (Castle and Byrnes, 2005).

	Rock Type	Depth, m	Average Permeability, mD	Average Porosity, %
Gross Schoenebeck	Conglomerates	4200 to 4230	0.003	4.8
	Volcanics	4230 to 4294	0.005	4.3
WVU	Tuscarora Sandstone	3200 to 3350	0.0048	6.8

### 3.3 Modeling the GDHC System on WVU Campus

This case study aims to find the levelized cost of heat (LCOH) for GDHC system on the Evansdale campus, WVU, to replace the current steam based heating and cooling system. Peak heating and cooling demand were estimated to determine the necessary amount of geothermal hot water production as well as to design the surface energy conversion facilities. Aspen Plus models of the geothermal water distribution network with building heating units and a centralized H<sub>2</sub>O/LiBr absorption chiller system were built to simulate the heating and cooling scenarios with various geothermal temperatures and flow rate profile. Cost estimation including cost of drilling geothermal wells, capital cost of surface equipment and operation and maintenance costs were made. Five pairs of temperature and flow rate cases were simulated to find the optimum state with the lowest LCOH. Moreover, three sub-cases representing three different economic settings were also calculated in comparison with the cost of the current steam based system, which is about \$ 12/MMBtu for heating and cooling.

### 3.3.1 Existing Heating and Cooling Basics

West Virginia University has three main campuses, the Health Sciences campus, downtown campus and the Evansdale campus. The Health Sciences campus is equipped with its own heating system, including two 600 hp Cleaver-Brooks boilers rated at 7.36 MW<sub>th</sub> each. Downtown campus primarily uses steam directly through the buildings, while the proposed GDHC system uses a secondary water to exchange heat with the geothermal water and then to heat the buildings. It would not likely be economical to replace the steam system on downtown campus since all the buildings' heating utilities would be retrofitted. Hence, only the Evansdale campus was considered for this case study. Most buildings on this campus use a steam/water heat exchanger system. Saturated steam is delivered to each building and exchanges heat with water which circulating through the building's radiation system. As long as the steam pipelines allow a sufficient flow rate of geothermal water to deliver the necessary heat, it is reasonable to replace the steam by geothermal hot water without a significant facility change. As for cooling, there are two 300 ton dual stage steam absorption chillers and two 600 ton dual stage steam absorption chillers in Evansdale campus, providing cooling for a total space of 75,000 m<sup>2</sup>.

The university's steam master plan is consulted to define the pipeline network. The campus is served by a 200 mm (8 inch) high pressure pipeline from Morgantown Energy Associates. The main steam enters from the northeast of the campus and is reduced to 0.86 MPa, 140 °C saturated steam which is then distributed throughout the campus. The main steam line is a 250 mm (10 inch) pipeline with a pressure drop of 226 Pa/m. The size of the sub-stream line varies with the heating load of different building, usually ranging from 100 mm (4 inch) to 200 mm (8 inch).

### 3.3.2 Proposed Heating and Cooling System

The university steam master plan estimates each building's peak heating demand by categorizing the buildings into classroom, greenhouse, and library. The heating demand coefficient for each category is 158 W/m<sup>2</sup> for the classroom, 79 W/m<sup>2</sup> for the green house, and 63 W/m<sup>2</sup> for the library from the steam master plan. Peak cooling demand was

estimated at 95 W/m<sup>2</sup> for all buildings from the steam master plan. Gross floor area of each building was consulted with the university facility office. Historical weather data in Morgantown area from the National Climatic Data Center database was used to curve-fit the monthly energy demand from the peak value, as shown in Equation 3.1, where  $\dot{H}$  and  $\dot{C}$  are heating and cooling demands,  $i$  is month index,  $HDD$  and  $CDD$  are degree heating day and degree cooling days.

$$\frac{\dot{H}_i}{\dot{H}_{peak}} = \frac{HDD_i}{HDD_{peak}}, \text{ and } \frac{\dot{C}_i}{\dot{C}_{peak}} = \frac{CDD_i}{CDD_{peak}} \quad (3.1)$$

Thermal energy delivered to surface ( $\dot{Q}$ ) by a GDHC system was defined in Equation 3.2, where  $\dot{m}_R$  is total mass flow rate (kg/s),  $C_{water}$  is specific heat of water (J/kg/°C),  $T_R$  is production temperature which is assumed to be the same as production temperature (°C), and  $T_r$  is reinjection temperature (°C).

$$\dot{Q} = \dot{m}_R \times C_{water} \times (T_R - T_r) \quad (3.2)$$

The delivered energy should be at least equal to the campus heating or cooling demand. With the constant geothermal gradient, the production temperature is positively linear to the drilling depth. The maximum flow rate per production well in this case study was assumed to be 50 kg/s. To provide a fixed amount of energy, the flow rate and the production temperature influences each other inversely based on Equation 3.2. Therefore, five pairs of flow rate and production temperature inputs were selected and modeled by Aspen Plus to find the lowest LCOH for the system.

The layout of the Evansdale campus buildings and pipeline was used to help build the Aspen Plus heating model, as shown in Figure 3.2. The heating model consists of the heat exchangers, the pipelines, and the stream splitting nodes. The geothermal water is not directly used to avoid potential corrosion and scaling inside the buildings' radiator systems. A secondary clean fluid is used to exchange heat with the geothermal water, and circulating through the building radiators. The stream fraction of each splitter was calculated based on the ratio of the downstream heating load to the main stream heat content. Overall heat loss coefficient ( $U$ ) of the pipeline was calculated at 0.1874 W/

$\text{m}^2 \cdot ^\circ\text{C}$ , based on a polyurethane insulation cover. Pipeline pressure drop due to frictional losses was assumed to be  $226 \text{ Pa/m}$ . The length of the pipeline was estimated at  $4.6 \text{ km}$ . No pressure drop was considered in the splitter. The system was designed to maintain the indoor temperature at  $23.9 \text{ }^\circ\text{C}$  in winter.

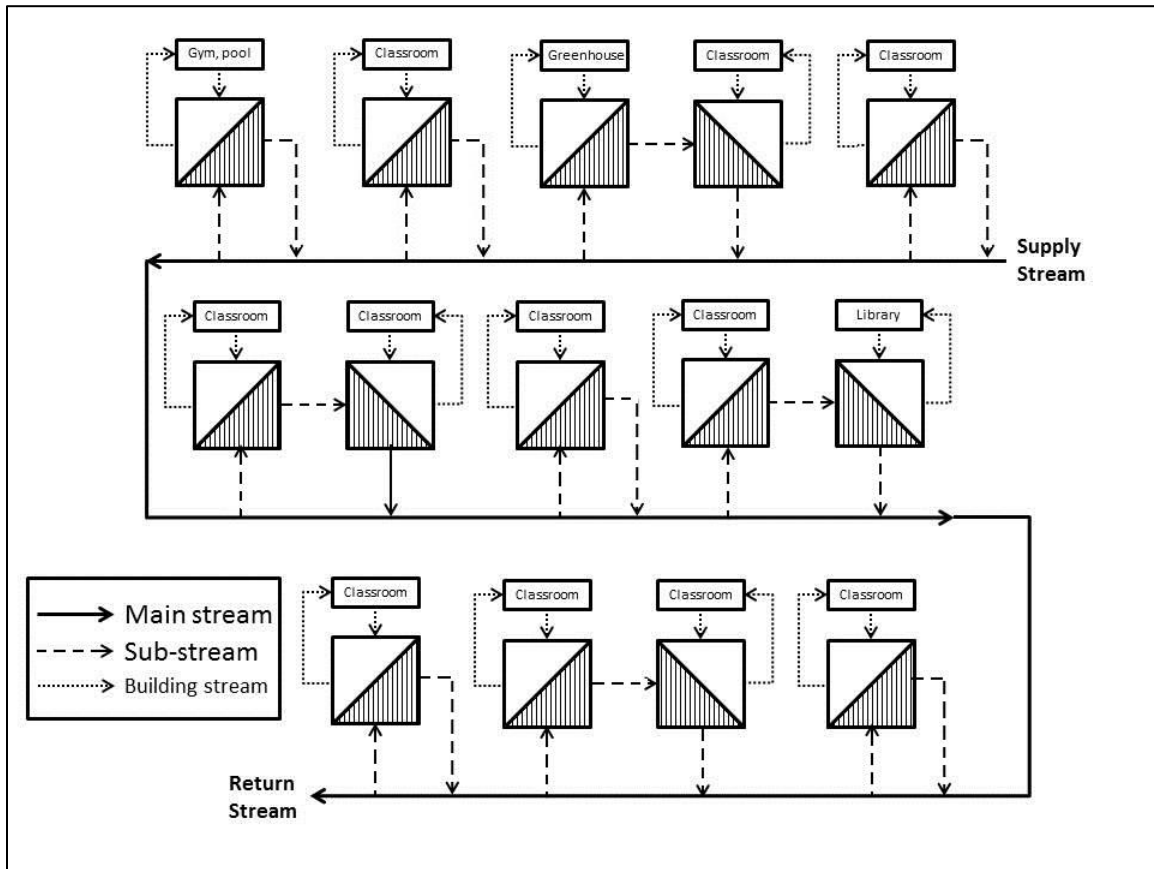


Figure 3.2: Layout of the Evansdale campus buildings (classroom, greenhouse, and library) and pipeline, based on which the Aspen Plus heating model was built.

Same centralized single-effect  $\text{H}_2\text{O}/\text{LiBr}$  absorption chiller system as discussed in Chapter 2 was assumed in this case study. The absorption chiller system was also modeled in the Aspen Plus to provide cooling for the campus. Simulations of the Aspen Plus heating and cooling model helped to determine the required production temperature and flow rate of the geothermal water, and to choose the candidate pairs of production temperature and flow rate for cost analysis.

### 3.3.3 LCOH Calculation for WVU Case Study

To ensure comprehensiveness and accuracy, three other sub-cases were also solved for different economic environments. Case I estimated the LCOH for a general EGS based GDHC system. Case II considered certain tax preferential regulations and incentives for a renewable energy project. On the basis of Case II, Case III solved the LCOH exclude the surface facility operation and maintenance costs. It is because currently the university is purchasing steam from the steam company at \$ 12/MMBtu, which also does not account for the surface operation and maintenance costs. Thus, the LCOH calculated in Case III was used to compare with this steam cost.

A geothermal project is characterized with a high initial investment and a relatively low operating and maintenance cost (Erdogmus, et al., 2006). The initial investment includes the surface heating and cooling capital plus the geothermal well drilling cost. The operation and maintenance costs for both heating/cooling process and geothermal wells are needed every year throughout the lifetime. For this case study, a 5% discount rate was assumed. Project lifetime was assumed to be 30 years.

The equipment cost of the heating/cooling system  $CAP_{surface}$ , is dominated by the cost of heat exchangers, which was estimated by the economic evaluation function of the Aspen Plus model. Estimation of drilling cost  $CAP_{drill}$ , followed the same as discussed in Chapter 2, as shown in Equation 3.3, where  $d_R$  is the desired drilling depth. The equation was derived based on drilling data from the Joint Association Survey on Drilling Costs 2009 of the American Petroleum Institute. For each drilling interval, the overall cost was divided by the overall depth; then a unified polynomial function was used to fit all the data from all the drilling intervals.

$$CAP_{drill} = 1.1592 - 1.908 \times 10^{-14} \times d_R^4 + 4.0292 \times 10^{-10} \times d_R^3 - 2.5874 \times 10^{-6} \times d_R^2 + 8.5065 \times 10^{-3} \times d_R \quad (3.3)$$

The geothermal field O&M cost  $OM_{well}$  calculation used Sanyal's equation, which is derived from actual cost data from GeothermEx power generation facility, as shown in

Equations 3.4 and 3.5 (Sanyal, 2004). The cost constant  $c_7$ , in cent/kWh, is a function of the power capacity  $P$ .  $G_s$  is the annual providing thermal energy.

$$c_7 = 2 \times \exp(-0.0025 \times (P/0.1 - 5)) \quad (3.4)$$

$$OM_{well} = c_7 \times G_s \quad (3.5)$$

The operating and maintenance cost of the heating/cooling system  $OM_{surface}$ , is associated with the day-to-day operation. The standard practice 18R-97 of the Association for the Advancement of Cost Engineering International (AACE) was used. Labor cost was assumed to be \$ 100,000/year. The utility cost of a GDHC system is mainly the pumping cost. The geothermal circulating water was assumed to be obtained from Monongahela River in close proximity to WVU with no cost. Equation 3.6 to 3.10 were used to estimate the annual pumping cost  $PC$ , where  $\Delta P_f$  is the pressure drop due to the friction,  $f$  is the friction coefficient,  $\rho$  is water density,  $v$  is the water flow velocity,  $Re$  is the Reynolds number,  $e$  is electricity rate,  $\dot{V}$  is the volume flow rate,  $\dot{m}_p$  is the mass flow rate,  $\eta_{pump}$  is the pump efficiency, and  $t$  is the pumping time. The friction coefficient  $f$  was calculated by Equation 3.7 for turbulent flow ( $10^4 > Re > 4 \times 10^8$ ), where  $\varepsilon$  is the average roughness for steel pipes, and was assumed to be 0.045 mm (Chen, 1979).

$$-\Delta P_f = \frac{2 \times f \times \rho \times v^2 \times L}{D} \quad (3.6)$$

$$\frac{1}{\sqrt{4f}} = -2 \times \log \left\{ \frac{\varepsilon}{3.7065D} - \frac{5.0452}{Re} \log \left[ \frac{1}{2.8257} \left( \frac{\varepsilon}{D} \right)^{1.1098} + \frac{5.8506}{Re^{0.8981}} \right] \right\} \quad (3.7)$$

$$v = \frac{\dot{V}}{\pi D^2 / 4} \quad (3.8)$$

$$\dot{V} = \dot{m}_p / \rho \quad (3.9)$$

$$PC_{surface} = \frac{e}{\eta_{pump}} \times (\Delta P_f) \times \dot{V} \times t \quad (3.10)$$



The above terms are the major cost terms for the EGS based GDHC project. Estimation of LCOH followed the same procedure as discussed in Chapter 2, as shown in Equation 3.11 to 3.14.

$$LCOH = \frac{\sum(CAP + OM + PC)}{\sum G_s} \quad (3.11)$$

$$\sum CAP = (CAP_{surface} + CAP_{well}) \quad (3.12)$$

$$\sum(OM + PC) = (OM_{surface} + OM_{well} + PC_{surface} + PC_{well}) \times \frac{(1+r)^{30} - 1}{r \times (1+r)^{30}} \quad (3.13)$$

$$\sum G_s = G_s \times \frac{(1+r)^{30} - 1}{r \times (1+r)^{30}} \quad (3.14)$$

### 3.4 Empirical LCOH Function Derivation

From LCOH analysis of hydrothermal resources and near hydrothermal EGS in Chapter 2, it was concluded that energy demand has the most negative effect while the drilling cost has the most positive effect on LCOH. To further look into the mathematical relations between them, two basic GDHC system metrics were selected as LCOH function variables, which are population density and geothermal gradient. WVU cost model was used to find the function by simply changing one variable while keeping the other constant.

The following part discusses several modifications of the WVU cost model for a more general LCOH estimation. The WVU case study directly estimated the energy demand by a building heating and cooling demand intensity constant, while here the energy demand was estimated based on population density, as shown in Equation 3.15, where  $P$  is the population density,  $A$  is the targeted area,  $hp$  is average household size, and  $\delta_h$  is household heating intensity.  $P$  is the census tract based population density in ppl/km<sup>2</sup>, which is available from the U.S. Census Bureau.  $A$  was assumed to be 2.56 km<sup>2</sup> which is consistent with the surface design in Chapter 2.  $hp$  in ppl/house and  $\delta_h$  in MW<sub>th</sub>/house are state wide constant available from the U.S. Energy Information Administration.

$$\dot{H} = \frac{P \times A}{hp} \times \delta_h \quad (3.15)$$

The WVU cost model did not include the surface distribution cost, while here estimation of the distribution network cost was needed, and followed the same procedure as discussed in Chapter 2. The WVU cost model assumed the system return temperature to be 40 °C, while here the return temperature was set as a variable. The cost model solved the minimum LCOH by varying the drilling depth, and was achieved by the Excel solver function.

The geothermal gradient was calculated by least square error fitting with the SMU geothermal temperature at depth data, with surface temperature assumed to be 10 °C, as shown in Equation 3.16, where  $G$  is the geothermal gradient,  $i$  is depth from 3.5 km to 9.5 km, with a 1 km interval, and  $T_{Ri}$  is geothermal temperature at depth  $i$ . Then a series of geothermal gradients were selected based on the gradient calculation results for WV. The LCOH function as an equation of population density at constant geothermal gradient was assumed similar to what have been found from the results of the hydrothermal resources in Chapter 2, as shown in Equation 3.17, where  $a$ ,  $b$ , and  $n$  are constants. For each gradient, different population densities were input into the cost model to calculate the LCOH. Constants  $a$ ,  $b$ , and  $n$  were calculated by least square error fitting Equation 3.18 with the population density and LCOH data. Finally, LCOH for an EGS based GDHC system for each of the census tract in WV was estimated.

$$\text{MINIMUM: } \sum_{3.5}^{9.5} (i \times G + 10 - T_{Ri})^2 \quad (3.16)$$

$$LCOH = a \times P^n + b \quad (3.17)$$

## 3.5 Results and Discussion

### 3.5.1 West Virginia Geothermal Maps

The geothermal temperature maps were generated by working with SMU Geothermal Lab. Figure 3.3 shows the geothermal temperature map of WV at 4.5 km. Other

geothermal temperature maps of WV can be found in Appendix B. SMU Geothermal Lab updated the temperature data from oil and gas wells, whose locations are also shown in Figure 3.3. To interpolate geothermal temperatures at other locations, the inverse distance weighted method was used and achieved by ArcGIS, which assumed the temperatures for the locations that are close to one another are more alike than those that are farther apart. Such an algorithm gives a more accurate estimation if the sample data is densely located. At 4.5 km, geothermal temperature in Morgantown is in the range of 130 to 150 °C. The geothermal gradient at WVU was calculated to be 26.5 °C/km.

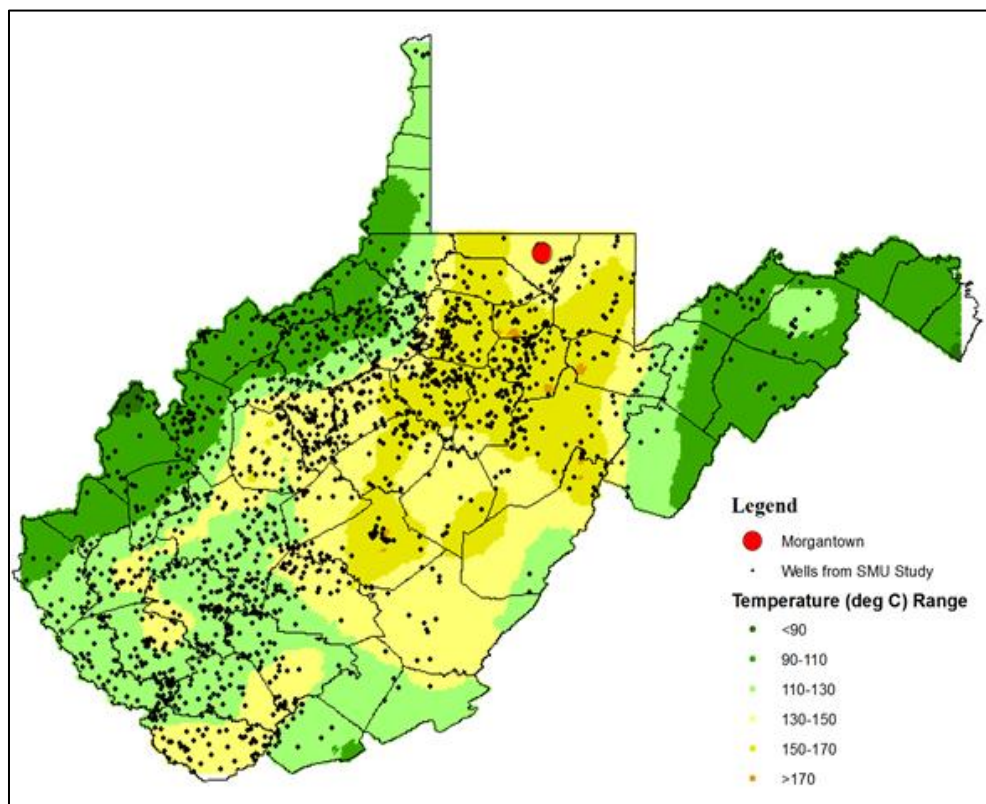


Figure 3.3: Geothermal temperature map of West Virginia at 4.5 km, black dots show the locations of oil and gas wells from which SMU updated their temperature profiles.

### 3.5.2 Campus GDHC Characterization

With the steam master plan, the campus peak heating and cooling demand were estimated at 22.9 MW<sub>th</sub> and 8.6 MW<sub>th</sub>, respectively. Annual energy consumption was estimated at 305,184 MMBtu. The monthly heating and cooling demand were also estimated, as shown in Figure 3.4. Peak heating demand was estimated in January, while peak cooling demand was estimated in July.

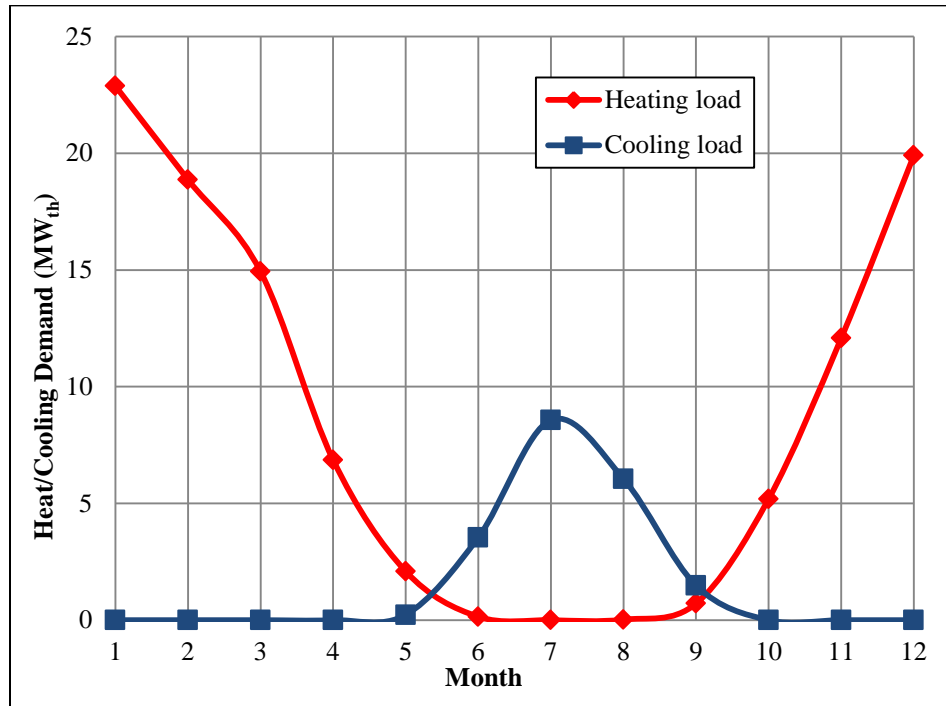


Figure 3.4: Monthly heating and cooling demand of the Evansdale Campus, WVU.

The GDHC system is designed to maintain the indoor temperature during winter at 23.9 °C (75 °F). As discussed in Chapter 2, geothermal hot water provides heating by a pair of heat exchangers. By assuming the overall pinch temperature of the two exchangers to be 16 °C, the minimum return temperature was calculated to be 40 °C (104 °F). Considering the geothermal gradient at 26.5 °C/km, four geothermal production temperatures were selected and simulated to ensure the drilling depth is less than 5 km, which are 80 °C, 100 °C, 120 °C, and 140 °C. A production temperature higher or lower than this range would result in either a prohibitively expensive drilling cost or an

unreasonably large number of production wells. Figure 3.5 shows the required flow rate versus the geothermal return temperature at different geothermal supply temperatures calculated by the Aspen Plus heating model, which agrees with Equation 3.2 that to provide a fixed amount of heating, geothermal mass flow rate and temperature drops between supply and return temperature affects each other inversely.

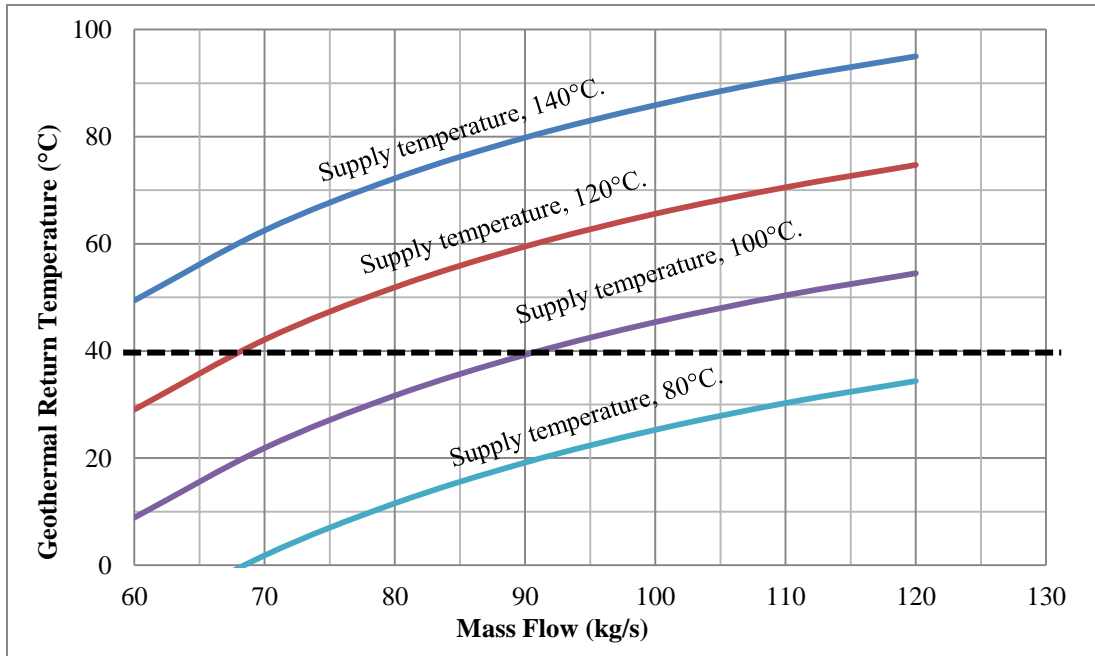


Figure 3. 5: Return temperature versus mass flow rate at selected supply temperatures to provide campus peak heating demand, dashed line indicates the minimum requirement for the return temperature.

By assuming the minimum return temperature as 40 °C, Figure 3.5 also reveals the required flow rate at each supply temperature so that the minimum return temperature is maintained. The Aspen Plus Design Spec function was used to find each minimum flow rate (variable) at each supply temperature (condition), to achieve a 40 °C return temperature (target). Results are shown in Figure 3.6. The curve divides the plot into two parts. To provide 22.9 MW<sub>th</sub> of heating, flow rate must be selected from the section above the curve at each supply temperature to ensure a normal operation of the heat exchangers. Given practical constrains on the flow rate that can be achieved for a production well, maximum flow rate per well was assumed to be 50 kg/s, as plotted by

the dashed lines in Figure 3.6. Once above the dashed line, one additional production well should be drilled. The Aspen Plus Design Spec function was again used to find the supply temperature at 148.9 °C when the flow rate is 50 kg/s, and the supply temperature at 95.6 °C when the flow rate is 100 kg/s. Therefore, five pairs of supply temperature and flow rate were selected for cost estimation, as shown in Table 3.2.

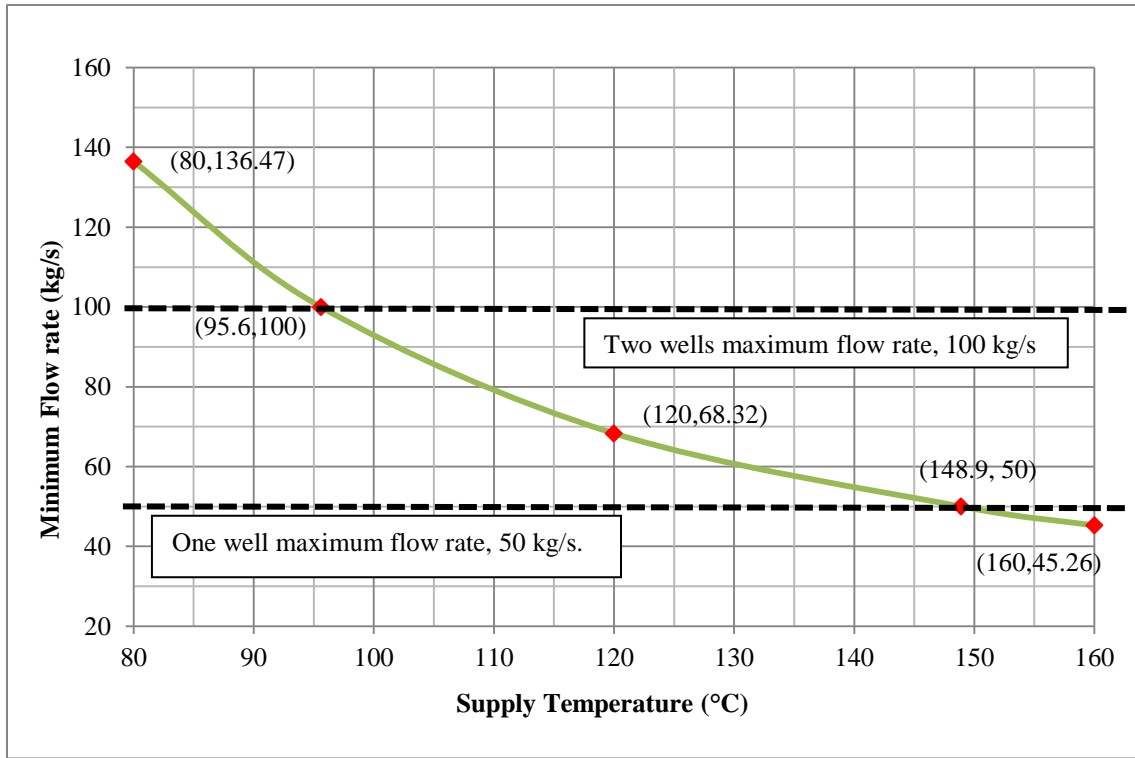


Figure 3.6: Minimum mass flow rate versus supply temperature to supply campus heating demand. Dashed lines indicate one production and two production wells' maximum flow rate. Red dots indicate the selected pairs of temperature and flow rate for cost estimation.

Since the campus heating demand is much higher than the cooling demand, any selected pair of supply temperature and flow rate from the heating model is able to provide sufficient cooling for the campus. Table 3.2 shows the five cases of supply temperature and mass flow rate which were investigated for WVU case study.

Table 3.2: Investigated cases of geothermal flow and temperature for WVU case study.

Index	Temperature, °C	Flow Rate, kg/s
1	160.0	45.26
2	148.9	50.00
3	120.0	68.32
4	95.6	100.00
5	80.0	136.47

### 3.5.3 Campus GDHC Cost Analysis

With geothermal gradient at 26.5 °C/km and surface temperature at 10 °C, drilling depths for case 1, 2, 3, 4, and 5 were calculated to be 5.67 km, 5.25 km, 4.16 km, 3.23 km, and 2.65 km, respectively. With the maximum flow rate of one production well at 50 kg/s, the number of wells including injection and production were calculated to be 2, 2, 3, 3, and 4 for each case. Overall drilling costs were calculated to be \$ 39.92, 36.67, 45.21, 39.48, and 48.35 million, respectively. The O&M cost of the reservoir field was estimated at \$ 1.79 million per year for all the five cases.

The Aspen Plus economic model directly evaluated the equipment purchase cost for the heating and cooling system, which is \$ 0.2 and 0.69 million. The ACEC recommended practice 16R-90 estimated another \$ 2.34 million for installation, handling, and other indirect cost such as general facilities and overhead. Thus the total surface capital was estimated at \$ 3.23 million. Annual pumping costs were estimated to \$ 21,467, \$ 23,715, \$ 32,405, \$ 47,431, and \$ 64,729 for case 1, 2, 3, 4, and 5, respectively. Table 3.3 shows the surface O&M cost breakdown by taking case 2 as an example. Surface O&M costs for five cases were estimated to be \$ 1.02, 1.02, 1.03, 1.05, and 1.06 million per year, respectively. Cost summary for all cases are shown in Table 3.4. On average, well capital accounts for 47.3% of the total investment, surface capital accounts for 3.7%, well field O&M accounts for 31.0%, and surface O&M accounts for 18.0%. So choosing a high temperature geothermal reservoir with a sufficient permeability is the most important factor for an economical GDHC project.

Table 3.3: Surface operation and maintenance cost estimation for case 2, in \$/per year, except for total direct cost, which is in \$.

Item	Calculation	Value
<b>Total Direct Cost</b>	$TDC$	3,226,212
Utility cost	$UC$	23,715
Labor cost	$C_{labor}$	100,000
Supervisory	$C_{super} = 0.18 \times C_{labor}$	18,000
Maintenance	$MC = 0.06 \times TDC$	193,573
Operation supply	$C_{supply} = 0.009 \times TDC$	29,036
Depreciation	$DC = 0.1 \times TDC$	322,621
Tax and insurance	$TI = 0.032 \times TDC$	103,239
Overhead	$OV = 0.708 \times C_{labor} + 0.036 \times TDC$	186,944
Administration	$AD = 0.177 \times C_{labor} + 0.009 \times TDC$	46,736
<b>Operation and Maintenance</b>	$O\&M = UC + C_{labor} + C_{super} + MC + C_{supply} + DC + TI + OV + AD$	1,023,864

Table 3.4: Cost summary of the proposed GDHC system on WVU campus, based on five selected temperature and flow rate cases.

	1	2	3	4	5
Wells capital , $\times 10^6$ \$	39.92	36.67	45.21	39.48	48.35
Wells O&M, $\times 10^6$ \$/year	1.79				
Surface capital, $\times 10^6$ \$	3.23				
Surface O&M, $\times 10^6$ \$/year	1.02	1.02	1.03	1.05	1.06



Finally, the LCOH for the proposed EGS based GDHC system on WVU campus was calculated with different production temperatures and flow rate, and in different economic scenarios. The results summary is shown in Table 3.5.

Table 3.5: LCOH (\$/MMBtu) for the WVU campus GDHC system, in different geothermal water characteristics (case 1, 2, 3, 4, and 5) and different economic scenarios (case I, II, and III)

	1	2	3	4	5
I	18.37	17.69	19.54	18.37	20.31
II	16.98	16.29	18.14	16.97	18.92
III	15.03	14.33	16.15	14.93	16.82

With certain preferential regulations and incentives, and by not considering the surface O&M cost, LCOH in economic case III is lower than that in other cases. Among the five candidate pairs of production temperature and flow rate, case 2 has the lowest LCOH. Figure 3.7 shows the calculated LCOH for five temperature and flow rate cases in economic Case III. Figure 3.7 shows that although a larger mass flow rate can efficiently offset the temperature decrease and hence decrease drilling cost, it may also require more production wells to be drilled. For WVU case study, one injection well and one production well with a 148.9 °C production temperature and a 50 kg/s flow rate provides the most economical geothermal energy.

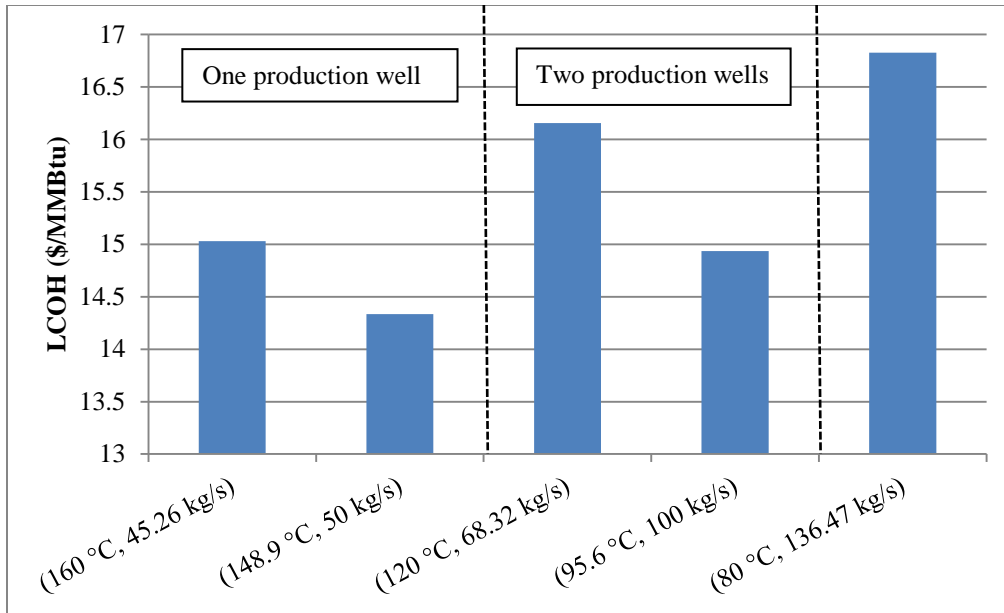


Figure 3.7: LCOH for the WVU GDHC project with selected temperature and flow rate.

Thus, for technical and economic consideration, the geothermal district heating and cooling system in West Virginia University should use one production and one injection well with a depth of 5.25 km for 148.9 °C geothermal temperature. Maximum flow rate should be maintained at peak heating. The levelized cost of heating is estimated as \$ 14.33/MMBtu, which is higher than cost of the current steam based heating and cooling system at \$ 12/MMBtu. To further decrease the LCOH, cascading applications to decrease the return temperature should be considered, such as geothermal based green house, or using geothermal heating for snow melting under pathways and for the tracks of the university personal rapid transition (PRT) system. In addition, increasing maximum flow rate of the production well is also recommended with improved well field technology in the near future. If a lower return temperature can be achieved at 30 °C, and the maximum flow rate can be achieved at 65 kg/s, LCOH for the WVU GDHC system can be as low as \$ 13.61/MMBtu.

### 3.5.4 LCOH Functions and State Wide Estimation

The geothermal gradient and the population density maps of WV were drawn by ArcGIS, as shown in Figures 3.8 and 3.9.

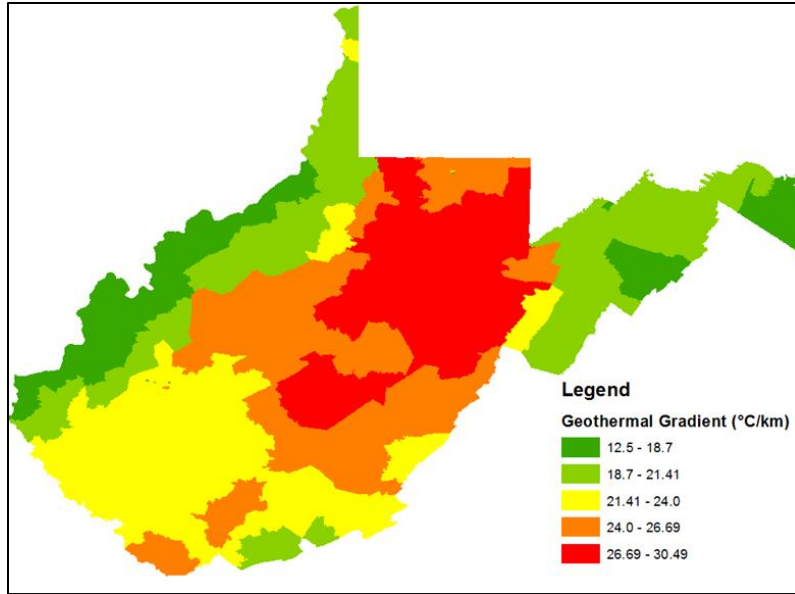


Figure 3. 8: Geothermal gradient map of WV, with a warmer color indicating a higher geothermal gradient.

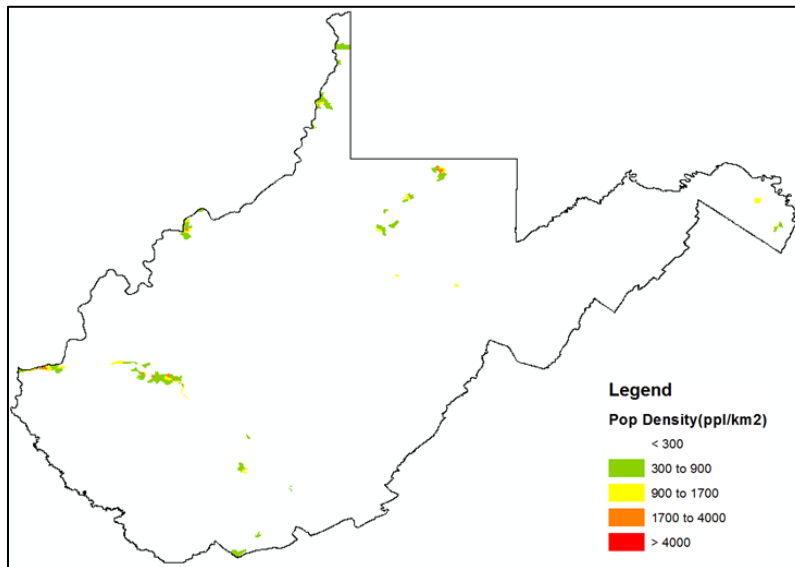


Figure 3.9: Population density map of WV, with a warmer color indicating a higher population density.

WV geothermal gradient was estimated in the range of 12 to 30 °C/km. For LCOH functions derivation, geothermal gradients were set at 14 to 30 °C/km, with 1 °C/km interval. For each gradient, the population densities were input to the cost model from

1,000 to 30,000 ppl/km<sup>2</sup>, and the LCOH results were recorded. The population density and LCOH results were fitted with Equation 3.18 by least square error analysis, to find the function constants a, b, and n. Results of a, b, and n for different geothermal gradients are shown in Table 3.6.

Table 3.6: Least square fitting results of LCOH function constants a, b, and n for different geothermal gradients (*G*).

<i>G</i> , °C/km	a	b	n	<i>G</i> , °C/km	a	b	n
14	22479.62	20	-0.97166	23	7270.58	12	-0.81079
15	14552.61	18	-0.90838	24	7932.52	12	-0.82534
16	14413.62	17	-0.90936	25	8533.13	12	-0.83772
17	13187.28	16	-0.89739	26	9269.50	12	-0.8549
18	19070.67	16	-0.95537	27	9952.80	12	-0.8708
19	15327.95	15	-0.92264	28	10636.10	12	-0.8867
20	39487.57	13	-1.05939	29	11319.40	12	-0.9026
21	5803.75	12	-0.77378	30	12002.70	12	-0.9185
22	6558.26	12	-0.79376				

There are 484 census tracts in West Virginia. Table 3.7 lists the 23 census tracts with the estimated LCOH below \$ 30/MMBtu. GEOIDs are numeric codes that uniquely identify all administrative/legal and statistical geographic areas by the U.S. Census Bureau. Among all the census tracts in WV, the one (with GEOID 54061010101) in Morgantown has the lowest LCOH. Potential places are concentrated in Monongalia county, Kanawha county, and Cabell county. Figure 3.10 shows the census tracts map of WV with their calculated LCOH, in which a warmer color represents a lower LCOH. It is clear that the warm colored areas in Figure 3.10 is very much overlapped with the populated areas as shown in Figure 3.9, indicating that a populated area is essential to an economical GDHC project.

Table 3.7: Potential places for GDHC systems development in WV, whose LCOH is less than \$ 30/MMBtu.

GEOID	LCOH	County	GEOID	LCOH	County
54061010101	15.44204	Monongalia	54039000800	27.26394	Kanawha
54061010202	20.95987	Monongalia	54061010201	27.32543	Monongalia
54039001300	22.69788	Kanawha	54039000600	27.74855	Kanawha
54061010102	23.76512	Monongalia	54039001200	27.97992	Kanawha
54069000500	24.71884	Ohio	54061012000	28.28341	Monongalia
54049020100	25.64488	Marion	54011001100	28.91448	Cabell
54039010200	25.88468	Kanawha	54039000700	28.94942	Kanawha
54061010901	26.04718	Monongalia	54011001300	29.17957	Cabell
54039013500	26.32721	Kanawha	54097966700	29.38451	Upshur
54011001400	26.69390	Cabell	54107000500	29.67028	Wood
54011000500	26.87133	Cabell	54107000300	29.70306	Wood
54011001200	26.96996	Cabell			

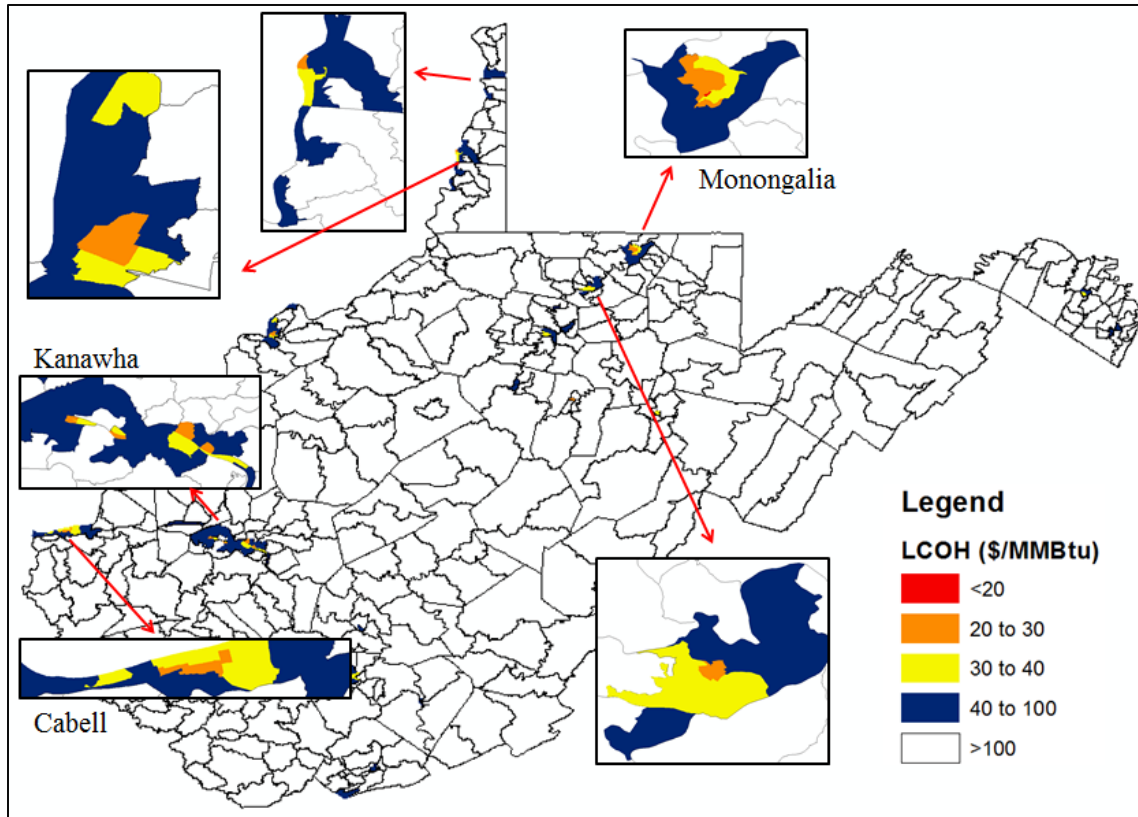


Figure 3.10: Census tracts map of WV, coupled with their estimated LCOH, with a warmer color representing a lower LCOH. Lowest LCOH is found at Morgantown, WV.

Finally, the LCOH functions were plotted by Matlab for gradients from 10 to 50 °C/km and for population densities up to 30,000 ppl/km<sup>2</sup>, as shown in Figure 3.11. The LCOH decreases with increase in geothermal gradient and population density. The population density shows a strong negative effect on LCOH at any geothermal gradient, while the gradient only shows a negative effect on LCOH at a low population density.

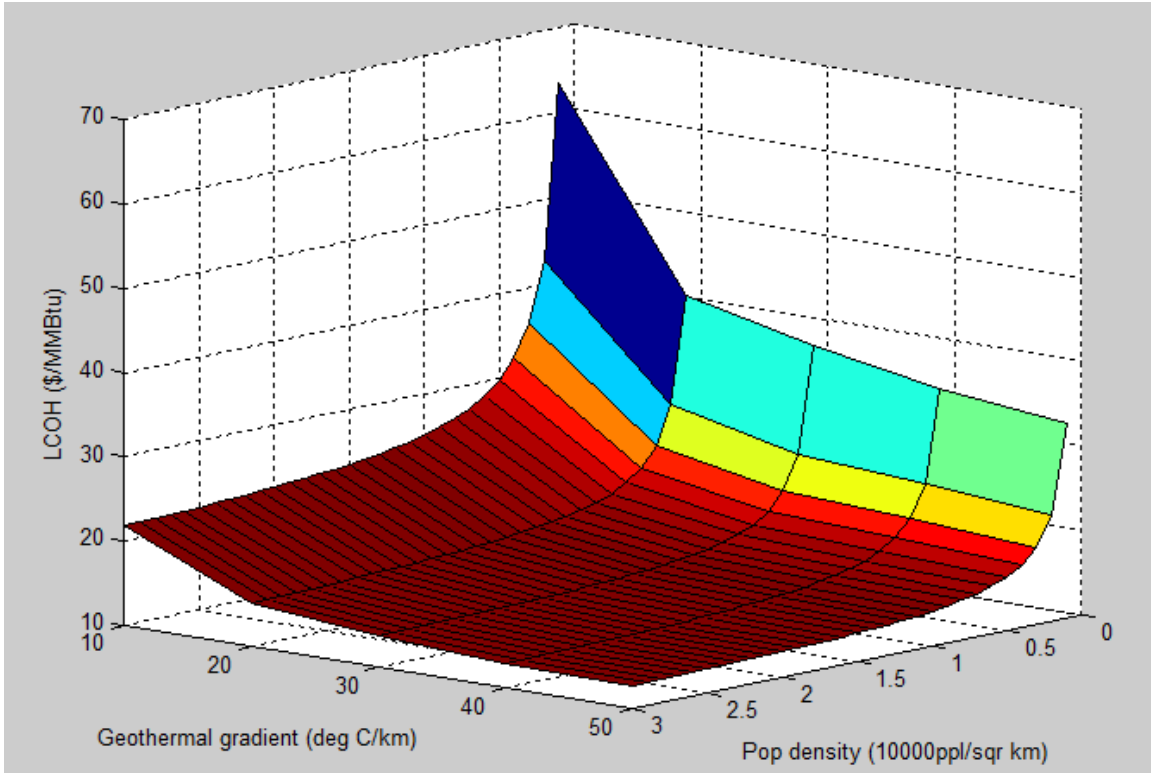


Figure 3.11: Plot showing the variation of LCOH function with population density and geothermal gradient.

### 3.6 Conclusion

This part of the study first conducted a techno-economic evaluation of an EGS based geothermal district heating and cooling system in the Evansdale campus, West Virginia University. The geological conditions at WVU and also reports from the SMU Geothermal Lab stating elevated geothermal temperatures in WV, fortify the fact that WVU has the potential to develop a GDHC system technically. Hence, the use of a geothermal system as a substitute to the current steam system particularly for heating and cooling has been the primary objective of this part of the study. To achieve the proposed objective, an Aspen Plus heating and cooling model was designed and simulated to provide the campus heating and cooling demand at 22.9 MW<sub>th</sub> and 8.6 MW<sub>th</sub>. To optimize the levelized cost of energy, five pairs of temperature and flow rate of geothermal production water were investigated. For the WVU case, a doublet system with a 50 kg/s flow rate was calculated to be more economical than a triplet (with two production well,

at a flow rate of 100kg/s) or a higher order geothermal system. Geothermal wells were calculated to be drilled to a depth of 5.25 km to ensure a geothermal temperature at 148.9 °C. Maximum production flow rate at 50 kg/s was recommended to ensure lowest LCOH. On Average, well capital accounts for 47.3% of the total investment, surface capital accounts for 3.7%, well O&M accounts for 31.0%, and surface O&M accounts for 18.0%. Well capital and O&M costs constitute the major portion of the overall investment. Drilling at a shallower depth might decrease the drilling cost significantly. However, it may require more production wells to ensure sufficient energy production. With certain tax preferential regulations and incentives, the LCOH for the WVU case was calculated at \$ 16.29/MMBtu. In comparison with the current steam purchase price which is \$ 12/MMBtu, surface O&M cost was excluded. The resulting LCOH was then calculated at \$ 14.33/MMBtu. To further decrease the LCOH, cascading applications to decrease the return temperature must be considered, which include geothermal based greenhouse heating or geothermal snow melting under pathways and for the tracks of the university personal rapid transition (PRT) system. Additionally, increase in the maximum flow rate of the production well along with improved well technology is recommended. From the cost model of WVU case study, it can be inferred that for a lower return temperature assumed at 30°C and for maximum flow rate of 65 kg/s, the LCOH for the GDHC system is calculated at \$ 13.61/MMBtu.

Based on the cost model of WVU case study, LCOH was derived as a function of population density and geothermal gradient. The geothermal gradient in WV was calculated in the range of 12 to 30 °C/km. There are 23 census tracts with the estimated LCOH below \$ 30/MMBtu, which are concentrated in Monongalia county, Kanawha county, and Cabell county. Minimum LCOH is observed in Morgantown, where WVU is located. LCOH decreases with the increase in geothermal gradient and population density. The population density shows a strong negative effect on LCOH at any geothermal gradient, while the gradient only shows a negative effect at a low population density.



# Chapter 4

## Conclusions and Recommendations

---

### 4.1 Significance and Conclusions

Geothermal district heating and cooling has the potential to offset a considerable amount of fossil fuels consumption in the U.S. The GDHC system produces a more stable base-load energy while produces much less greenhouse gas and particulates emissions than conventional heating and cooling systems. However, the literatures on studies analyzing the economic impacts of installing or retrofitting existing systems are few in number. This study is unique in that its purpose was to utilize supply analyses for the GDHC systems and determine an appropriate economic assessment of the viability and sustainability of the systems. The significance of this study is to present a cost model for the GDHC system which for the first time takes the energy market demand into consideration for a geothermal project. By showing the technical feasibility and economic benefits of the GDHC systems, this study bridges the gap between theoretic design of the system and popularizing it among the public. Developing GDHC systems will help the national energy industry restructure to a more renewable and sustainable oriented system, and protect the national energy security. By evaluating the opportunities to develop GDHC systems in the United States, the following conclusions were made by this study:

- The western U.S. is much more geothermally active than the eastern part. The overall geothermal potential is estimated with a mean of 273,100 MW<sub>th</sub>, with levelized cost of heat (LCOH) as low as \$ 6.74/MMBtu, at Weiser in Idaho. Usually, the LCOH of the identified hydrothermal resource is the cheapest. The reservoir stimulation cost causes the near hydrothermal EGS has a higher LCOH. The most expensive one is the undiscovered hydrothermal resource due to the high exploration cost.

- The undiscovered hydrothermal resources are predicted to be concentrated in the states of California, Nevada, Hawaii, Alaska, and Oregon. Future geothermal exploration activities should more on such areas. Among the undiscovered resources, over 60 GW<sub>th</sub> of geothermal energy is with a LCOH lower than natural gas based heating system (\$ 9.2/MMBtu), and other 35 GW<sub>th</sub> of geothermal energy is with a LCOH lower than \$ 25/MMBtu.
- The hot impermeable surroundings of the hydrothermal reservoir can also be used for geothermal applications, which are known as the near hydrothermal EGS resources. Apart from the fact that the near hydrothermal EGS resources have a bit higher LCOH than their corresponding hydrothermal resources, this category is the least expensive EGS resource. With the fact that most of the high quality hydrothermal resources have already been developed for other geothermal applications, the near hydrothermal EGS resources are worth considering for expanding the current energy system.
- The high temperature and high flow rate of the geothermal resources are the key parameters when choosing a GDHC site. The local energy demand is the most important factor for the success of a GDHC system. Long distances between source and supply of the hot water would cause severe heat loss, so the GDHC system must built close to the energy market.
- For hydrothermal and near hydrothermal EGS, since the reservoir depth is fixed, the geothermal gradient effect on LCOH is not significant. Sensitivity analysis shows that local energy demand, reservoir temperature and project lifetime have negative effects on LCOH, while discount rate, well capital and surface capital have positive effects on LCOH. Increasing the energy demand is the most effective way to decrease LCOH.
- A GDHC system based on West Virginia University campus is simulated as a preliminary case study which helps for detailed EGS based GDHC system research in the future. Results show that a doublet geothermal well system (one injection and one production), which is drilled to 5.25 km to ensure a geothermal

temperature of 148.9 °C can provide sufficient energy for the Evansdale campus heating and cooling demand. Maximum flow rate of 50 kg/s should be maintained at peak energy demand. The LCOH is calculated as \$ 14.33/MMBtu, which is higher than the current steam based system (\$ 12/MMBtu).

- With Southern Methodist University Geothermal Lab's finding of the elevated geothermal temperature in WV, the LCOH of developing GDHC systems in WV is calculated for every census tract. The potential locations are concentrated in Monongalia County, Kanawha County, and Cabell County. Minimum LCOH is observed in Morgantown, where WVU is located. LCOH results show that the target area's population density has a strong negative effect on LCOH at any geothermal gradient, while the gradient only has a negative effect on LOCH at a low population density.

## **4.2 Recommendations**

This project serves as a basis about where to develop the GDHC systems. People should consider the following aspects when developing any practical GDHC project based on this research, since assumptions and simplifications have been used.

- In this research, the GDHC system is designed to provide heating and cooling energy for all the people in the target location. Study of Bloomquist and Lund shows consumers still have great reluctance in accepting the GDHC systems, especially if an extra fee for retrofit is needed (Bloomquist and Lund, 2000). Therefore, a careful energy market evaluation is recommended.
- To further extract energy from geothermal water, cascading applications are recommended to decrease the return temperature. If the return temperature of WVU case study decreases from 40 to 30 °C, the LCOH can decrease by 5%. For EGS resources, any technique that can increase the maximum flow rate of the production well is also recommended.

- The WVU case study does not provide in depth study on reservoir availability for a GDHC system. Future work is recommended to focus on geologic study, lithology study, and seismic study in Morgantown area, to ensure the availability of a sufficient water flow rate for the system.
- The cost model in this research is the first ever cost model of geothermal energy which is designed for the GDHC system. It is recommended to couple this cost model with the reservoir simulation software to enable a more comprehensive analysis of the GDHC system. It is also recommended to enable this cost model for other kinds of geothermal direct uses.
- Population density varies with the size of the target area. This research assumes the target area to be one square mile when designing the distribution network. The effect of choosing a larger or smaller target area remains unknown. In one hand, it changes the population density, and hence the energy demand; on the other hand, it changes the surface distribution network. Further work is recommended which enables the facility of choosing an optimum target area for the GDHC system.

This study proposed a novel method of analyzing the feasibility of geothermal energy, in addition to illustrating the need for environmentally-safe, renewable energy sources to meet legislation requirements. As demand for energy continues to rise, GDHC development may provide key assistance in providing a cleaner future on a global scale.

## Reference

- Asif, M., Muneer, T. (2007) Energy supply, its demand and security issues for developed and emerging economies. *Renewable and Sustainable Energy Reviews*, 11:1388–1413.
- Augustine, C., Young, K. R., and Anderson, A. (2010). Updated US geothermal supply curve. *Proceedings, 35th Workshop on Geothermal Reservoir Engineering, Stanford University, Stanford, USA*.
- Blackwell, D., Richards, M., Frone, Z., Batir, J., Williams, M., Ruzo, A., and Dingwall, R. (2011) SMU Geothermal Laboratory Heat Flow Map of the Conterminous United States. Supported by Google.org. Available at <http://www.smu.edu/geothermal>.
- Blackwell, D., Frone, Z., Richards, M., (2010). Elevated Crustal Temperatures in West Virginia: Potential for Geothermal Power. Huffington Department of Earth Sciences Geothermal Laboratory, Southern Methodist University.
- Blackwell, D., and Richards, M. (2004). Geothermal map of North America, AAPG Map, scale 1:6,500,000, Product Code 423. Southern Methodist University Geothermal Lab.
- Blair, J. M. (1978). Control of oil. *Vintage Books*.
- Bloomquist, R. G. (1985). Evaluation and ranking of geothermal resources for electrical generation or electrical offset in Idaho, Montana, Oregon and Aashington, Executive Summary. *Washing State Energy Office, Olympia, USA*.
- Bloomquist, R. G., and Lund, J. (2000). Resource development potential-revenue generation potential: only a balanced approach can lead to district energy development. *TRANSACTIONS-GEOTHERMAL RESOURCES COUNCIL*, 13-18.
- Bowman, R. A., Mueller, A. C., & Nagle, W. M. (1940). Mean temperature difference in design. *Trans. ASME*, 62(4), 283-294.

- Bureau of Labor Statistics (BLS) Employment Cost Index (ECI) (2013). Private industry – Utilities. CIS2014400000000I at <http://www.bls.gov/ncs/ect/data.htm>
- Castle, J.W., Byrnes, A.P., (2005) Petrophysics of Lower Silurian sandstones and integration with the tectonic-stratigraphic framework, Appalachian basin, United States. *American Association of Petroleum Geologist Bulletin*, 89-1, pp. 41-60.
- Chamorro César, Mondéjar Mar á, Ramos Roberto, Segovia José Mart ín Mar á, Villamañán Miguel. (2012) World geothermal power production status: Energy, environmental and economic study of high enthalpy technologies. *Energy*, 42(2012):10-18.
- Chen, N. H. (1979). An explicit equation for friction factor in pipe. *Industrial & Engineering Chemistry Fundamentals*, 18(3), 296-297.
- Cook, T. R., Dogutan, D. K., Reece, S. Y., Surendranath, Y., Teets, T. S., and Nocera, D. G. (2010). Solar energy supply and storage for the legacy and nonlegacy worlds. *Chemical reviews*, 110(11), 6474-6502.
- Edenhofer, O., Pichs-Madruga, R., Sokona, Y., Seyboth, K., Matschoss, P., Kadner, S., Zwickel, T., Eickemeier, P, Hansen, G., Schl ömer, S., Stechow, C. (2011) IPCC
- Entingh, D. J., Petty, S., and Livesay, B. J. (1988). IMGEO-Impact of R&D on cost of geothermal power: Documentation and model version 2.09. *Sandia National Laboratory*.
- Entingh, D. J. (2006). Introduction to the geothermal electricity technology evaluation model (GETEM), *Princeton Energy Resources International*.
- Erdogmus, B., Toksoy, M., Ozerdem, B., and Aksoy, N. (2006). Economic assessment of geothermal district heating systems: A case study of Balcova–Narlıdere, Turkey. *Energy and buildings*, 38(9), 1053-1059.
- Fraas, A. P. (1989). Heat exchanger design. *John Wiley & Sons*.

- Gao, H., Chen, Z., Osadetz, K. G., Hannigan, P., and Watson, C. (2000). A pool-based model of the spatial distribution of undiscovered petroleum resources. *Mathematical Geology*, 32(6), 725-749.
- Garside, L., (1994). Description of Nevada Thermal Springs and Wells by County. *Nevada Bureau Geothermal Technologies Program*.
- Gifford, J.S., Grace, R.C. (2011). CREST: Cost of renewable energy spreadsheet tool. *National Renewable Energy Laboratory*.
- Giggenbach, W. F. (1988). Geothermal solute equilibria. derivation of Na-K-Mg-Ca geothermometers. *Geochimica et cosmochimica acta*, 52(12), 2749-2765.
- Gilman, P., and Dobos, A. (2012). System Advisor Model, SAM 2011.12. 2: General Description (No. NREL/TP-6A20-53437). *National Renewable Energy Laboratory*.
- Glassley, W. (2010) Geothermal Energy: Renewable Energy and the Environment. *CRC Press*.
- Gordon, R. L. (1975). Economic analysis of coal supply: an assessment of existing studies (No. PB-243220). Pennsylvania State Univ., University Park, USA.
- Gudmundsson, J., Freeston, D., Lienau, P. (1985) The Lindal Diagram. *Geothermal Resources Council Transaction*, Vol 9-Part 1.
- Gunnlaugsson, E. (2008). District heating in Reykjavík; past–present–future. In *UNU Geothermal Training Programme. 30th Anniversary Workshop, Reykjavík, Iceland*.
- He, X., and Anderson, B. J. (2012). Low-temperature geothermal resources for district heating: an energy-economic model of West Virginia University case study. *Proceedings, 37th Workshop on Geothermal Reservoir Engineering, Stanford University, Stanford, USA*.

- Hefley, B., and Seydor, S. (2011). The economic impact of the value chain of a Marcellus shale well. University of Pittsburgh.
- Hurter, S., Kohler, S., Saadat, A., Holl, H.G., Rockel, W., Trautwein, U., Zimmermann, G., Wolfgramm, M., and Huenges, E., (2002) Stimulating low permeability aquifers: Experiments in Rotliegend Sandstones, NE Germany. Geothermal Resources Council Transactions.
- Karingithi, C.W., (2009). Chemical geothermometers for geothermal exploration. *Proceedings, Exploration for Geothermal resources, Lake Naivasha, Kenya.*
- Kasameyer, R. (1997). Brief guidelines for the development of inputs to CCTS from the technology working group-working draft, *Lawrence Livermore Laboratory, Livermore, CA.*
- Kilian, L. (2006). Not all oil price shocks are alike: disentangling demand and supply shocks in the crude oil market. CEPR Discussion Paper No. 5994, available at SSRN: <http://ssrn.com/abstract=975262>.
- Klein, C.W., Lovekin, J.W., Sanyal, S.K. (2004). New geothermal site identification and qualification. *GeothermEX, Inc.*
- Kline, D., Heimiller, D., and Cowlin, S. (2008). A GIS method for developing wind supply curves. *National Renewable Energy Laboratory.*
- Labay, D. G., and Kinnear, T. C. (1981). Exploring the consumer decision process in the adoption of solar energy systems. *Journal of consumer research*, 271-278.
- Lashof, D., Ahuja, D. (1990) Relative contributions of greenhouse gas emission to global warming. *Nature*, 344: 529-531.
- Lee, K. C. (1996). Classification of geothermal resources an engineering approach. *Proceedings, 21th Workshop on Geothermal Reservoir Engineering, Stanford University, Stanford, USA.*



- Lei, H., and Valdimarsson, P. (2009). District heating modelling and simulation. *Proceedings, 34th Workshop on Geothermal Reservoir Engineering, Stanford University, Stanford, USA.*
- Lienau P., Lunis B. (1998) Geothermal direct use engineering and design book. Oregon Institution of Technology.
- Lovekin, J. (2004). Geothermal inventory. *Bulletin Geothermal Resources Council, 33(6), 242-244.*
- Lund, J., Freeston, D., Boyd, T., (2010). Direct application of geothermal energy: 2010 worldwide review. *World Geothermal Congress.*
- Lund, J. W., Freeston, D. H., and Boyd, T. L. (2011). Direct utilization of geothermal energy 2010 worldwide review. *Geothermics, 40(3), 159-180.*
- Special Report on Renewable Energy Sources and Climate Change Mitigation. *Cambridge University Press. Cambridge, United Kingdom and New York, USA.*
- Mahone, D. (1998). Absorption chillers. *Southern California Gas Company.*
- Marcel, R. G., (2007). Technology status of direct geothermal utilization. Paper presented at *European Geothermal Congress, Unterhaching, Germany.*
- McVeigh, J., Cohen, J., Vorum, M., Porro, G., and Nix, G. (2007). Preliminary technical risk technical risk analysis for the geothermal technologies program. *National Renewable Energy Laboratory.*
- Mock, J. E., Tester, J. W., and Wright, P. M. (1997). Geothermal energy from the earth: its potential impact as an environmentally sustainable resource. *Annual review of Energy and the Environment, 22(1), 305-356.*
- Muffler, L. J. P., and Guffanti, M. (1979). Assessment of geothermal resources of the United States--1978. *US Geological Survey.*

- Muffler, P., and Cataldi, R. (1978). Methods for regional assessment of geothermal resources. *Geothermics*, 7(2), 53-89.
- Nathenson, M. (1975). Physical factors determining the fraction of stored energy recoverable from hydrothermal convection systems and conduction-dominated areas (No. USGS-OFR-75-525). *Geological Survey, Menlo Park, USA*.
- New York State oil, gas and mineral resources annual report 2010. New York State Department of Environmental Conservation, Division of Mineral Resources.
- Ozgener, L., Hepbasli, A., and Dincer, I. (2005). Energy and exergy analysis of Salihli geothermal district heating system in Manisa, Turkey. *International Journal of Energy Research*, 29(5), 393-408.
- Pan, G. (1993). Indicator favorability theory for mineral potential mapping. *Nonrenewable Resources*, 2(4), 292-311.
- Persson, U., AND Werner, S. (2011). Heat distribution and the future competitiveness of district heating. *Applied Energy*, 88(3), 568-576.
- Petty, S., Livesay, B. J., Long, W. P., and Geyer, J. (1992). Supply of geothermal power from hydrothermal sources: A study of the cost of power in 20 and 40 years. *Sandia National Laboratories*.
- Petty, S., Porro, G. (2007). Updated US geothermal supply characterization. *Proceedings, 32th Workshop on Geothermal Reservoir Engineering, Stanford University, Stanford, USA*.
- Priest, S. S., Blanton, A. J., Sackett, P. C., Welch, S. L., and MA, W. (2000). Geothermal industry temperature profiles from the Great Basin. *US Geological Survey*.
- Reed, M. J. (1982). Assessment of low-temperature geothermal resources of the United States-1982 (No. USGS-CIRC-892). *US Geological Survey, Menlo Park, USA*.

- Ryder, R.T., Crangle, R.D., Trippi, M.H., Swezey, C.S., Lentz, E.E., Rowan, E.L., and Hope, R.S. (2009). Geologic cross section D–D' through the Appalachian basin from the Findlay arch, Sandusky County, Ohio, to the Valley and Ridge province, Hardy County, West Virginia. U.S. Geological Survey Scientific Investigations Map 3067, 2 sheets, 52-p. pamphlet.
- Sanyal, S. K. (2004). Cost of geothermal power and factors that affect it. *Proceedings, 29th Workshop on Geothermal Reservoir Engineering, Stanford University, Stanford, USA.*
- Shah, R. K., and Sekulic, D. P. (2003). Fundamentals of heat exchanger design. *John Wiley & Sons.*
- Smith, R. L., and Shaw, H. R. (1979). Igneous-related geothermal systems. *US Geologic Survey Circular, 790*, 12-17.
- Somers, C., Mortazavi, A., Hwang, Y., Radermacher, R., Rodgers, P., & Al-Hashimi, S. (2011). Modeling water/lithium bromide absorption chillers in ASPEN Plus. *Applied Energy*, 88(11), 4197-4205.
- Stevenson, P. (2014). The potential for recovering and using surplus heat from industry. *Department of Energy & Climate Change, UK.*
- Tenzer, H. (2001). Development of hot dry rock technology. *Bulletin Geo-Heat Center, Oregon Institution of Technology, USA.*
- Tester, J. W., Anderson, B. J., Batchelor, A. S., Blackwell, D. D., DiPippo, R., Drake, E. M., ... and Veatch, R. W. (2006). The future of geothermal energy: Impact of enhanced geothermal systems (EGS) on the United States in the 21st Century. Massachusetts Institute of Technology, Cambridge, USA.
- Thorsteinsson, H. H. (2008). US geothermal district heating: barriers and enablers. Doctoral dissertation, Massachusetts Institute of Technology.

- Turton, R., Bailie, R. C., Whiting, W. B., and Shaeiwitz, J. A. (2008). Analysis, synthesis and design of chemical processes. *Pearson Education*.
- U.S. Energy Information Administration Heating Fuels Comparison Calculator, (2013).
- U.S. Energy Information Administration. (2013). Assumptions to the Annual Energy Outlook 2013.
- U.S. Energy Information Administration. (2011). International Energy Statistics.
- U.S. National Aeronautics and Space Administration. (2012). GISS Surface Temperature Analysis.
- Valdimarsson, P. (1993). Modelling of geothermal district heating systems. University of Iceland, Faculty of Engineering.
- White, D. E., and Williams, D. L. (1975). Assessment of geothermal resources of the United States--1975 (No. USGS-75-726). *Geological Survey Circular*.
- Williams, C. F. (2004). Development of revised techniques for assessing geothermal resources. *Proceedings, 29th Workshop on Geothermal Reservoir Engineering, Stanford University, Stanford, USA*.
- Williams, C. F., and DeAngelo, J. (2008). Mapping geothermal potential in the western United States. *Geothermal Resources Council Transactions*, 32, 181.
- Williams, C. F., Reed, M. J., Mariner, R. H., DeAngelo, J., and Galanis Jr, S. P. (2008). Assessment of moderate-and high-temperature geothermal resources of the United States. *US Geological Survey fact sheet*, 3082(4).
- Williams, C. F., Reed, M. J., Mariner, R. H., DeAngelo, J., and Galanis Jr, S. P. (2009). Quantifying the undiscovered geothermal resources of the United States. *US Geologic Survey, Geothermal Resources Council Transactions*, 33, 995-1001.
- Xia, L., Lorente, S., and Bejan, A. (2011). Constructal design of distributed cooling on the landscape. *International Journal of Energy Research*, 35(9), 805-812.

Yildirim, N., Toksoy, M., and Gökçen, G. (2006). District heating system design for a university campus. *Energy and buildings*, 38(9), 1111-1119.

Young, K. R., Augustine, C., and Anderson, A. (2010). Report on the US DOE Geothermal Technologies Program's 2009 Risk Analysis. *Proceedings, 35th Workshop on Geothermal Reservoir Engineering, Stanford University, Stanford, USA*.

# Appendix A: Geothermal Reservoir Characteristics and LCOH

Table A-1: Identified Hydrothermal Resources and Near Hydrothermal EGS

Reed River HS, AK	Moana area, NV	Upper Division HS, AK	White Arrow HS, ID	Clear Lak, CA	Medical HS, OR	Weiser area, ID	Name
1520	300	1520	50	3660	1520	200	Depth, m
100	95	110	100	300	105	90	Most Likely Temperature, °C
60.31165	51.0325	93.80333	67.29111	234.2778	72.72476	77.00354	Most Likely Flow, kg/s
4.102068	2.770325	7.016337	4.136771	160.9913	4.934121	2.893585	5 Percentile Potential, MW
18.22352	15.4184	33.51187	20.05965	259.1721	22.86808	25.66704	Most Likely Potential, MW
33.71864	29.60166	61.757	37.41907	360.6215	42.31748	53.86502	95 Percentile Potential, MW
68.10	18.14	67.95	12.17	8.33	14.95	6.74	Mean LCOH, \$/MMBtu
15.2847	14.9988	29.3545	17.8717	102.0594	19.6911	26.2325	Near-hydro EGS Potential, MW
74.06	20.49	73.90	14.00	9.13	16.55	8.27	Mean LCOH, \$/MMBtu

<b>Gregson, MT</b>	<b>Wabuska HS, NV</b>	<b>Crane Creek- Cove Creek, ID</b>	<b>Baker HS, WA</b>	<b>Mt. Princeton HS Area, CO</b>	<b>Steamboat Springs, NV</b>	<b>Cove Fort-Sulphudale- Liquid, UT</b>	<b>Weberg HS, OR</b>	<b>Hawthorne, NV</b>
1520	1520	3050	1520	100	1520	760	1520	300
110	115	150	115	95	165	150	100	100
99.25969	123.0655	672.7746	316.4298	58.72556	246.2934	324.472	51.44187	60.17994
6.924541	10.43071	56.71734	32.89482	3.290118	74.00257	61.17487	3.453342	4.366492
33.90166	46.63593	367.6885	118.8314	17.32173	134.5907	151.3959	14.92811	19.29539
63.47525	86.68188	722.8973	213.1016	33.05362	196.377	241.5638	27.59139	36.12956
18.43	18.27	14.73	17.31	20.17	21.59	20.88	13.98	18.64
28.7181	39.4196	341.3776	92.9902	15.5185	62.5481	91.6737	12.7956	16.2610
20.34	19.82	16.18	19.00	22.69	23.42	22.84	15.67	20.78

<b>Poncha HS, CO</b>	<b>Belknap/Foley HS, OR</b>	<b>Huckleberry HS, WY</b>	<b>Magic Reservoir, ID</b>	<b>Kahneetah HS, OR</b>	<b>Vale HS, OR</b>	<b>Sleeping Child HS, MT</b>	<b>Newcastle area, UT</b>	<b>Pilger Estates HS, CA</b>
1520	1070	1520	1220	1070	1070	1520	760	100
100	105	120	110	115	145	90	110	95
70.37774	114.1827	521.6244	126.1802	90.25096	628.8612	44.14491	157.0936	41.0147
4.538174	9.154249	19.25648	9.296733	7.405873	106.5377	2.458282	14.51284	2.902536
21.4982	34.78578	213.5304	45.76589	31.10351	294.6788	11.51134	57.53948	11.57896
40.50217	66.34979	442.1266	86.37421	57.4391	505.872	21.38255	102.8176	21.29332
20.77	20.87	19.82	22.35	23.95	26.92	18.82	26.71	19.68
18.9065	30.5612	216.4650	40.9373	25.8217	211.2541	9.9876	46.8019	9.7652
22.49	23.06	21.46	24.27	26.08	29.41	20.79	29.36	22.23



<b>Wilson HS, NV</b>	<b>South Brawley, CA</b>	<b>Montezuma HS, NM</b>	<b>Wilbur Spring, CA</b>	<b>Klamath Falls, OR</b>	<b>Banbury area, ID</b>	<b>Chena, AK</b>	<b>Heber, CA</b>	<b>Ashton Warm Springs, ID</b>	<b>Waunita HS, CO</b>
1520	3050	1520	1070	500	1520	1520	1220	1520	1520
100	250	95	160	105	95	95	205	90	120
57.48225	369.3383	69.987	404.8407	159.459	55.33792	36.37633	468.8722	71.01262	172.4222
3.89805	180.4352	3.913915	62.03762	15.44777	3.20474	1.859729	140.5149	2.894579	15.218
17.48853	299.4625	21.21033	236.9922	51.85093	16.24961	9.147946	351.1519	22.56644	69.73813
32.47181	405.8185	40.39243	432.3329	92.3336	30.60834	17.448	570.1365	45.70165	129.9488
24.31	47.80	22.97	36.36	27.72	22.08	15.98	27.92	19.84	23.21
15.5493	106.2982	19.8752	193.6915	39.8498	14.9028	8.5413	224.3831	22.8894	59.2586
26.39	52.11	25.17	39.73	30.86	24.56	17.55	30.14	21.90	25.22

<b>Murphy HS, ID</b>	<b>Salton Sea area, CA</b>	<b>Radium HS, NM</b>	<b>Marysville Test Well, MT</b>	<b>Deer Creek HS, ID</b>	<b>McCredie HS, OR</b>	<b>Routt, CO</b>	<b>Broadwater HS, OR</b>	<b>Joseph HS, UT</b>	<b>Roystone HS, ID</b>
1520	2290	1520	2000	1830	1520	1520	100	1520	1520
100	310	90	100	125	95	110	105	90	90
64.12922	14955.53	103.6346	214.2619	208.6867	64.81048	103.0423	67.15143	67.44923	63.77011
3.731768	8685.287	4.425418	19.12483	17.20811	3.861332	7.776062	3.531235	4.256367	2.802134
19.25659	17098.54	38.19545	61.19292	91.02058	20.35728	35.94886	20.78286	18.55446	19.84647
36.62798	25348.34	79.95217	106.4327	172.3423	39.40747	67.14848	40.22373	35.16983	39.01156
26.66	57.88	27.17	21.94	25.96	25.12	25.23	29.03	25.29	24.74
16.9566	8393.8914	43.4129	45.2802	83.8709	17.5303	30.1834	20.5740	15.7537	19.9954
28.95	63.11	29.40	23.86	28.20	27.30	27.45	33.07	27.86	27.21

<b>Long Valley caldera, CA</b>	<b>White Licks HS, ID</b>	<b>Paso Robles, CA</b>	<b>Calistoga HS, CA</b>	<b>Mt. Signal, CA</b>	<b>Boulder HS, MT</b>	<b>Bonneville HS, ID</b>	<b>Abraham, UT</b>	<b>Puna, HI</b>	<b>Ennis HS, MT</b>
3050	1220	1520	1520	1520	1520	1520	1520	1070	1520
205	110	95	140	135	100	95	90	350	115
593.49	122.4839	44.59001	254.4245	204.8355	74.72856	87.94863	52.77516	1342.265	178.2607
224.9385	9.109507	2.960946	31.034	39.62491	3.891207	4.769915	2.750873	855.106	12.49922
421.4186	44.86515	12.95496	121.6241	87.56237	23.20993	28.89252	14.78484	1832.4	74.24186
626.4832	84.16948	24.54632	219.4041	137.8905	44.78856	56.30999	28.87128	2880.983	146.6945
35.28	34.30	31.23	41.79	48.28	23.83	25.19	27.16	54.18	25.60
205.4234	41.2692	11.1446	97.7867	51.5756	22.0959	27.0507	13.8096	1036.8243	71.3336
38.60	37.67	33.86	45.55	52.64	25.88	27.39	29.71	59.61	27.89

<b>Great Boiling Springs, NV</b>	<b>Fly Ranch HS, NV</b>	<b>Umpqua HS, OR</b>	<b>Warfield, ID</b>	<b>Sharkey HS, ID</b>	<b>Silver Sta HS, MT</b>	<b>Indian Valley HS, CA</b>	<b>Gila HS, NM</b>	<b>Raft River, ID</b>	<b>Geysers, CA</b>
610	300	1520	1520	1830	1520	460	1520	1830	1830
175	100	95	100	115	115	100	100	145	242
676.8956	77.40904	55.66516	69.37702	146.1291	133.4778	44.51721	55.17069	634.8605	6069.534
130.1218	6.777298	3.2755	4.158055	11.36126	9.706345	2.734547	3.499102	97.25794	3273.672
443.5424	23.06132	15.96612	21.1954	55.33368	49.17673	12.80974	15.38193	314.9663	5088.796
794.7499	40.85536	29.67088	39.47845	106.5543	93.80151	24.00618	28.10283	558.0048	6910.492
47.31	42.60	32.06	29.38	28.30	29.93	46.55	34.92	34.32	53.26
351.3090	18.4880	14.1416	18.9873	49.5755	43.4340	11.3856	12.5496	237.1176	1819.6718
53.15	48.46	34.99	31.95	30.81	32.69	52.03	37.98	37.44	58.13

<b>Sulphur HS, NV</b>	<b>Gillard HS, AZ</b>	<b>Sierra Valley, CA</b>	<b>The Needles, NV</b>	<b>Bailey Bay HS, AK</b>	<b>San Emidio Desert, NV</b>	<b>Roosevelt HS, UT</b>	<b>Newberry Caldera, OR</b>	<b>Reese River, NV</b>	<b>Big Bend HS, CA</b>
1830	1520	680	1070	1520	1070	1220	2130	760	1520
165	110	100	120	125	190	250	275	135	105
460.288	163.535	43.32188	235.1046	225.1675	734.3458	1319.79	1155.411	237.4577	62.21403
64.08805	11.427	3.395778	24.0183	20.71745	219.785	655.8656	355.2305	25.35848	4.608232
276.2973	65.20031	12.80751	93.17335	107.7152	437.0271	1194.466	1120.681	110.9365	20.34447
506.9267	127.6664	23.21675	168.1606	203.4031	655.9171	1747.939	1880.773	205.3299	38.10838
45.46	48.26	56.51	46.26	30.20	53.21	60.12	53.97	48.80	38.87
228.6890	57.7338	10.3125	75.5457	95.9820	208.4173	544.8216	746.7514	94.4547	18.6522
49.83	52.72	62.92	51.23	32.70	59.06	66.57	59.18	54.53	42.29

<b>Kyle HS, NV</b>	<b>Maazama Well, OR</b>	<b>Randsburg area, CA</b>	<b>Olene HS, OR</b>	<b>Thermo HS, UT</b>	<b>Tassajara HS, CA</b>	<b>Makushin, AK</b>	<b>Amedee, CA</b>	<b>Fernley area, NV</b>	<b>North Brawley, CA</b>	<b>Brady HS, NV</b>
100	3050	235	1520	760	1520	1520	460	1680	1520	300
105	140	105	110	125	95	205	115	155	250	185
114.5675	412.3264	85.01758	114.5464	209.0704	40.61264	1460.886	113.5632	295.3076	1430.957	535.8664
5.199309	40.81067	10.23177	8.443935	21.73872	2.894041	527.7139	10.81847	45.88587	695.9479	123.0237
47.0425	230.3145	25.60278	40.34779	81.23604	11.44494	1104.48	42.52989	163.3714	1202.17	369.4121
99.67924	442.3019	42.54198	74.80349	143.471	20.68282	1736.657	77.57538	295.3049	1665.135	635.1034
56.26	38.31	73.91	43.74	54.42	40.08	39.84	51.59	50.32	93.20	53.77
56.9978	211.5711	16.4475	34.6137	66.8122	9.3759	614.7899	33.9796	125.4089	471.2043	276.7140
65.15	42.05	84.30	47.99	60.83	43.56	43.28	58.16	55.30	102.50	61.51

<b>Big Creek HS, ID</b>	<b>Neal HS, OR</b>	<b>Humboldt House- Rye Patch, NV</b>	<b>Wedell H, NV</b>	<b>Willow Well, AK</b>	<b>Red River HS, ID</b>	<b>Desert Peak, NV</b>	<b>Soda Lake area, NV</b>	<b>Breitenbush HS, OR</b>	<b>Medicine Lake, CA</b>
1520	1070	910	1520	1520	1520	1680	1370	2130	2740
135	150	205	140	75	85	215	205	150	255
307.6634	434.9324	1258.349	235.4954	16.63204	26.88255	434.072	680.1049	97.73271	3920.362
31.10038	47.95675	452.0184	23.72482	0.59375	1.279206	169.2262	216.3139	22.72209	1928.733
147.9668	235.7882	912.0538	112.4273	3.249519	5.982393	335.1686	489.3567	44.50549	3440.531
277.2496	441.4846	1407.075	217.5376	6.239365	11.11227	511.9545	769.9207	67.83698	4886.071
56.90	68.80	75.54	58.31	49.74	39.15	75.95	72.33	47.51	71.42
132.4631	213.4928	491.9067	99.4818	2.8373	5.1408	171.8453	294.3678	22.9393	1374.8260
62.80	76.33	84.37	64.32	54.40	42.90	83.84	80.11	51.94	78.73

<b>Smith Creek Valley, NV</b>	<b>Blue Mt, NV</b>	<b>Squaw HS area, ID</b>	<b>Mitchell Butte, OR</b>	<b>Little Valle, OR</b>	<b>Brockway HS, CA</b>	<b>Slate Creek HS, ID</b>	<b>Krigbaum HS, ID</b>	<b>Little HS, CA</b>	<b>Coso area, CA</b>
1830	910	1520	1070	1070	1520	1520	1520	1520	1520
125	205	130	120	125	90	105	90	100	285
171.4853	911.7914	189.0057	133.4278	202.5697	28.29068	80.95521	40.10262	51.96978	3613.732
17.00911	194.2523	13.09017	9.791687	18.65698	1.753681	5.639034	2.170961	3.635679	2092.683
73.30246	781.7431	81.70904	50.8055	87.0364	6.75606	26.3395	10.51036	15.94177	3579.93
137.125	1457.884	166.9124	99.35578	162.3316	12.15396	49.05385	19.85297	29.80339	5002.87
59.50	79.91	47.65	60.26	68.88	55.66	47.14	43.78	48.53	95.81
61.8910	654.0641	82.6088	48.5905	74.3509	5.3084	22.8902	9.3664	13.1905	1415.3482
65.43	89.48	52.33	66.71	76.41	60.78	51.97	48.12	53.32	105.62



<b>Buffalo Valley HS, NV</b>	<b>East Basin Creek, ID</b>	<b>Sunbeam HS, ID</b>	<b>Maple Grove HS, ID</b>	<b>Wendel, CA</b>	<b>Valles Caldera- Sulphur Springs, NM</b>	<b>Lakeview area (Hunters and Barry Ranch HS), OR</b>	<b>Idaho bath-Mid Fk Salmon, ID</b>
1520	1520	1520	1520	1520	3350	1070	1520
100	95	100	95	125	225	135	95
57.70993	49.73996	65.96276	58.92955	161.5903	378.1515	284.0206	61.82475
3.755887	2.624444	3.712555	3.196647	17.41901	83.14885	37.47027	3.559621
17.57898	13.87623	20.29621	17.10373	68.09601	311.6943	128.0184	18.30509
33.15726	25.9576	38.72387	33.09994	123.9109	548.3919	225.8615	35.32358
57.18	47.29	47.21	47.88	65.81	75.49	72.70	47.22
15.4987	12.6459	19.2445	15.3845	55.5412	235.2486	100.1593	16.4064
63.00	52.12	52.04	52.56	72.47	83.95	80.07	52.06

<b>Pumper nickel, NV</b>	<b>Jemez Springs, NM</b>	<b>Wayland HS, ID</b>	<b>Tuscarora, NV</b>	<b>Clifton HS, AZ</b>	<b>Black Warrior, NV</b>	<b>Beowawe HS, NV</b>	<b>Darrrough HS, NV</b>	<b>Sonama Mission Inn, CA</b>	<b>Boyes HS, CA</b>
1520	1520	1830	760	1520	1520	2440	610	1520	1520
125	110	130	155	110	135	215	120	110	110
140.796	115.5799	183.0985	389.445	190.1302	227.8228	701.3386	159.2396	78.72844	109.1478
12.8889	8.30342	12.87712	79.36054	6.349235	24.36681	211.6201	14.49277	6.677214	9.207602
58.45756	41.40807	78.37528	208.7569	81.88608	106.4804	573.0754	66.20633	27.34295	41.73151
110.8814	79.50682	156.9741	353.7363	185.322	198.0134	959.5735	123.3386	49.87146	78.61295
71.16	61.82	49.68	77.42	49.42	74.28	83.20	77.35	69.28	69.25
51.9466	37.4996	79.4383	144.6394	106.3806	92.1071	383.3947	54.1233	22.7431	36.7243
78.61	68.16	54.44	87.03	54.01	82.11	91.78	87.53	76.03	75.99

<b>Pinto HS, NV</b>	<b>Luce HS, OR</b>	<b>Marble Hot Well, CA</b>	<b>Owl Creek HS, ID</b>	<b>Cherry Creek , NV</b>	<b>Kellog HS, CA</b>	<b>Travertine HS, CA</b>	<b>Colado area, NV</b>	<b>Riggins HS, ID</b>	<b>Baltazor HS, NV</b>
1520	1520	1520	1830	1520	1520	300	1070	1520	1070
145	105	90	110	100	110	100	110	90	140
330.1972	108.9119	48.92979	107.4388	63.55881	72.57341	35.62978	145.7858	38.14889	291.7778
51.22281	7.276363	2.61828	7.802804	4.001865	6.337751	1.656368	13.69468	2.07925	38.92332
165.5717	38.58819	14.89046	37.53196	19.74539	24.03829	10.20437	56.60806	9.969305	136.7411
288.7083	73.08218	29.20224	69.88318	37.39454	43.62772	20.46836	107.7293	18.69272	244.7388
90.44	74.77	66.94	59.60	70.80	68.13	75.38	78.62	55.15	83.11
127.0818	34.9357	15.0110	33.5502	17.5525	19.2819	10.6812	48.8660	8.5925	106.9731
100.15	82.40	73.44	65.61	77.90	75.05	86.48	87.45	60.77	92.69

<b>Dann Ranch HS, NV</b>	<b>West Valley Reservoir, CA</b>	<b>Lightning Dock, NM</b>	<b>Railroad Valley, NV</b>	<b>McDermitt area, OR</b>	<b>Canby (T'SOT), CA</b>	<b>Fireball Ridge, NV</b>	<b>Spencer HS, NV</b>	<b>Leach HS, NV</b>	<b>Tecopa HS, CA</b>
1520	1830	2740	1520	1520	1520	1520	1520	1520	1520
140	130	130	135	95	120	100	95	120	120
296.2726	175.5308	199.9207	224.4395	62.54326	119.0921	69.15941	33.68077	98.30701	124.1854
16.82584	20.09404	17.69008	24.18751	3.599233	11.85335	3.934055	1.607453	15.28097	12.02075
154.8256	75.46734	85.65165	104.7164	18.32076	47.4529	22.20394	8.706601	35.80278	48.57111
323.7682	134.9124	164.0567	193.4701	34.25499	86.2273	41.9255	16.67823	59.03813	88.79816
74.20	90.30	71.23	95.44	74.92	86.37	74.50	57.47	85.37	96.07
166.0357	58.0063	75.9762	89.8334	16.3822	39.1912	20.6518	8.0562	22.4666	40.2722
82.07	99.63	78.27	105.78	82.55	95.53	82.33	63.28	94.33	105.88

<b>Tolvana, AK</b>	<b>Latty HS, ID</b>	<b>Dyke HS ara, NV</b>	<b>Kelly HS, CA</b>	<b>McLeod 88, NV</b>	<b>Double HS, NV</b>	<b>Butte Springs, NV</b>	<b>Black Rock Point, NV</b>	<b>Mono Lake, CA</b>	<b>Arrowhead HS, CA</b>
1520	1520	1520	1830	1520	1520	1520	1520	750	1370
110	110	110	120	120	120	115	120	95	115
188.3777	79.85676	74.52967	131.3175	132.469	112.1908	101.0209	113.5732	30.99444	86.7385
13.63052	5.178329	6.283927	13.75916	11.27161	9.996554	7.116378	7.86549	1.763327	8.477391
87.47186	26.22365	25.64388	51.88433	52.42566	42.01083	36.31562	43.70508	7.906014	31.5996
181.1549	49.45485	47.41064	94.74472	97.3985	76.36397	69.36931	85.12225	15.0753	57.13064
113.93	86.03	90.61	90.33	95.51	90.55	85.43	85.41	88.65	127.39
87.5099	23.5463	21.1808	40.9932	44.5635	35.5458	31.7315	40.2025	6.7991	25.1907
126.26	95.19	100.32	99.67	105.85	100.26	94.39	94.37	99.71	140.96

<b>Neinmeyer HS, ID</b>	<b>Circle, AK</b>	<b>Mineral (San Jacinto)HS, NV</b>	<b>Bradfield Canal HS, AK</b>	<b>Fish Lake Valley, NV</b>	<b>Goddard HS, AK</b>	<b>Sitka Hot Spring, AK</b>	<b>MacFarlan e's HS, NV</b>	<b>McGee Mt, NV</b>	<b>Rowland HS, NV</b>
1520	1520	1520	1520	1520	1520	1520	1520	1520	1520
100	105	100	110	205	135	125	95	100	110
84.00511	77.57599	48.02429	98.25099	760.2189	191.4963	170.2347	46.6366	72.12264	75.58854
4.28847	5.676473	2.848492	7.255519	151.3034	18.42286	15.81501	3.069745	4.440148	5.916402
27.38484	26.24304	13.73769	35.49332	600.4133	88.18119	74.32748	13.06182	23.32744	25.57659
55.14058	48.19397	25.30877	67.40578	1085.742	165.4311	137.1548	24.42186	44.91846	47.39544
86.11	124.24	91.40	68.24	155.50	75.05	75.07	90.77	90.68	91.28
28.0045	22.4682	11.9541	30.9063	489.2731	80.5918	64.1018	10.7600	21.4460	22.3817
95.27	137.99	101.17	75.05	173.33	82.67	82.68	100.48	100.39	101.05

<b>East Brawley, CA</b>	<b>Near Fish Bay, AK</b>	<b>Worswick HS, ID</b>	<b>Dulbi, AK</b>	<b>Manley, AK</b>	<b>Stillwater area, NV</b>	<b>Okpilak Springs, AK</b>	<b>Leonards HS/Seyferth HS, AK</b>	<b>Radio Towers, ID</b>
3050	1520	1220	1520	1520	1010	1520	1520	1520
285	95	105	110	90	160	85	120	90
2839.484	59.10699	82.77949	122.8341	31.79192	784.6502	28.66955	146.8647	14.68217
1236.599	3.689646	5.611402	9.59068	1.805723	172.5264	1.318873	12.23384	1.072684
2870.89	18.43961	26.82504	47.56398	7.894888	433.3244	6.27275	59.63678	2.820622
4502.38	34.94097	49.89528	90.28429	14.66775	710.2309	11.6487	111.3496	4.487772
286.59	75.39	114.21	137.90	114.37	154.95	61.11	103.33	86.27
1608.8842	16.4874	24.0838	42.6815	6.7404	283.5461	5.5416	53.3381	1.6348
318.93	82.86	127.44	153.28	126.70	174.33	66.15	114.33	95.43

<b>Icy Point HS, AK</b>	<b>Vulcan HS, ID</b>	<b>Melozi HS, AK</b>	<b>Fallon naval Air Station, NV</b>	<b>West Ukinrek Maar, AK</b>	<b>Barron's HS, ID</b>	<b>Blossom HS, NV</b>	<b>Dixie Valley Geothermal field, NV</b>	<b>Pilgrim HS, AK</b>
1520	1520	1520	2130	1520	1220	1520	1520	1220
90	115	90	195	200	95	70	225	140
96.60615	133.4567	39.14353	727.0816	303.3864	56.12638	14.20462	1550.58	203.3952
4.053017	11.28635	2.358829	133.7043	75.56249	2.998102	0.187705	702.366	18.72355
36.37459	50.29692	9.944863	555.8766	234.4488	16.24265	3.052279	1130.399	93.57762
75.74091	93.93421	18.21053	1012.948	415.1513	31.21205	6.810592	1527.773	174.4616
80.91	133.00	138.19	187.95	119.29	114.33	4010.66	184.87	93.06
37.2634	42.6781	8.3169	449.5441	178.4933	15.2560	3.9196	376.6711	83.3262
89.11	147.82	153.58	208.52	132.28	127.57	79.88	205.18	103.22



Lava Creek, AK	Boiling Springs, ID	Carson Lake Corral, NV	Clear Creek, AK	East Mesa, CA	Tenakee Inlet, AK	Serpentine Springs, AK	Tungsten Mt, NV	Carson River, CA	Lee HS, NV
1520	1520	1520	1520	1520	1520	1520	1520	1520	1520
100	100	125	100	190	100	145	125	145	150
66.08748	69.99592	159.4415	63.27105	735.2811	51.01204	220.375	161.6788	210.1265	352.3517
4.205189	4.485071	14.20742	4.486489	215.3667	3.013373	17.85523	16.11247	21.32004	41.88003
20.11371	21.9108	66.33571	19.94445	508.9405	14.26862	107.113	69.01781	98.07053	190.0474
37.246	41.77865	122.5668	37.09547	820.7258	27.44706	212.024	126.7669	188.2112	352.8538
98.50	133.11	172.18	98.47	308.33	81.07	98.14	172.16	134.53	172.12
17.3007	19.1226	58.2726	17.3958	297.9690	12.8120	101.7814	58.5005	90.3068	160.3785
108.63	147.92	191.83	108.60	346.61	89.20	108.42	191.82	149.61	191.78

Lake City HS, CA	Sespe HS, CA	South, AK	Fort Bidwell, CA	Mickey HS, OR	Grovers HS, CA	Cabarton HS, ID	Dunes, CA	Emigrant, NV	Molly's HS, ID	Indian Cr. HS, ID
1520	1520	1520	760	1070	1520	1520	1070	2440	1520	1520
160	120	85	110	170	90	85	145	165	95	95
1415.221	145.0304	23.0441	136.3384	595.9009	35.82224	35.84295	250.7555	471.9739	61.59263	76.71652
308.35	13.46609	0.947453	15.19567	121.117	1.864289	1.758981	26.77565	60.92238	3.536061	4.500932
767.7539	60.05329	4.89302	48.30144	362.5965	10.06157	8.975237	127.1637	306.7326	18.03351	24.34969
1261.213	112.1767	9.646627	85.30214	624.718	18.90588	17.00609	243.0642	587.1843	34.05296	47.55276
248.94	221.67	139.08	208.60	227.16	134.85	133.37	308.36	176.24	133.17	133.14
492.1676	52.2881	4.6373	36.5975	260.6095	9.4305	7.6968	115.4149	280.8019	16.1463	22.4501
277.78	246.41	154.53	237.00	255.68	149.92	148.19	346.65	195.67	147.99	147.95

Surprise Valley HS, CA	Leonards HS/Seyferth HS, CA	Shakes Springs, AK	Ophir, AK	Hot (Borax)Lake, OR	Alvord HS, OR	Trout Creek, OR	Fales HS, CA
1520	1520	1520	1520	1520	1220	910	1520
115	125	90	85	150	135	115	100
107.3385	134.3958	21.74556	30.18927	558.3922	258.0293	134.2128	36.31292
10.19334	15.11597	0.614589	1.013299	88.48586	31.14793	10.10275	1.107341
40.03748	50.10267	4.790522	7.265129	288.6783	115.3123	49.47313	10.19384
73.88567	88.93948	10.6256	15.01218	504.8285	206.1675	93.32312	21.78234
248.96	178.53	72.44	86.06	249.03	235.03	218.02	105.21
31.8287	38.2158	5.4975	7.5130	217.0563	90.2453	43.7824	11.9026
277.80	198.81	75.75	94.13	277.93	263.63	246.49	116.00

<b>Little Melozitna, AK</b>	<b>Carey HS, OR</b>	<b>Kanuti, AK</b>	<b>Crump's HS, OR</b>	<b>Mother Goose, AK</b>	<b>Harney Lake, OR</b>	<b>Lake HS, OR</b>	<b>Crane HS, OR</b>	<b>Clark Ranch, OR</b>	<b>Big Windy Hot Springs, AK</b>
1520	1520	1520	1520	1520	1520	1010	1520	1520	1520
88	100	105	150	70	105	110	105	110	95
52.6684	53.02581	68.72665	617.6216	18.96662	84.81492	114.4134	76.74252	100.8365	68.56086
2.714749	3.643137	4.883822	73.17696	0.887386	5.829065	8.528034	5.451008	7.125057	1.314628
15.15577	16.04595	21.97207	315.5927	3.556425	27.56488	40.51582	24.82954	34.11933	23.39581
28.86523	29.86074	40.97174	585.4492	6.700678	52.26625	75.65394	46.34696	62.63833	55.11879
363.64	328.70	363.49	370.48	121.10	249.12	334.07	249.12	249.09	125.39
13.6016	13.7373	18.7112	275.0830	3.4060	24.5346	35.3105	21.2617	29.9340	31.0326
406.77	367.22	406.63	412.25	133.30	278.02	375.25	278.01	278.00	143.67

<b>Cold Bay HS, AK</b>	<b>Akutan Island, AK</b>	<b>Kwiniuk, AK</b>	<b>Kilo, AK</b>	<b>Ray River, AK</b>	<b>Lower Ray River, AK</b>	<b>Fisher HS, OR</b>	<b>Ishtalitna HS, AK</b>	<b>Dall Hot Spring, AK</b>	<b>Akutan Fumaroles, AK</b>
1520	1520	1520	1520	1520	1520	1520	1520	1520	1520
90	130	75	75	80	80	95	105	95	250
52.27738	211.5767	37.36023	23.81891	21.42665	29.77639	39.73665	63.9024	47.84932	687.1911
3.885423	25.45575	0.322212	0.460481	0.950799	1.435263	2.83497	3.898082	2.813418	191.8327
17.11266	96.33973	9.648837	2.955521	4.168001	6.539144	11.17506	19.0727	13.17487	653.1399
33.13752	177.846	24.53881	5.015495	7.689242	12.12677	20.29013	36.09072	24.49546	1173.233
355.47	354.95	103.28	364.29	364.60	364.33	370.65	363.57	363.65	354.58
15.8213	79.2848	14.2057	2.1457	3.4649	5.7299	9.1208	17.5459	11.5566	506.5320
396.04	395.73	109.99	407.43	407.74	407.47	412.42	406.70	406.79	395.52

<b>HS Cove, AK</b>	<b>Adak, AK</b>	<b>Korovin, AK</b>	<b>Geyser Bight, AK</b>	<b>Kluichef, AK</b>	<b>Milky River- Atka Island, AK</b>	<b>False Pass, AK</b>	<b>Emmons Lake, AK</b>	<b>Akun Strait, AK</b>	<b>Port Moller HS, AK</b>
1520	1520	1520	1520	1520	1520	1520	1520	1520	1520
110	155	170	182	230	245	85	95	80	80
67.68594	183.7457	338.9077	1218.647	481.7151	647.2661	20.94978	48.34987	88.4	39.71711
7.315627	31.70111	67.2368	336.857	263.5567	210.3446	1.146882	2.622475	7.766521	2.288984
23.0169	97.23731	201.7962	995.5329	398.3411	569.6212	4.157919	11.26852	16.75436	11.23467
39.85787	166.653	348.6701	1744.931	557.0229	924.7217	7.86155	21.83767	27.07888	23.3061
969.83	969.37	969.30	969.16	969.14	969.10	356.96	356.35	356.61	356.13
17.7403	71.0987	143.0746	751.8375	157.6610	357.7881	3.5267	10.2871	10.1995	11.6289
1087.36	1087.15	1087.12	1087.09	1087.09	1087.09	396.90	396.55	396.71	396.42

<b>Heber Shallow, CA</b>	<b>East Mesa shallow, CA</b>	<b>Valles Caldera- Redondo, NM</b>	<b>Geysers High Temp Reservoir, CA</b>	<b>Steamboat Hills, NV</b>	<b>Milky River, AK</b>	<b>Hson Umnak Island, AK</b>	<b>Great Sitkin Island, AK</b>
1220	1070	3350	1830	1520	1520	1520	1520
170	165	275	315	210	80	100	130
1689.077	2119.468	933.9149	3597.185	623.513	15.88285	49.94445	191.5738
415.3966	329.2829	385.4019	2692.503	276.9756	0.391261	4.211458	21.47753
965.8546	1184.942	928.2215	4270.408	474.0698	2.20678	14.95252	87.43508
1529.261	2097.353	1470.772	5898.282	682.0894	3.97975	27.07184	166.3115
27.92	308.32	75.49	53.26	21.59	972.30	970.16	969.55
573.5017	895.3173	551.8197	1611.9597	204.5252	1.7239	12.4758	78.0518
346.61		83.95	58.13	23.42	1088.79	1087.54	1087.23

<b>Cove Fort-Sulphur dale-Vapor, UT</b>	<b>Long Valley shallow, CA</b>	<b>Dixie HS, NV</b>	<b>Dixie Valley Power Partners, NV</b>
760	3050	2900	1520
155	175	130	280
22.8741	200.6693	138.1177	956.9031
5.416439	57.61784	18.29709	545.8747
12.23601	123.5377	59.16885	977.2432
19.36002	195.0783	103.9202	1415.21
21.32	35.28	184.87	184.87
7.1093	70.6214	45.7965	435.2396
22.84	38.6	205.18	205.18



Table A-2: Undiscovered Hydrothermal Resources

<b>AZ&gt;150 °C</b>	<b>AZ&lt;150 °C</b>	<b>CA&gt;150 °C</b>	<b>CA&lt;150 °C</b>	<b>HI&gt;150 °C</b>	<b>HI&lt;150 °C</b>	<b>AK&gt;150 °C</b>	<b>AK&lt;150 °C</b>	<b>Regions</b>
0	85.5019	246.0216	108.9220	3350	0	192.3831	102.2556	<b>Lowest Temperature, °C</b>
0	110	260.2538	120.5360	350	0	211.1510	116.7506	<b>Most Likely Temperature, °C</b>
0	156.7126	276.7380	130.7090	360	0	243.9285	138.3075	<b>Highest Temperature, °C</b>
0	29.0071	2380.4132	41.0598	661.7692	0	423.7725	36.7759	<b>5 Percentile Flow, kg/s</b>
0	178.3509	3958.5507	138.5869	1342.2650	0	938.4917	145.8905	<b>Most Likely Flow, kg/s</b>
0	456.4035	5432.7507	292.7723	2206.1298	0	1689.4726	329.1093	<b>95 Percentile Flow, kg/s</b>
0	13.98	34003.31	499.96	11413.93	0	4486.95	733.63	<b>5 Percentile Potential, MW</b>
0	104.68	64033.79	1912.69	24650.15	0	11231.77	3554.28	<b>Most Likely Potential, MW</b>
0	216.76	94121.22	3485.73	38421.15	0	18702.93	6806.39	<b>95 Percentile Potential, MW</b>
NA	51.93	8.39	32.52	57.67	NA	42.74	14.70	<b>Mean LCOH, \$/MMBtu</b>

NV>150 °C	NV<150 °C	NM>150 °C	NM<150 °C	MT>150 °C	MT<150 °C	ID>150 °C	ID<150 °C	CO>150 °C	CO<150 °C
187.7668	111.3985	247.4267	97.4707	0	96.7339	0	107.5986	0	106.5417
204.7271	126.3234	262.4267	112.3640	0	108.1950	0	125.9540	0	111.5417
224.4467	140.6107	277.4267	132.0083	0	123.8462	0	141.8374	0	122.1418
390.0393	53.5047	315.3487	32.3282	0	40.8248	0	86.6979	0	32.5952
842.0240	192.8611	794.1590	139.7108	0	152.0717	0	338.3592	0	126.3641
1411.2248	421.1843	1300.0543	323.7266	0	332.3233	0	758.4500	0	276.2296
13840.88	1555.56	519.75	40.37	0	23.73	0	656.32	0	31.58
33293.41	6751.41	1401.30	228.46	0	108.86	0	3302.25	0	147.43
54194.27	12582.59	2285.61	443.83	0	205.91	0	6309.94	0	275.26
22.57	18.99	89.73	24.76	NA	19.51	NA	9.36	NA	21.48

<b>WY&gt;150 °C</b>	<b>WY&lt;150 °C</b>	<b>WA&gt;150 °C</b>	<b>WA&lt;150 °C</b>	<b>UT&gt;150 °C</b>	<b>UT&lt;150 °C</b>	<b>OR&gt;150 °C</b>	<b>OR&lt;150 °C</b>
0	950	0	110	228.5931	102.8024	198.3270	112.7035
0	120	0	1150	237.9903	113.2126	212.2641	126.2858
0	1350	0	1250	247.5679	127.8024	229.7716	140.9792
0	63.5389	0	104.7015	666.2056	49.6009	259.1973	96.3180
0	521.6244	0	316.4298	1197.0887	163.0336	833.8158	297.3143
0	1328.4072	0	661.4359	1804.3986	337.1512	1459.9217	613.5476
0	12.11	0	13.01	1030.34	60.97	1214.98	606.02
0	125.48	0	46.36	1954.90	247.89	4021.44	2413.62
0	263.45	0	83.53	2888.39	452.19	6946.29	4458.75
NA	21.16	NA	18.26	63.84	21.57	55.85	14.66

## Appendix B: WV Geothermal Temperature Maps

